UNIVERSIDADE FEDERAL DO RIO GRANDE DO SUL

INSTITUTO DE GEOCIÊNCIAS

PROGRAMA DE PÓS-GRADUAÇÃO EM GEOCIÊNCIAS

ANÁLISE INTEGRADA PELO MÉTODO U-Pb E TRAÇOS DE FISSÃO EM ZIRCÃO: CARACTERIZAÇÃO, DATAÇÃO E INTERPRETAÇÃO

AIRTON NATANAEL COELHO DIAS

ORIENTADOR – Prof. Dr. Farid Chemale Jr.

CO-ORIENTADOR - Prof. Dr. Carlos Alberto Tello Saenz

Volume Único

Porto Alegre – 2012

UNIVERSIDADE FEDERAL DO RIO GRANDE DO SUL

INSTITUTO DE GEOCIÊNCIAS

PROGRAMA DE PÓS-GRADUAÇÃO EM GEOCIÊNCIAS

ANÁLISE INTEGRADA PELO MÉTODO U-Pb E TRAÇOS DE FISSÃO EM ZIRCÃO: CARACTERIZAÇÃO, DATAÇÃO E INTERPRETAÇÃO

AIRTON NATANAEL COELHO DIAS

ORIENTADOR: Prof. Dr. Farid Chemale Jr.

CO-ORIENTADOR: Prof. Dr. Carlos Alberto Tello Saenz

BANCA EXAMINADORA

Prof. Dr. Elton Dantas – Instituto de Geociências, UnB

Prof. Dr. Júlio Cesar Hadler Neto - Instituto de Física "Gleb Wataghin", UNICAMP

Prof. Dr. Léo Afraneo Hartmann – Instituto de Geociências, UFRGS

Tese de Doutorado apresentada como requisito parcial para a obtenção do Título de Doutor em Ciências.

Porto Alegre – 2012

"O amor recíproco entre [o que se] aprende e [o que se] ensina é o primeiro passo e mais importante degrau para se chegar ao conhecimento."

Erasmo de Roterdã

"Quase todos podem fazer ciência; quase ninguém consegue fazer boa ciência"

Larison Cudmore

"Ó profundidade das riquezas, tanto da sabedoria, como da ciência de Deus! Quão insondáveis são os seus juízos, e quão inescrutáveis os seus caminhos."

Romanos 11:33

DEDICATÓRIA

À

Hélida, motivo e combustível da minha vida!

À meus amados sobrinhos *Vinicius, Tamyres, Nicolas e Rafael;*

à, meu melhor amigo e pilar, *Preto;*

e à *Farid,* o responsável por renovar minhas esperanças.

AGRADECIMENTOS

A Deus por ter me sustentado, suprido minhas necessidades e ter sido meu porto seguro. Ele entendeu meus medos, minhas ansiedades e colocou no meu caminho pessoas dispostas e me reergueu quando caído estava. A Ele meu primeiro e mais importante agradecimento;

À Helida, por estar ao meu lado nesta etapa. A carga que você suportou não foi pequena. Sua presença, suas palavras e seu carinho me mantiveram em pé. Olhar pra um futuro com você me fez continuar. Meus sonhos eram (e são) os seus sonhos e por isso chegamos (e chegaremos) ao fim da estrada das nossas vidas juntos. Amo você, "em tudo, tudo, tudo".;

Ao meu pai, meu exemplo de homem honesto, correto, sério e dedicado ao seu trabalho. Pelo seu amor, consideração, incentivo e por jamais me permitir desistir. Tudo que sou devo a esse homem, meu exemplo e meu herói;

A minha mãe pelo seu amor imensurável dedicado a mim em todos os momentos que pensava estar só e a duvidar da realização dos meus sonhos. Seu amor incomparável me assistia e dava toda a confiança que precisava pra seguir em frente. Nunca conheci uma mulher tão forte e tão especial;

Aos meus irmãos, Artaxerxes e Arley, e cunhadas Patrícia e Karina, simplesmente por serem quem são. Sou privilegiado pelo amor de vocês e por sempre acreditarem em mim, mesmo quando eu mesmo não acreditei;

Aos meus sogros, Doniel e Asenathi pelo incentivo que sempre me deram. Eles estiveram presentes em cada etapa desta tese. Das primeiras idéias e expectativas às mudanças. Muito obrigado!;

Ao Prof. Farid por me orientar, instruir e guiar no caminho da ciência, introduzindo-me a um novo método. Só isso já seria suficiente pra que eu lhe agradecesse, mas além da chance de conhecimento, o senhor (e a Lucy) me brindaram com uma amizade especial. O senhor confiou em mim e incentivou sempre, mesmo sabendo das minhas limitações. Muito obrigado por renovar minha esperança. Essa tese, eu dedico ao senhor também. Ela é sua!

Ao Prof. Carlos por tudo o que fez por mim. Sempre serei grato ao senhor;

Ao Prof. Carlos José, querido Casé, pelos incontáveis momentos que pude aprender, discutir, questionar e desabafar. Apesar de todos seus afazeres em nenhum momento deixou de me escutar e instruir com grande cuidado e carinho. Que a minha admiração e respeito fique registrada;

Aos meus tios Nely e Tonhão que sempre me incentivaram; Aos meus primos Gisely, Larissa, Leonardo e Tiago pelo amor e preocupação.

SUMÁRIO

LISTA DE FIGURAS E TABELAS

ANÁLISE INTEGRADA PELO MÉTODO U-Pb E TRAÇOS DE FISSÃO EM ZIRCÃO: CARACTERIZAÇÃO, DATAÇÃO E INTERPRETAÇÃO

RESUMO

Datação dupla com os métodos de Traços de Fissão (TF) e U-Pb *in situ* via LA-ICP-MS em zircões extraídos de rochas sedimentares foi utilizada para gerar informação das áreas fontes, da história térmica e dos eventos crustais (incluindo formação de Supercontinentes) que podem ser descortinados em uma bacia intracratônica. Assim, análises em zircões da Bacia Bauru, formada no Neocretáceo (73-90 Ma) e localizada no centro-sul da Plataforma Sul-americana, foram realizadas nas formações Caiuá (Sequência Deposicional 1) e Santo Anastácio (Sequência Deposicional 2) e membros Vale do Rio do Peixe e Presidente Prudente da Formação Adamantina (Sequência Deposicional 3). Os resultados de U-Pb em zircão nas três sequências deposicionais, permitiram identificar áreas fontes de zircões formados nos ciclos Brasiliano (Neoproterozóico) e Transamazônico (Paleoproterozóico), e subordinadamente, nos ciclos Estateriano e Sunsás. Localmente, foram encontrados zircões de idade mesozóica e arqueana. Os dados de TF em zircão dos sedimentos da Bacia Bauru contêm preciosa informação sobre os eventos de denudação rápida dos cinturões neoproterozóicos (idades U-Pb a TF próximas). Por outro lado, alguns zircões registram o processo de acreção crustal na margem da placa, distante a mais de 1000 km da bacia, com reflexo na sua porção intracratônica por soerguimento rápido das áreas cristalinas e, consequentemente, passagem da zona de apagamento total para zona de retenção parcial de TF (180 à 320 ºC), os quais foram disponibilizados no ciclo sedimentar durante o Paleozóico e Mesozóico. Assim, as idades aparentes de TF em zircão concentram-se no Neoproterozóico, Siluro-Ordoviaciana, Carbonífero Superior a Triássico e Cretáceo, que são em parte registro dos eventos de: (i) acreção do Ciclo Brasiliano e Brasiliano Precoce (ou Arco Magmático de Goiás), decorrente da aglutinação do Gondwana Oeste; (ii) dos ciclos Famatiniano e Gondwanides (formação do Supercontinente Pangea) ocorrentes na margem oeste da Placa Sul-Americana e com reflexos no interior da placa; (iii) ciclo extensional relacionado a separação das placas sul-americana e africana. A aplicação da presente técnica de datação dupla é uma ferramenta poderosa para o estudo das bacias intracratônicas onde os grãos dos zircões têm uma história muito complexa, com histórias de resfriamento único ou múltiplos (ZAP).

ABSTRACT

Fission Track (FT) and U-Pb in situ by LA-ICP-MS double-dating in zircon grains extracted from sedimentary rocks was applied to get information of the source areas, thermal history and crustal events (including formation of supercontinents) which can be unraveled in an intracratonic basin. Thus, zircon analyzes from the Bauru Basin, formed in the Late Cretaceous (73-90 Ma) and located in south-central South American Platform, were carried out in the Caiuá (Depositional Sequence 1) and Santo Anastácio (Depositional Sequence 2) formations and Vale do Rio do Peixe and Presidente Prudente members of the Adamantina Formation (Depositional Sequence 3). Based on the U-Pb results in zircon grains from three depositional sequences were possible to recognize main source areas: from Brasiliano (Neoproterozoic) and Transamazionian (Paleoproterozoic) cycles, and subordinately from Statherian and Sunsás cycles. Locally, were found Mesozoic and Archean zircons. The zircon FT data of the Bauru Basin sediments contain valuable information about the rapid denudation events of the Neoproterozoic belts (those U-Pb and FT ages are very close). Moreover, some zircons records the accretion crustal process in the western margin of Gondwana, far more than 1000 km from the studied basin, which reflected in its intracratonic portion by rapid uplift of crystalline areas and hence the zircon passed from total annealing zone to partial annealing zone (PAZ) (180 to 320 ° C). This material was thus available in the sedimentary cycle during the Paleozoic and Mesozoic. In this way the FT apparent zircon ages concentrated in the Neoproterozoic, Silurian-Ordoviacian, Upper Carboniferous to Triassic and Cretaceous, which are in part a record of events: (i) Accretion of Early Brasiliano cycles (or Goiás Magmatic Arc) and main Brasiliano Cycle (650-500 Ma), as result of West Gondwana agglutination; (ii) Famatinian and Gondwanides cycles (formation of Pangea Supercontinent) occurred on the west margin of the present-day South American Platform and with reflections inside of the plate; (iii) extensional cycle related to separation of South American and African Plates. The present double dating is a powerfull tool for the study of intracratonic basins where the zircons grains have a very complex history with single or even multiple cooling histories (PAZ).

ESTRUTURA DA TESE

Esta tese está estruturada em torno de artigos publicados e submetidos a periódicos durante o desenvolvimento do Doutorado. Portanto, sua organização compreende duas partes principais, :

A primeira parte é composta pelos capítulos I a III e suas referências (IV), como segue:

- O Capítulo I refere-se à *introdução* da Tese, que apresenta o tema e seus objetivos gerais e específicos e métodos e materiais.

- O Capítulo II apresenta um estado da arte sobre as *metodologias empregadas* na tese.

- O *texto integrador dos artigos* foi desenvolvido no Capítulo III , que sintetiza os resultados da pesquisa nas diferentes áreas geológicas e física da tese e referências utilizadas nesta primeira parte da Tese.

- No Capitulo IV constam as *referências* decorrentes dos três primeiros.

- A segunda parte consiste do *corpo principal* da Tese com os artigos publicados e submetidos (V), que são:

    Artigo 1. Este trabalho apresenta idades obtidas via metodologia combinada de MTF e U-Pb *in situ* aplicada a zircões pertencentes à Formação Rio Paraná (de acordo com Fernandes e Coimbra, 1996) pertencente à Bacia Bauru, estado de São Paulo, Brasil. Foi o primeiro trabalho de uma série que envolve a análise integrada para estudos de proveniência dentro desta bacia intracratônica.

    Artigo 2. Em sequência ao trabalho de análise integrada pelas metodologias de TF e U-Pb, neste trabalho são apresentadas idades e interpretações provenientes de zircões pertencentes à Formação Vale do Rio do Peixe, de acordo com Fernandes e Coimbra (1996) ou Formação Adamantina Inferior (segundo Paula e Silva et al., 2009) pertencente a Bacia Bauru, sudeste do Brasil..

    Artigo 3. Por fim, este trabalho, completa as análises realizadas dentro da Bacia Bauru no estado de São Paulo. São acrescentadas análises de mais doze amostras pertencentes às formações já citadas acima, e da Formação Caiuá e Membro Presidente Prudente. Neste trabalho a carga interpretativa é maior

e objetiva-se delinear claramente quais são as áreas fontes da bacia, bem como identificar os fenômenos geológicos que ocorreram nas margens e no interior da Plataforma Sul-americana.

- Nos *anexos* encontra-se um artigo publicado na qual o doutorando é coautor e que está relacionado ao tema central da tese. A lista de anexos é complementada com resumos de participação em congresso durante o desenvolvimento do doutorado.

I. INTRODUÇÃO

1.1. Apresentação do tema e justificativa

O zircão, $ZrSiO_4$, é um mineral fundamental para as chamadas Ciências da Terra. Acessório comum em rochas ígneas, sedimentares, e metamórficas, o zircão é física e quimicamente resistente, podendo "sobreviver" durante muitos períodos geológicos, e em muitos casos, fornece um registro de cada evento geológico a qual foi submetido nestes períodos. Tornou-se um dos mais importantes minerais para o estudo da evolução de bacias sedimentares através de diferentes métodos de datação.

Tais minerais podem, muitas vezes, apresentar um zoneamento complexo, como resultado de sua história geológica, no entanto, os recentes desenvolvimentos na microanálise tem reforçado a utilidade deste mineral, permitindo a amostragem mais detalhada destas estruturas de pequena escala.

Uma das características mais importantes do zircão é a sua capacidade para incorporar os elementos traços, tais como U, Th e Pb que estão presentes em quantidades de ppm (partes por milhão), o que é crucial para as análises geocronológicas. Especificamente, nesta tese foram utilizadas duas destas técnicas geocronológicas: o Método de Traços de Fissão (MTF) e U-Pb *in situ* via LA-ICP-MS (Laser Ablation – Ion Coupled Plasma – Mass Spectrometer).

O método U-Pb em zircões detríticos vem sendo aplicado no estudo de diferentes tipos de bacia para revelar a sua *i)* proveniência ou origem sedimentar, *ii)* a correlação de sequencias sedimentares, *iii)* idades deposicionais máximas e *iv)* ambiente tectônico. Por outro lado, o MTF é aplicado a análises de processos geológicos de intermediária/baixa temperatura, 200-320 °C (Garver and Brandon, 1994; Tagami, 1998; Carter e Moss, 1999; Liu et al., 2001; Bernet et al., 2001). Tal análise possibilita o entendimento de *i)* processos de denudação nas diferentes situações tectônicas, e *ii)* na estimativa da idade deposicional máxima.

A combinação das duas técnicas, aplicadas a zircões detríticos em rochas sedimentares, pode, portanto, trazer informações muito importantes sobre eventos geológicos de alta e intermediária/baixa temperatura. Informações tais como: *i)* cristalização ígnea e metamórfica de zircões, *ii)* eventos morfotectônicos (*uplift*, denudação, etc.), e *iii)* proveniência sedimentar, como já citado. Essa análise

combinada é utilizada em diferentes tipos de bacia para melhor entendimento da relação existente entre a origem sedimentar e o preenchimento da bacia (Carter & Moss, 1999). Em alguns casos, é possível identificar eventos de deposição acrescionais e de metamorfismo ao longo da margem ancestral (Thomson and Hervé, 2002).

As amostras selecionadas para compor esta tese são da à Bacia sedimentar Bauru, no estado de São Paulo, sudeste do Brasil. Trata-se de uma bacia intracratônica. Nesta área foram coletadas e datadas cerca de 50 amostras de zircão. No entanto, nos artigos selecionados (publicados e submetidos) serão apresentados resultados de 29 amostras.

Bacias sedimentares como a Bacia Bauru, estão localizadas em uma região continental estável, a alguma distância das margens esticadas ou convergentes (Allen & Armitage, 2012). São caracterizadas por uma baixa taxa de sedimentação dominante durante centenas de milhões de anos, de espessura não superior a 5 km e distribuição amplamente superficial (milhões de quilômetros quadrados). A sedimentação pode se estender por mais de 600 Ma, como é o caso das bacias Australiana Central e Espinhaço (Shaw et al., 1991;. Chemale et al., 2012.) Ou pode ocorrer em menos de 400 Ma como é o caso das bacias Fanerozóica de Michigan e Paraná (Sloss, 1963; Zalan et al., 1990). Seus sedimentos podem assim, registrar múltiplas histórias das áreas cratônicas, sendo que estas histórias podem ser associadas aos eventos geológicos ocorridos nas margens extensionais ou convergentes. Muitos registros importantes destes eventos podem ser encontrados no ambiente continental intraplaca, como descrito por Lindsay (2002) em bacias intracratônicas fanerozóicas.

1.2. Objetivos

A metodologia de trabalho empregada nesta tese buscou aprimorar os conhecimentos acerca das técnicas MTF e U-Pb *in situ,* utilizadas na geocronologia.

1.2.1. Objetivos gerais

Foram objetivos gerais deste trabalho compreender a história geológica da bacia intracratônica do Bauru, formado durante o Mesozóico na posição central da Plataforma Sul-Americana.

1.2.2. Objetivos específicos

Com base nos objetivos gerais, alguns objetivos específicos foram delimitados:

- Aplicação da técnica combinada de MTF e U-Pb *in situ* via LA-ICP-MS em zircões detríticos;
- Desenvolvimento e aprimoramento da técnica combinada implementada por Carter and Moss (1999);
- Datação e interpretação das formações geológicas da Bacia Bauru, no estado de São Paulo, sudeste do Brasil;

CAPÍTULO II

II. METODOLOGIAS EMPREGADAS

2.1. Método de Traços de Fissão (MTF)

A análise de traços de fissão como uma ferramenta de datação geológica foi primeiramente proposta na década de 1960, por P. B. Price e R. M. Walker. Trabalhos como os de R. L. Fleischer, P. B. Price e R. M. Walker, da General Eletric (EUA) descobriram:

- a possibilidade de se revelar quimicamente os traços decorrentes dos danos de radiação, produzidos por partículas carregadas ao longo de seus percursos nos sólidos; é importante mencionar que a revelação química permitiu a observação dos traços através de microscópios óticos comuns, evitando-se o uso de microscópios eletrônicos, que são menos apropriados para esta tarefa, embora as primeiras observações de traços em minerais tenham sido feitas no microscópio eletrônico e;

- a existência dentro de alguns minerais e vidros naturais de traços que poderiam ser classificados como traços fósseis, porque tinham sido produzidos durante a história geológica do mineral.

Com base nestes trabalhos, foram observadas as maiores expansões na sua aplicação em estudos geológicos. Tal fato deve-se a um maior entendimento da dependência da ferramenta na chamada temperatura de *annealing* e informações sobre sua cinética. A datação por traços de fissão tem sido aplicada na tentativa de maior explicação de uma grande variedade de problemas geológicos, tais como: proveniência sedimentar, modelagem de histórias térmicas de bacias sedimentares, evolução crustal de cinturões orogênicos e episódios de denudação/exumação nos continentes (Franco, 2006).

Comparado com outras técnicas de datação baseadas em radioisótopos naturais, o MTF é diferente porque ele não se baseia na medição da abundância isotópica por espectrometria de massas, mas sim, na contagem individual de traços de fissão (Wagner and Van der Haute, 1992). Essa contagem, que permite determinar a densidade superficial de traços de fissão, é feita em um microscópio ótico após um ataque químico (característico de cada mineral) que aumenta o diâmetro dos traços de fissão que se estendem até a superfície do mineral, tornando-os oticamente visíveis.

Além das aplicações supracitadas, o MTF é, atualmente, a técnica mais utilizada na reconstrução da história térmica de rochas em tempos geológicos, permitindo obter a idade de minerais cristalinos e amorfos, tais como obsidianas, apatita, zircão, epídoto, dentre outros (Green et al., 1986; Crowley et al., 1991; Carlson et al., 1999; Osório et al., 2003; Barbarand et al., 2003; Ravenhurst et al., 2003; Tello et al., 2005, Curvo et al., 2005; Tello et al., 2006; Dias et al., 2009; Dias et al., 2010), que em geral contêm algumas partes por milhão (ppm) de urânio.

A partir da fissão espontânea do isótopo ^{238}U ou da fissão induzida por nêutrons térmicos do isótopo ^{235}U, dois fragmentos de fissão são emitidos em sentidos contrários com energias totais (fragmentos leves + fragmentos pesados) de aproximadamente 200 MeV. A grande massa, carga e energia dos fragmentos de fissão alteram a estrutura cristalina do zircão deixando um traço latente (uma zona de rede desarranjada onde átomos e moléculas foram deslocados pela passagem dos fragmentos).

A figura 01 apresenta o modelo *"íon explosion spike"* de Fleischer et al (1965h) modificado, que explica como ocorre o processo de formação do traço latente, onde (A) ocorre a ionização dos átomos da rede cristalina devido à fissão nuclear e, (B) por repulsão Coulombiana, ocorre um afastamento desses átomos. Em seguida há uma (C) relaxação da rede cristalina que resulta na formação do traço latente com aproximadamente 16 μm de comprimento no caso da apatita e 11 μm no zircão. O diâmetro em ambos minerais é da ordem de alguns angstrons. Em relação á estes, Wagner and Van der Haute (1992) afirmam que: *i)* Os átomos fissionados são distribuídos homogeneamente no volume do detector; *ii)* Todos os traços possuem comprimento *l* igual e o início da fissão é o centro de cada traço; *iii)* Os traços são isotropicamente distribuídos, sem nenhuma orientação preferencial, cuja probabilidade de formação no detector é a mesma em todas as direções.
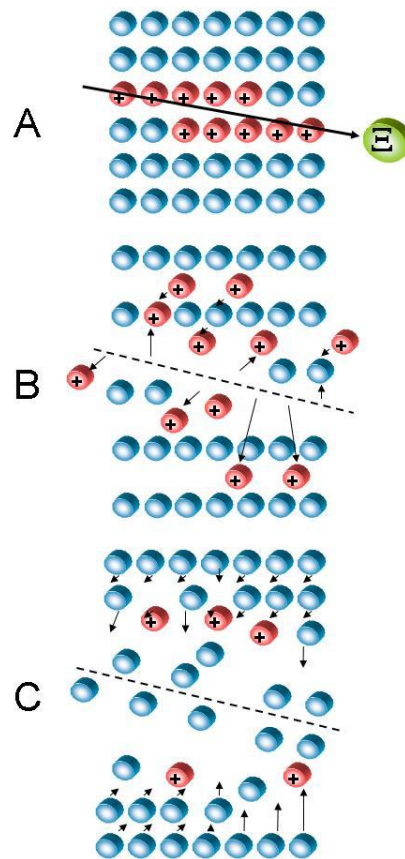
Figura 1. Formação do traço latente (modificado de Wagner and Van der Haute, 1992)

Os traços latentes são continuamente produzidos no mineral durante sua história geológica e podem ser observados ao microscópio óptico após um ataque químico conveniente. Devido sua largura inicial estar na ordem de angstrom, sua observação direta só é possível através de um microscópio de transmissão eletrônica (TEM) (Wagner and Van der Haute. 1992). Comumente, no MTF os minerais são submetidos a um tratamento químico (*etching*), cuja técnica consiste em imergir o mineral em uma solução. A reação que ocorre é uma corrosão da superfície do mineral, sendo que esta corrosão é preferencial ao longo dos traços. Somente os traços que cruzam a secção de polimento do mineral serão atacados, ou aqueles que estão totalmente contidos no interior do mineral e são cortados por outro traço ou por uma fratura que permitam o acesso da solução ao traço (figura 2). Os traços que não interceptam a seção de polimento do mineral são chamados de traços confinados. Os traços confinados que estão paralelos a seção de polimento são avaliados em seu comprimento para fim de estudos de *annealing,* como será discutido mais adiante. É necessário que esta reação seja cuidadosamente controlada através do monitoramento, da concentração e temperatura da solução

utilizada, monitorando-se inclusive o tempo de imersão. O ataque químico padrão utilizado no zircão é NaOH:KOH a 225 ± 2 ^{o}C em tempos que podem variar de 4 à 72 horas (Garver, 2003).
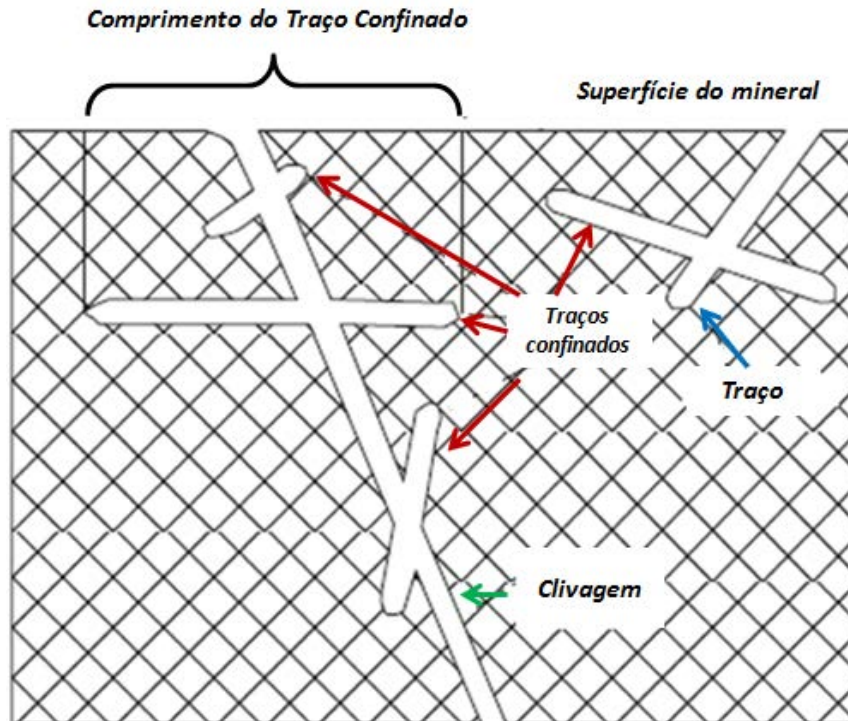
Figura 2. Disposição dos traços durante o ataque químico (*etching*). Os traços que cortam a superfície são os contados (obtenção da densidade), e os traços confinados paralelos à superfície, são medidos para utilização na reconstrução da história térmica do mineral e estudos de *annealing* (modificado de Godoy, 2006).

Um ponto que tem que ser destacado é que a velocidade do ataque químico é diferente no interior do traço e na superfície do mineral, influenciando em sua eficiência. Para maiores detalhes sobre eficiência do ataque químico veja Wagner and Van der Haute (1992).

Os procedimentos metodológicos foram desenvolvidos por vários pesquisadores (Fleischer et al., 1975; Naeser et al., 1979b; Gleadow, 1981; Hurford and Green, 1981; Storzer and Wagner, 1969). A principal diferença existente entre tais procedimentos está na análise dos traços induzidos. Se os traços induzidos e espontâneos forem obtidos a partir do mesmo grão,mas com a utilização de um detector externo (mica muscovita) o procedimento é denominado grão por grão (Método do Detector Externo, MDE). Se os traços induzidos e espontâneos são obtidos a partir de grãos diferentes tem-se um procedimento por população de grãos (Curvo, 2002).

O MDE, desenvolvido por Hurford and Carter (1991), é o mais utilizado dentro da comunidade científica de MTF. Para a datação utilizando o Método do Detector Externo (MDE), os grãos de zircão e apatita são escolhidos e montados de forma ordenada (matriz) com aproximadamente 100 grãos. Os traços de fissão espontânea são revelados através de ataque químico conveniente e analisados em microscópio óptico. Posteriormente a mesma amostra é acoplada a uma mica muscovita (que faz o papel de detector externo) para ser irradiada com nêutrons térmicos. Os traços induzidos do ^{235}U que se estenderem até a superfície do mineral, serão detectados pela mica muscovita, deixando na mesma uma imagem especular dos grãos contidos na montagem. Após um ataque químico feito com HF (ácido fluorídrico) ao 48% a 15 ºC durante 90 minutos pode ser feita a análise dos traços de fissão induzida revelados na mica muscovita. Tal método é bastante apropriado para amostras retiradas de bacias sedimentares ou locais onde se podem ter grãos de diferentes populações, mesmo que estes grãos tenham sido retirados de uma mesma rocha anfitriã. Nos dois casos, a quantidade de urânio pode variar de grão para grão. Como cada grão é datado separadamente, a quantidade de traços observados na mica pode trazer informações sobre a diferença no conteúdo de ^{235}U existentes em cada um grãos (Dias, 2008).

O MTF em zircão, especificamente, pode ser aplicado para determinar a idade e os eventos térmicos em regiões de interesse geológico. Uma vez que a temperatura de fechamento zircão é a ~240 °C, o que corresponde a temperatura em que os traços são retidos (no mineral) em tempos geológicos, é possível determinar as idades próximas as idades de cristalização de alguns minerais (Tagami, 2005). Este método pode também ser utilizado na investigação da prospecção de petróleo em profundidades onde o mineral apatita (com temperatura de fechamento em ~ 120 °C) sofreu *annealing* total, pois o zircão ainda pode dar informação da evolução térmica da bacia onde a perfuração é feita (Yamada et al., 1998, 2003). Por essas e outras razões o MTF tornou-se uma das técnicas mais úteis utilizadas por toda a comunidade geológica para reconstruir a história térmica de baixa/intermediária temperatura das rochas.

Ademais, o zircão tornou-se um dos mais importantes para o estudo de proveniência de sedimentos e da história exumação de cinturões orogênicos. Dentre as razões para isto está o fato do zircão ser comum em muitas rochas ígneas, metamórficas e sedimentares; resistente ao desgaste e à abrasão, e pode ser

datado com vários métodos isotópicos com razoáveis concentrações de urânio e tório (Bernet and Garver, 2005; Tagami, 2005).

A capacidade do zircão para reter informações sobre a história térmica mais recente de uma área fonte é de valor inestimável para elucidar os processos geológicos decorrentes de uma variedade de configurações geodinâmicas. Em consequência, MTF em zircão tem sido extensivamente utilizada, juntamente com outros métodos de datação radiométricos, tais como U-Pb (por exemplo, em Davis et al., 2003; Chemale et al., 2012; Barredo et al., 2012) e U-Th/He (Reiners, 2005), para compreender a termocronologia de rochas em uma variedade de ambientes geológicos: isto é, a análise da história térmica de rochas do embasamento orogênicos, termocronologia usando grãos detríticos em rochas sedimentares para análise de proveniência e análise da história térmica em, ou, perto de falhas (Carter, 1999; Garver et al., 1999;. DeCelles et al., 2000;. Hasebe and Tagami, 2001; Spikings et al., 2001;. Yamada et al., 2003;. Hasebe and Watanabe, 2004; Garver, 2003; Dias et al., 2010, 2011).

Equação da idade

A primeira instância, o MTF obedece aos mesmos princípios dos outros métodos geocronológicos, baseados no decaimento natural de átomos-pai instáveis para átomos-filho estáveis. Por assim dizer, o método fundamenta-se na equação diferencial que rege o decaimento radioativo, cuja integração permite que se descreva a acumulação de traços fósseis. Esta equação requer a medida direta da quantidade de urânio presente no mineral e dos átomos-filho de ^{238}U. Este último equivale ao número de decaimentos por fissão espontânea ocorridos e, consequentemente, ao número de traços espontâneos por unidade de volume do mineral. No MTF, estes parâmetros são obtidos indiretamente através da medida da densidade de traços de fissão. Dentro da comunidade cientifica de MTF a idade por Traços de Fissão pode ser obtida utilizando-se dois tipos de calibração: calibração Zeta e Absoluta. A calibração Zeta utiliza-se de idades-padrões (idades bem documentadas por outros métodos geocronológicos, tais como Ar/Ar, Rb/Sr, K/Ar); maiores detalhes podem ser encontrados em Green (1985), Wagner and Van der Haute (1992) e Hurford (1990, 1998). Nesta tese discorreremos sobre a calibração Absoluta.

A contagem dos traços, para obter as densidades fóssil e induzida, é realizada em uma área específica denominada campo que é escolhida aleatoriamente na parte central de cada grão.

Os erros das medidas das densidades são desvios padrões de médias de distribuições poissonianas enquanto que os erros das medidas de comprimentos correspondem a desvios padrões de médias de distribuições gaussianas. As medições de densidade foram feitas ao microscópio óptico com um aumento nominal de 10X150 à seco.

Os dados utilizados na equação da idade são obtidos após a análise ao microscópio dos traços de fissão espontânea, obtendo-se a densidade, ρ_S, e a densidade dos traços de fissão induzida, ρ_I. A densidade, ρ_S, está relacionada com o número de átomos de urânio, ^{238}U e outros parâmetros através da equação 1:

$$\rho_S = \varepsilon^{238}.N_U.C_{238}.\frac{\lambda_F}{\lambda}.[\exp(\lambda.T)-1] \qquad (1)$$

Onde ε^{238} é um fator de detecção, que representa a razão entre o número de traços de fissão do ^{238}U, observados por unidade de superfície e o número de fissões espontâneas ocorridas no mineral, por unidade de volume; N_U é o número de átomos de urânio por unidade de volume, presente no mineral; C_{238} é a concentração isotópica do ^{238}U no urânio natural; λ_F é a constante de decaimento por fissão espontânea do ^{238}U; e λ é a constante de decaimento alfa do ^{238}U.Para evitar a medida direta de urânio presente na amostra, ela é irradiada com nêutrons térmicos, os quais vão induzir a fissão do isótopo de ^{235}U. Este procedimento é respaldado pela invariabilidade da razão isotópica de ^{238}U e ^{235}U em amostras naturais, ou seja, $C_{238}/C_{235} = \eta$ (ver, por exemplo, Iunes, 1990).

A idade dos grãos de zircão foram obtidas utilizando a equação 2 e levando em consideração as demais equações explicitadas em 3, 4 e 5. Esta equação foi amplamente estudada pelo Grupo de Cronologia do IFGW/UNICAMP onde se inseriu o fator R_M ao considerar a calibração absoluta (Iunes, 1990, 1999; Iunes et al., 2002a; Iunes et al., 2002b; Iunes et al., 2004; Iunes et al., 2005) e se determinou o valor do λ_F obtido por diferentes métodos radiométricos (Hadler et al., 1981; Hadler, 1982; Guedes et al., 2000; Guedes et al., 2001; Guedes et al., 2003a; Guedes et al., 2003b; Hadler et al., 2003).

$$T = \frac{1}{\lambda} \ln \left[1 + \frac{g\,(\rho_S/\rho_I)}{(\varepsilon^{238}/\varepsilon^{235})} \left(\frac{\lambda}{\lambda_F} \right) \left(\frac{R_M}{C_{238}} \right) \right] \qquad (1)$$

$$\rho_I = \varepsilon^{235}.N_U.R_M \qquad (3)$$

$$R_M = R_U + \left(\frac{N_{Th}}{N_U} \right).R_{Th} \qquad (4)$$

$$R_U = \frac{\rho_U^V}{N_U^V \varepsilon^V} \qquad (5)$$

Onde **λ** é a constante de decaimento alfa do ^{238}U cujo valor é 1,55125 X 10^{-10} a^{-1} (Iunes et al., 2002a); **λF** é a constante de decaimento por fissão espontânea do ^{238}U cujo valor é (8,35 ± 0,24) X 10^{-17} a^{-1} (Guedes et al., 2000); **ε^{238}** (**ε^{235}**) é a razão entre o número de traços de fissão do ^{238}U (^{235}U) observados por unidade de superfície e o número de fissões espontâneas (induzidas) ocorridas no mineral por unidade de volume; **ρS** (**ρI**) é a densidade superficial de traços de fissão espontânea (induzida) de cada grão da amostra; **C$_{238}$** é a concentração isotópica do ^{238}U no urânio natural cujo valor é 0,99275 (Lederer and Shirley, 1978); **RM** é um parâmetro relacionado com a dosimetria de nêutrons ao qual a amostra foi submetida e é determinado utilizando a calibração absoluta como explicado em Iunes et al., (2002a); ρ^V_U é a densidade de traços induzidos na mica acoplada aos vidros dopados com urânio; N^V_Uε^V é um fator de calibração obtido usando filmes de urânio e tório natural (Iunes et al., 2002a); **N$_{Th}$/N$_U$** é a razão tório-urânio do mineral (Iunes et al., 2002a; Iunes et al., 2002b) e **g** é um fator de geometria relacionado ao detector externo e vale 0.684 (Iwano and Danhara, 1998).

A calibração absoluta é um procedimento adotado para determinar, de forma direta, a fração de átomos de ^{235}U que efetivamente fissionaram no mineral em decorrência da irradiação com um fluxo de nêutrons térmicos. Neste caso, exclui-se a necessidade de utilizar uma amostra padrão que tenha sido datada através de outros métodos radiométricos, como por exemplo, Ar/Ar, U/Pb, etc. Esta calibração é realizada através de dosímetros (vidros dopados com urânio e tório com concentrações conhecidas) acoplados a micas e intercalados com as amostras a

serem analisadas. Posteriormente, as micas acopladas aos dosímetros são analisadas sob um microscópio ótico a fim de determinar a densidade superficial de traços de fissão.

As medidas de λ_F foram feitas considerando os principais erros sistemáticos identificados na literatura através de dois experimentos: usando filmes finos de urânio natural como dosímetros de nêutrons e filmes infinitos dopados com ^{242}Pu como fontes de fragmentos de fissão, utilizados com o intuito de calibrar o detector usado na coleta de fragmentos de fissão espontânea do ^{238}U. Na literatura este parâmetro foi medido mais de 50 vezes sem que se chegasse a um valor comum (Hadler et al., 1981; Hadler, 1982; Guedes, 2001).

Annealing no MTF

As causas geológicas capazes de influenciar a estabilidade dos traços de fissão latentes nos minerais têm como candidatos: tempo, temperatura, pressão, soluções intergranulares e radiações ionizantes (Fleischer et al., 1965h; Ahrens et al., 1970; Gleadow, 1978; Tagami et al., 1990). Destes, a temperatura é o mais importante para os minerais utilizados comumente em aplicações geológicas (Gallagher et al., 1998).

O fenômeno conhecido como *annealing* é capaz de reordenar a estrutura do sólido que foi desordenada pela passagem de um fragmento de fissão (Fracalossi, 2007), isto é, os átomos que foram deslocados com a formação dos traços podem retornar ao seu local de origem quando expostos a um tratamento térmico. Este fato indica que os traços latentes são processos reversíveis. É o *annealing* dos traços de fissão é o fenômeno que qualifica o método como a única ferramenta termocronológica capaz de reconstruir eventos geológicos, a temperaturas não superiores a 120 ºC, no caso da apatita e 320 ºC, no caso do zircão (Carter and Bristow, 2000 e referências correlatas).

Quando uma amostra sofre um *annealing*, a idade obtida é menor que a idade de formação do mineral, isto acontece porque o *annealing* faz com que os traços de fissão espontânea sofram uma redução no seu comprimento e densidade, com isso haverá uma diminuição nas eficiências de observação desses traços fosseis em relação aos traços induzidos que são isentos de *annealing* (ε^{238} é menor em comparação com ε^{235}). Assim a idade obtida é uma idade aparente (idade menor que a de formação dos cristais), e podem ser corrigidas para obtenção da idade em que os traços começaram a ser gravados na amostra. O grau de *annealing* é

comumente expresso pela redução da densidade do traço ρ ou tamanho do traço l – normalizado para o valor original ρ_0 ou l_0 antes do apagamento – sobre várias condições de tempo e temperatura (Wagner and Van der Haute, 1992).

Portanto, o fenômeno de redução do comprimento dos traços devido ao *annealing* é de fundamental importância na datação de traço de fissão porque serve de uma base para a obtenção das histórias térmicas de regiões de interesse geológico. Como a idade termocronológica é determinada pela comparação da quantidade de traços do mineral e a temperatura afeta esta quantidade (como já comentado acima), consequentemente, a evolução da idade reflete a evolução da temperatura. O que distingue um método termocronológico de um geocronológico convencional é que os nuclídeos filhos (ou traços) são perdidos através da difusão (no caso de análises U-Th/He) ou através do *annealing*, onde os traços de fissão podem ser parcialmente ou completamente apagados (Reiners and Shuster, 2009). Considerando-se este fator no momento de aplicar as densidades de traços obtidas à equação da idade, obtemos a idade termocronológica, que, na grande maioria das vezes, é muito menor que a de formação do mineral. Portanto, a interpretação das idades termocronológicas requer conhecimento da cinética de *annealing* (ou difusão) dos traços no mineral hospedeiro (Jelinek et al., 2010). Conhecer este fenômeno é muito importante caso o interesse está em decodificar a história geológica registrada pelo mineral.

É possível se obter uma descrição quantitativa do *annealing* dos traços de fissão em função do tempo e da temperatura, através de modelos. Basicamente, são feitas duas abordagens. A primeira é utilizar uma equação empírica, mas cineticamente possível, para ajustar os dados e a segunda é propor um modelo teórico para o *annealing* dos traços e com o auxílio de um conjunto de dados experimentais fazer ajustes para se encontrar os parâmetros desconhecidos, cada qual com um significado físico. A vantagem em se utilizar uma modelagem com parâmetros com significado físico é que isso pode permitir que parâmetros relacionados com os fenômenos envolvidos no processo de *annealing* sejam determinados também de forma independente, sem o auxílio dos dados utilizados exclusivamente para o ajuste dos modelos. Com isso, em princípio, pode-se obter uma extrapolação mais confiável para tempos geológicos de milhões de anos (Palissari, 2007). Um modelo basicamente empírico foi descrito por Yamada et al., (2007) e outro com uma abordagem mais física foi descrita por Guedes et al., (2005a).

Cada mineral possui suas próprias características frente ao fenômeno de encurtamento dos traços devido à ação da temperatura (*annealing*). No caso da apatita a temperatura de *annealing* total é ~ 120 ^{o}C e no zircão é de ~ 320 ^{o}C em tempos geológicos. Ou seja, a datação destes minerais nos fornece a idade do último evento térmico que causou o apagamento total dos traços. Quando o *annealing* é parcial (o que pode acontecer mesmo à temperatura ambiente e em tempos geológicos) a idade pode ser obtida via os métodos de correção que levam em conta o quanto os traços foram apagados.

Infelizmente, a compreensão atual do processo de *annealing* ainda é limitada, principalmente no que diz respeito à cinética do fenômeno em função da temperatura, tempo e composição.

A estrutura interna de traços latentes controla o processo de *annealing* e, consequentemente, o encurtamento do comprimento do traço. No entanto, as equações empíricas não refletem a relação entre a estrutura interna dos traços e o seu comportamento no *annealing*, pois a informação estrutural de traços é perdida devido a ataque químico. A descrição quantitativa da cinética de *annealing* é fornecida pelos modelos de *annealing* (Yamada et al., 1995; Galbraith and Laslett, 1997; Tagami et al., 1998; Guedes et al., 2005a; Murakami et al., 2006;. Moreira et al., 2010). Alguns destes modelos estabelecem correlação entre os parâmetros e os fenômenos físicos (Carlson, 1990; Guedes et al, 2005a, 2005b).

No entanto, mesmo os modelos na literatura possuem ausência de observações do processo em escala atômica (Carlson, 1990; Crowley, 1991; Green et al., 1993) e estudos em escala atômica são essenciais para o desenvolvimento de modelos quantitativos que relacionem a formação do traço e o processo de *annealing* (Rabone et al., 2008; Li et al., 2011).

De acordo com Tagami e O'Sullivan (2005) o processo de *annealing* é caracterizada pelo desenvolvimento de uma morfologia irregular no limite dos traços, gerando uma segmentação do mesmo. Consequentemente, o *annealing* deve ocorrer pela difusão de átomos intersticiais como resultado da ativação térmica. Ademais, Gallagher et al. (1998) também afirmam que o *annealing* é consequência de um processo de difusão ativada termicamente e o intervalo de temperatura necessário varia de mineral para mineral (ver Wagner e Van der Haute, 1992).

Um conceito associado ao fenômeno de *annealing* é o *lag-time*. O *lag-time* de uma amostra é o tempo necessário para a amostra ser exumada, resfriar, e em seguida ser depositada numa bacia adjacente. Eventualmente, uma rocha atinge a

superfície onde é sujeita a erosão. O tempo de erosão e transporte sedimentar é geralmente considerado como geologicamente instantânea (Heller et al., 1992; Bernet et al., 2004a.), mas isso nem sempre é o caso. O *lag-time* integra o tempo entre aexumação e a deposição (Bernet and Garver, 2005).

Talvez este seja o aspecto distintivo do uso do MTF em zircão que não tenha seus traços total ou parcialmente apagados após a deposição: as idades de resfriamento registrados nos detritos sedimentares podem ser relacionados aos eventos térmicos ocorridos na área fonte. Em muitos casos, estes eventos estão diretamente relacionados com o resfriamento devido ao *uplift* e a exumação de rocha fonte. Desta forma, as idades podem estar ligadas diretamente à formação da bacia sedimentar (ver figura 3c). Neste caso, o *lag-time* é definido como a diferença entre o pico de idade e a idade de deposição (Garver and Brandon, 1994a; Garver et al., 1999) e estará relacionado também ao encerramento da fonte de sedimentos e a deposição numa bacia adjacente.

No contexto geológico de vulcanismo ativo o *lag-time* é quase zero, devido à erupção e deposição em bacias de flanco. Por outro lado, nos casos onde não há vulcanismo, o *lag-time* representa o tempo necessário para a rocha a ser exumada, erodida e, em seguida o zircão ser transportado para uma bacia adjacente, portanto, este será uma função da taxa de exumação na área fonte (Bernet and Garver, 2005).

Estudos de evolução de bacias sedimentares via MTF

O zircão desempenha um papel importante na interpretação da composição e história dos sedimentos antigos e modernos. Por ocorrer em praticamente todos os depósitos sedimentares, fornece um elo crítico na compreensão na história de origem de um depósito. Twenhofel (1941), em um trabalho pioneiro sobre as fronteiras de mineralogia e petrologia sedimentar, observou que a simples presença de um zircão detrítico seria importante para estudos de proveniência de uma bacia sedimentar. Desde então, o zircão é reconhecido como uma ferramenta poderosa na compreensão de proveniência e de sistemas de dispersão sedimentar (Fedo et al., 2005). O MTF tornou-se uma importante ferramenta para o estudo de proveniência de sedimentos e processos de exumação de cadeias de montanhas orogênicas (Bernet et al., 2004a).

A densidade de traços de fissão observáveis em zircão é dependente da história térmica refletida por uma Zona de *Annealing* Parcial (ZAP) que ocorre a

temperaturas que variam entre 180-320 ºC (em 10^6 - 10^8 anos). Essa informação é fundamental para compreender as relações temporais entre o desenvolvimento da área fonte e a sedimentação em bacias adjacentes.

A utilização de dados obtidos de zircões detríticos para o estudo da evolução das fontes, numa bacia sedimentar, é dependente do ambiente geológico e de vários fatores que devem ser considerados. Idades de zircões detríticos obtidos via MTF, por conseguinte, referem-se ao tempo de resfriamento através deste intervalo de temperatura. Para amostras vulcânicas ou ígneas, que não experimentaram apagamento dos traços após sua cristalização, a idade MTF obtida fornece a idade original da formação. No entanto, zircões derivados de um terreno metamórfico irá fornecer a idade do resfriamento pós-metamórfismo, e esta idade estará relacionada com a trajetória de resfriamento através das isotermas que definem a ZAP do zircão (Carter and Bristow, 2000).

A figura 3a (modificado de Carter e Bristow, 2000) mostra um conjunto de zircões detríticos associados às trajetórias de resfriamento. Zircões derivados de erupções vulcânicas e denudação tectônica sofrerá resfriamento geologicamente instantâneo (trajetórias A e B), enquanto zircões derivados do interior de crátons estáveis, geralmente irão experimentar algumas trajetórias de resfriamento com histórias mais prolongadas (trajetórias C e D). Sedimentos reciclados podem conter zircões derivados de uma variedade de trajetórias de resfriamento (trajetórias A, B, C e D).

Grandes lacunas temporais entre erosão, resfriamento e deposição podem introduzir grandes incertezas quanto à proveniência dos zircões (esta incerteza aumenta ainda mais quando se avalia sedimentos reciclados ou retrabalhados). Eis a razão para a utilização de duas técnicas de datação combinadas. As incertezas são bruscamente diminuídas quando usamos metodologias que estão ligadas a diferentes temperaturas de fechamento.
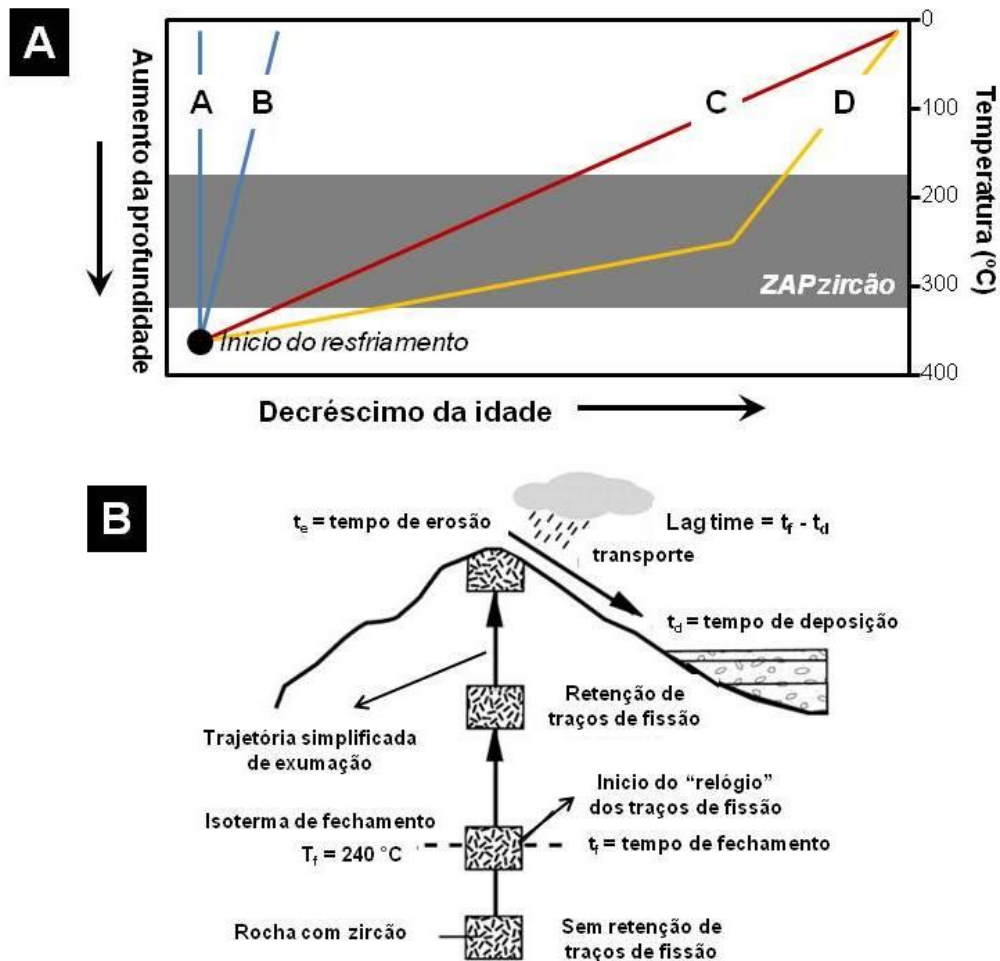
Figura 3. (A) Conjunto de zircões detríticos associadas as trajetórias de resfriamento. Para um resfriamento pós-metamórfico e/ou exumacional, a idade obtida estará relacionada com taxa na qual as amostras resfriaram através da ZAP (trajetórias A e D). No caso de sedimentos, estes podem conter proporções variáveis de qualquer um destas diferenças de idades, bem como é o caso de grãos policíclicos (modificado de Carter and Bristow, 2000). Abaixo (B) é apresentado a dinâmica simplificada associada ao *lag-time.* O tempo de transporte é considerado instantânea em tempos geológicos (modificado de Bernet and Garver, 2005).

2.2. Método U-Pb *in situ* via LA-ICP-MS

A metodologia U-Pb em zircão representa um dos métodos mais acurados para a datação radiométrica de rochas ígneas, metamórficas e sedimentares. Essa técnica de datação consiste em obter as idades de cristalização e/ou metamorfismo dos minerais, com base no decaimento radioativo do U para Pb traçando-se uma curva (Concórdia) com as razões isotópicas de $^{235}U/^{207}Pb$ e $^{238}U/^{206}Pb$. A utilização de LA-ICP-MS permite a obtenção das razões isotópicas de U e Pb por meio de análises pontuais no mineral, fundamentais para cristais com mais de uma fase de crescimento, como o zircão. Tal metodologia possibilita datações mais rápidas e sem risco de contaminação, porém com menor precisão, em relação à metodologia

tradicional de dissolução isotópica de grão a grão com TIMS (Espectrômetro de Massa com Ionização Térmica). Precisão essa é compensada por análises em um grande número de grãos, permitindo obter idades de boa confiabilidade.O método U-Pb *in situ* fornece uma excelente resolução espacial, o que permite datar cristais de zircões ou fases de cristalização ígnea ou metamórfica de zircões de forma rápida e com bom grau de acurácia e precisão (por exemplo: Compston et al., 1994; Gray and Zeitller, 1997; Jackson et al., 2004; Koesler et al., 2002; Williams, 1998).

As análises de U-Pb das amostras desta tese foram executadas no LGI-UFRGS com o equipamento MC-ICP-MS (Neptune, ThermoFinnigan) e uma microssonda a laser acoplada (UP 213, Nd:YAG, New Wave) (figura 4), cuja metodologia segue os padrões internacionais de análises de U-Pb em *zircão in situ* (Chemale et al., 2012b). A seguir, descreve-se o método de análise *in situ* em zircões com o equipamento LA-MC-ICP-MS.

Figura 4 – Ilustração do MC-ICP-MS Neptune (ThermoFinnigan) com a microssonda a laser UP213 (New Wave) acoplada, utilizados para as análises *in situ* de U-Pb em zircão no LGI-UFRGS.

A configuração mista dos coletores Faraday e multiplicadores de íons (MIC's) utilizada para as medidas simultâneas dos isótopos de Th, U, Pb e Hg é apresentada na tabela 1.

Tabela 1. Configuração dos coletores Faraday e MIC's adotada para as análises de U-Th-Pb.

MIC3	MIC4	L4	MIC6	L3	Axial	H2	H4
^{202}Hg	^{204}Hg+ ^{204}Pb	^{206}Pb	^{207}Pb	^{208}Pb		^{232}Th	^{238}U

A calibração de ganho dos coletores Faraday é realizada rotineiramente antes da realização da seção de análises, enquanto a calibração cruzada (cross calibration) envolvendo um dos Faraday de referência e os 3 MICs só é efetuada quando a sensibilidade de um deles é afetada de forma significativa, tornando necessário, por exemplo, a mudança da voltagem de operação ou mesmo uma troca. Para o fator de ganho para calibração dos copos Faraday, aplica-se um sinal constante de 33 volts. Para a calibração cruzada, ou cálculo do fator de conversão das leituras em volts (Faraday) para contagens por segundo (cps) dos MICs envolvidos, utiliza-se uma solução diluída e própria para o Neptune com concentração da ordem de 220 ppt acrescida de Th. O valor teórico para a conversão é de 62.440 cps/mV quando se usa um resistor de 10^{11} ohms nos medidores Faraday.

No ICP, os íons são muito abundantes e sofrem repulsão eletrostática em que os elementos leves são mais repelidos que os pesados, e também os elementos com massas até da ordem de 90 são menos ionizados, causando fracionamento isotópico. Deve-se acrescer ainda ao processo de fracionamento o que se verifica durante o processo de ablação no laser por envolver elementos como Pb e U com volatilidades muito distintas. Assim, as razões isotópicas são afetadas por estes processos, mas podem ser corrigidas utilizando-se um padrão internacional cujas concentrações e razões foram aferidas pelo clássico método de diluição isotópica e utilizando espectrômetros de ionização térmica (TIMS).

O presente método U-Pb utilizou o zircão GJ-1 (Simon et al., 2004), padrão internacional do GEMOC ARC National Key Center, Austrália, para as correções nas razões isotópicas. Os teores de U, Th e Pb variam consideravelmente, mas trata-se de um padrão muito homogêneo em termos de razão entre os radiogênicos e respectivos isótopos pais, da mesma forma que razões (^{207}Pb/^{206}Pb)* (onde * refere a fração radiogênica).

As análises pontuais são procedidas em grupo de 4 até 10 determinações intercalados com o padrão acima. O número de pontos ou *"spots"* varia em função

da homogeneidade dos zircões em estudo e também dos teores de U e Pb nas áreas selecionadas. O tamanho dos grãos deve ter ao menos 20 μm, pois os spots podem ser de 10, 25, 40 ou até de 60 μm. O tamanho é muitas vezes estabelecido no momento, tendo como base as intensidades dos sinais. Neste quesito o sinal correspondente ao ^{207}Pb é o determinante principal. Quando este for menor que 10.000 cps, é necessário aumentar o tamanho do spot ou a intensidade da potência do laser. A amostra padrão é montada sobre um cilindro também de epóxi e é inserido na cavidade apropriadamente feito em cada pastilha.

Os parâmetros usuais do laser aparecem na tabela 2. A aquisição de dados de forma simultânea é procedida em 50 ciclos de 1,049 segundos de integração e sem tempo de espera entre os ciclos. Com este tempo de ablação o laser chega a "escavar" cerca de 20 μm de profundidade. Para cada conjunto de medidas do padrão e amostras são adquiridos também os valores de branco nas mesmas condições analíticas. Os valores de branco são subtraídos das leituras do conjunto. O valor do ^{204}Pb é corrigido para ^{204}Hg, para estimar o chumbo comum, assumindo-se que a razão de ^{202}Hg/^{204}Hg é igual 4,355.

O método contumazmente utilizado para correção de Pb comum em zircões, baseia-se na presença do isótopo de ^{204}Pb. No caso do laser, o sinal do ^{204}Pb varia intensamente e é afetado fortemente pela presença do ^{204}Hg proveniente dos gases de Ar e He, o que resulta em uma estimativa imprecisa do Pb comum. Uma das maneiras de minimizar tais incertezas é realizar o cálculo da fração do Pb comum na amostra, de modo a utilizar as seguintes equações (Williams, 1998): $f_{206} =$ $[^{206}Pb/^{204}Pb]_c/[^{206}Pb/^{204}Pb]_s$ e $\quad f_{207} = [^{207}Pb/^{204}Pb]_c/[^{207}/^{204}]_s.$

Para as razões isotópicas do Pb comum, utiliza-se a curva de evolução proposta por Stancey e Kramers (1975) em que é requerida uma idade estimada inicial. As razões de $^{207}Pb*/^{206}Pb*$ e $^{206}Pb*/^{238}U$ (onde * refere a fração radiogênica) são corrigidas a partir das equações de f_{206} e f_{207} para ciclos individuais. Em termos gerais, os ciclos com valores de f_{206} acima de 0.0025 (i.e., 0.25% de presença de Pb comum) não são incluídos no cálculo, pois resultam em idades discordantes e não se dispõem junto a curva concórdia. Áreas esbranquiçadas (alteradas por algum processo) ou metamitizadas (escuras neste caso) e áreas cortadas por micro-fissuras preenchidas no zircão revelam quase sempre alto teor de Pb comum. Assim, é adotado nesta metodologia, evitar tais áreas para efetuação do spot valendo-se de imagens de retroespalhamento ou catodoluminescência.

As razões isotópicas necessárias para o calculo de idades convencionais ou elaboração de diagramas tipo concórdia seguem um procedimento sistemático envolvendo primeiramente correção para branco. Após as correções de branco as razões de interesse são calculadas e podem variar devido a processos de fracionamento conforme comentado anteriormente. Neste aspecto, as razões $^{206}Pb^*/^{238}U$ variam visivelmente durante os 50 ciclos de medição. As razões aumentam em razão do Pb (mais volátil) condensar progressivamente nas paredes do tubo de ablação à medida que o laser vai aprofundando.

Na maior parte dos casos o fracionamento que ocorre é linear. Como razão real da amostra utiliza-se o intercepto da melhor reta em que os 6 primeiros pontos são geralmente descartados, de acordo com a formulação proposta por Youden (1951) e também adotada por Koŝler et al., (2002). Em geral calcula-se a média aritmética dos valores, eliminando valores discrepantes (ao nível de 2SD). Nos casos em que $^{207}Pb^*/^{206}Pb^*$ e, também $^{232}Th/^{238}U$, apresentam fracionamento inverso, utiliza-se o mesmo método do fracionamento induzido por ablação a laser e aplicado para obtenção da razão $^{206}Pb/^{238}U$. A etapa seguinte envolve correções devidas a Pb comum e cálculos de razões corrigidas e respectivos erros (1SD). As idades individuais ou construção de diagramas tipo concórdia são obtidas valendo-se do Isoplot (Ludwig, 1998). O detalhamento da metodlogia U-Pb em zirção pelo método LA-IMC-ICPMS utilizado no presente trabalho pode ser encontra em Chemale Jr. et al., (2012b).

Nas análises feitas para esta tese, todas as montagens de zircão utilizados para determinação da idade via MTF (1 cm X 1 cm) foram montados em um epóxi (2,5 cm de diâmetro circular). Imagens de zircão foram obtidos usando um Microscópio Óptico (Leica MZ 125) e um Microscópio eletrônico de Varredura (Jeol JSM 5800).

Os dados isotópicos foram adquiridos com *spots* de 25 μm, no mesmo zircões e, especificamente, na mesma área do grão datada pelo MTF. Para a correção de Pb comum, assumimos que os valores obtidos a partir de ^{204}Pb zircões têm uma composição Pb comum (Stacey e Kramers, 1975), assumindo uma idade concordante de $^{206}Pb/^{238}Pb$ e $^{207}Pb/^{206}Pb$ como idade estimada. A tabela 2 mostra as condições de operação do LA e do ICP-MS na ocasião das análises. Maiores detalhes sobre o método de análise e tratamento de dados por ser encontradas em Guadagnin et al., (2010) e Chemale et al. (2012 b).

Tabela 2. Condições de operação do laser e do MC-ICP-MS

Laser type New Wave UP213:	Energia: 6 J/cm^2; Frequência: 10 Hz; *Spot* do laser: 25 μm.

MC-ICP-MS Neptune:	Potência 1200 W;
	Detecção:
	    Faradays ^{206}Pb, ^{208}Pb, ^{232}Th, ^{238}U;
	    MIC's ^{202}Hg, ^{204}Hg+^{204}Pb, ^{20}7Pb;
	Fluxo de Gás:
	    Ar resfriados (Ar) 15 l/min;
	    Ar auxiliar (Ar) 0.8 l/min;
	    Ar transporte 0.75 l/min (Ar) + 0.45 l/min (He);
	    Aquisição: 50 cycles de 1.048 s.

2.3. Metodologia combinada de MTF e U-Pb *in situ*

Uma das vantagens do zircão, frente a outros minerais, é que seus grãos podem ser datados por MTF and U-Pb, que, devido às suas diferentes sensibilidades térmicas, podem fornecer informações únicas, tanto sobre a idade e estrutura da fonte de sedimentos, bem como da evolução da própria bacia.

O pioneirismo na metodologia combinada de MTF e U-Pb *in situ* em zircões detríticos deve-se à Carter and Moss (1999) e Carter and Bristow (2000). Embora cada técnica aplicada à zircões detríticos possa fornecer um informação específica sobre a área fonte, em qualquer estudo, invariavelmente, permanecem questões pendentes que surgem das limitações de cada método.

Enquanto MTF em zircão fornece informações preferencialmente sobre eventos de baixa temperatura, o U-Pb registra a idade de cristalização ígnea ou metamórfica de zircões que é fundamental para estudos de proveniência sedimentar (áreas fonte) assim como definição de eventos geológicos de magmatismo, metamorfismo e sedimentação e eventos de acresção de crosta nos mais diversos ambientes tectônicos..

Ao adotar uma abordagem de datação combinada para o zircão, usando o MTF e U-Pb sobre as mesmas amostras e/ou grãos, é possível superar as limitações de cada metodologia e extrair uma quantidade ideal de informações de procedência que se relaciona tanto com a idade da formação (ou área) geológica de interesse e sua evolução térmica.

III. TEXTO INTEGRADOR DOS ARTIGOS

CAPITULO III

Com base ao tema desta tese, foram desenvolvidas análises em zircões da bacia sedimentar Bauru. A Bacia Bauru formou-se no Neocretáceo (70-100 Ma), no centro-sul da Plataforma Sul-americana, em evento de compensação isostática posterior ao acúmulo de quase 2000 m de lavas basálticas, ocorrido no Cretáceo Inferior (~ 140 Ma). Desenvolveu-se como bacia continental interior, pós-ruptura do continente gondwânico, acumulando uma sequência sedimentar essencialmente arenosa, hoje com espessura máxima de cerca de 300 m e área de 370.000 Km^2. A sequência tem por substrato basaltos da Formação Serra Geral. No Brasil, ocorre na parte ocidental do estado de São Paulo, no noroeste do Paraná, no leste do Mato Grosso do Sul, no Triângulo Mineiro e no sul de Goiás.

Os dados aqui apresentados estão limitados a amostras do estado de São Paulo. Estas análises culminaram em três artigos. Outros trabalhos ligados a tese em que o doutorando é coautor e/ou colaborador são apresentados na seção "anexos"., que, em parte, trazem contribuições sobre os estudos de TF em zircão e a sua própria estrutura molecular.

O **primeiro artigo** (Dias et al., 2010) é o primeiro de uma série que aplica a metodologia combinada de MTF e U-Pb *in situ* via LA-ICP-MS. Este foi o responsável por aguçar nossa curiosidade sobre a eficiência da nova metodologia. Neste trabalho são apresentadas idades de zircões extraídos de rochas sedimentares na Formação Rio Paraná (Fernandes e Coimbra, 1996), pertencente à Bacia Bauru, no estado de São Paulo, Brasil, que correspondem às rochas sedimentares da Sequência Deposicional 1 (Paulo e Silva et al., 2009). Foram datadas quatro amostras via MTF e duas via técnica combinada U-Pb e MTF. Suas interpretações forneceram as primeiras informações sobre as áreas fonte para os sedimentos e os eventos morfotectônicos na Bacia Bauru.

Neste trabalho, as idades obtidas via MTF foram assim interpretadas: três grupos de idades aparentes foram identificados: Brasiliano (800 a 480 Ma), com o principal grupo no final do ciclo (480-500 Ma); Devoniano (350 a 420 Ma), que podem corresponder a elevação principal da Plataforma Sul-americana durante a formação da Bacia do Paraná; e o terceiro grupo com idades Permiano-Caborníferas (293-267 Ma), que está ligada com a Formação Pangea ou a orogenia Gondwanides. O método U-Pb forneceu informações sobre as possíveis áreas fontes: as idades dominantes são Brasilianas (795 a 485 Ma), sendo que fontes

subordinadas foram identificadas no Mesoproterozóico e Paleoproterozóico (Transamazônico).

A avaliação integrada do conjunto de dados permitiu-nos distinguir as diferentes áreas fontes dos sedimentos da Bacia Bauru (Brasiliano, Mesoproterozóico e Paleoproterozóico), bem como identificar zircões que foram reciclados ou passaram por processos de denudação em dois importantes eventos ocorridos na Plataforma Sul-americana: orogenias Devoniana e Gondwanides (Permiano-Carbonífero).

No *segundo artigo* (Dias et al., 2011), o método combinado foi aplicado à Formação Vale do Rio do Peixe (Fernandes e Coimbra, 1996) ou base da Sequência Deposicional 3 (Paulo e Silva et al., 2009), também na Bacia Bauru. Neste trabalho nove amostras foram datadas via MTF e três via técnica combinada U-Pb e MTF. Mais uma vez, a técnica combinada mostrou-se muito importante para revelar a área fonte das rochas, bem como, os eventos morfotectônicos ocorridos durante o processo evolutivo da Plataforma Sul-americana.

A metodologia U-Pb forneceu informações consistentes de que os zircões da bacia são dominantemente Brasilianos e Rhyacionos, com fontes subordinadas do Neo até Mesoproterozóico. A principal fonte desta formação originada de sedimentos da Bacia do Paraná contêm zircões retrabalhados do Paleoproterozóico ao Eopaleozóico. Os zircões Neoproterozóicos inferior podem ter sido transportados do Maciço Goiás, região à oeste da Bacia Bauru e que contêm em si o cinturão orogênico Mara Rosa, que se formou nesta época.

Os dados obtidos via MTF puderam ser agrupados em quatro grupos de idades distintos: o Neoproterozóico inferior, Brasiliano, Ordoviciano-Siluriano e Carbonífero-Triássico inferior. Os processos de exumação do Neoproterozóico e Brasiliano inferior estão relacionados com *inliers* situados a oeste da Bacia Bauru (Maciço Goiás Central). As idades do Paleozóico aqui analisados são agrupados nas duas principais formações montanhosas à oeste da Plataforma Sul-americana: orogenias Famatiniana e Gondwanide. Especificamente, a orogenia Gondwanide é bem representada por idades aparentes de 370 à 250 Ma e indicam a passagem de zircão pela zona de *annealing* parcial (ZAP) durante este ciclo.

Um *terceiro artigo* visou apresentar novos dados sobre a datação combinada aplicada à Bacia Bauru. Neste artigo são divulgados os resultados da datação em vinte e nove amostras (29 datadas via MTF e 10 via U-Pb). Três formações foram avaliadas: Formação Caiuá (Sequência Deposicional 1), Formação

Santo Anastácio (Sequência Deposicional 2) e Formação Adamantina (Sequência Deposicional 3), Membros Vale do Rio do Peixe e Presidente Prudente (Paula e Silva et al., 2009). O conjunto mais abrangente de dados foi elementar para concluir de forma muito mais precisa e substancial as interpretações preliminares obtidas nos primeiros trabalhos. Trata-se de um artigo muito mais contextualizado do que os anteriores, e com as interpretações e argumentações bem mais fundamentadas..

As análises de U-Pb em zircões detríticos *in situ* permitiu distinguir os principais eventos acrecionais ocorridos durante o Pré-Cambriano na Plataforma Sul-americana, são eles: Arqueano (Ciclo Jequié em 3,0-2,7 Ga), Rhyaciano (Ciclo Transamazônico em 2,2-1,90 Ga), Statheriano (1,80-1,68 Ga), Sunsas (1,2-0,90 Ga) e Toniano (Brasiliano precoce, 0,9-075 Ga), e finalmente, Neoproterozóico superior (Brasiliano, 0.65-0,50 Ga).

As idades aparentes obtidas via MTF, permitiram complementar a análise da proveniência dos unidades sedimentares da Bacia Bauru, bem como estabelecer os principais períodos de da acresção crustal ocorridos na Plataforma Sul-americana do Neoproterozóico ao Mesozóico. As idades Tonianas e Criogeniana-Ediacaranas sugerem que estes zircões passaram pela ZAP durante o processo de exumação do Ciclo orogênico Brasiliano precoce e principal. No entanto, duas grandes concentrações de idades entre 500-360 Ma e 345-230 Ma também são reconhecidas, o que pode estar acompanhando os dois principais ciclos orogênicos paleozóicos na fronteira ocidental da Plataforma Sul-americana, o Famatiniano e Gondwanides, no Cretáceo Superior da Bacia Bauru. Desta forma, as informações sobre o fluxo sedimentar através da paleocorrentes durante a deposição da bacia de Bauru, as potenciais áreas fontes e datação combinada via U-Pb e MTF em zircão foram fundamentais para distinguir as áreas fontes principais, bem como, os principais eventos tectônicos na a Plataforma Sul-americana a partir de zircões extraídos de rochas sedimentares intracratônicas. A aplicação deste tipo de metodologia ou mesmo com combinação de outras técnicas (ex.: U-Th/He) em bacias intraplacas (incluindo as bacias intracratônicas) é tão importante como os estudos aplicados em margens ativas para definir ciclos de acresção crustais e formação de supercontinentes.

IV. REFERÊNCIAS

Ahrens, T. J.; Fleischer, R. L.; Price, P. B.; Woods, R. T.; 1970. Erasure of fission tracks in glasses and silicates by shock waves. Earth Planet. Sci. Lett., 8, 420-426.

Allen, P. A. and Armitage, J.J. 2012 Cratonic Basins. In: Busby, C. and Azor, A. (eds) 2012.Tectonics of sedimentary basins: Recent advances. Wilery-Blackwell, 602-620.

Barbarand, J.; Carter, A.; Wood, I.; Hurford, T.; 2003. Compositional and structural control of fission-track annealing in apatite. Chem. Geol. (Isot. Geosci. Sect.) 198, 107-138.

Bernet, M.; and Garver, J. I.; 2005. Fission-track Analysis of Detrital Zircon. Reviews in Mineral. and Geoch., 58 (1), 205-237.

Bernet, M.; Brandon, M. T.; Garver, J. I.; Molito, B. R., 2004a. Downstream changes of Alpine zircon fission-track ages in the Rhône and Rhine rivers, J. Sed Res., 74, 82-94.

Bernet, M.; Zattin, M.; Garver, J.I.; Brandon, M. T.; Vance, J.A., 2001. Steady-state exhumation of the European Alps. Geology 29, 35-38.

Carlson, W. D.; Donelick, R. A.; Ketcham, R. A.; 1999. Variability of apatite fission-track annealing kinetics I: Experimental results. Am. Mineral. 84, 1213-1223.

Carlson, W. D.; 1990. Mechanisms and kinetics of apatite fission-track annealing. Amer. Mineral. 75, 1120-1139.

Carter, A. and Bristow, C. S.; 2000. Detrital zircon geochronology: enhancing the quality of sedimentary source information through improved methodology and combined U-Pb and fission-track techniques. Basin Research, 12, 47-57.

Carter, A., 1999. Present status and future avenues of source region discrimination and characterization using fission track analysis. Sedimentary Geology, 124, 31-45.

Carter, A. and Moss, S. J.; 1999. Combined detrital-zircon fission-track and U-Pb dating: A new approach to understanding hinterland evolution. Geology, 27 (3), 235-238

Chemale Jr., F., Dussin, I. A., Alkmim, F. F., Martis, M. S., Queiroga, G., Armstrong, R., Santos, M. N. 2012a. Unravelling a Proterozoic basin history through detrital zircon geochronology: The case of the Espinhaço Supergroup, Minas Gerais, Brazil. Gondwana Research (*in press*).

Chemale Jr., F.; Kawashita, K.; Dussin, I. A.; Ávila, J. N.; Justino, D.; Bertotti, A. L.; 2012b. U-Pb zircon dating with MC-ICP-MS using mixed detector configuration. An. Acad. Bras. Ciências, 84(2), 43-63 (*in press*).

Compston,W., Williams, I.S., Meyer, C., 1984. U–Pb geochronology of zircons from lunar breccia 73217 using a sensitive high-resolution ion-microprobe. J. Geophys. Res. B 98, 525–534.

Crowley, K. D.; Cameron, M.; Shaefer, R. L.; 1991. Experimental studies of annealing of etched fission tracks in fluor apatite. Geoch. Cosmoch., 55, 1449-1465.

Curvo, E. A. C.; J.C. Hadler; P.J. Iunes; S. Guedes; C. A. Tello; S. R. Paulo; P.C. Hackspacher; R. Palissari; P. A. F. P. Moreira; 2005. On epidote fission track dating, Radiation Measurements, 39, 641 – 645.

Curvo, E. A. C., 2002. **Estudo da datação por traços de fissão em epídoto**. Dissertação de Mestrado, UNICAMP, Campinas, SP, 50p..

Davis, D. W.; Williams, I. S.; Krogh, T.E.; 2003. Historical development of zircon geochronology. Reviews in Mineralogy & Geochemistry, 53, 145-181.

DeCelles, P. G.; Gehrels, G. E.; Quade, J.; LaReau, B.; Spurlin, M.; 2000. Tectonic Implications of U-Pb zircon ages of the Himalayan Orogenic Belt in Nepal. Science, 288, 497.

Dias, A. N. C.; Tello, C. A. S.; Chemale Jr., F.; Godoy, M. C. T. F.; Guadagnin, F.; Iunes, P. J.; Soares, C. J.; Osório, A. M. A.; Bruckmann, M. P.; 2011. Fission track and U-Pb in situ dating applied to detrital zircon from the Vale do Rio do Peixe Formation, Bauru Group, Brazil. Journal of South American Earth Sciences, 31, 298-305.

Dias, A. N. C.; Tello, C. A.; Chemale Jr.; F., Iunes, P. J.; Soares, C. J.; Curvo, E. A.; Guedes, S.; Barra, B. C.; Constâncio Jr.; M. and Hadler, J.C.; 2010. Zircon fission track and U-Th-Pb in situ dating of Rio Paraná Formation, Parana Basin, Brazil. Revista Mexicana de Fisica, 56 (1), 16-21.

Dias, A. N. C.; Tello S., C. A.; Constantino, C. J. L.; Soares, C. J.; Osório, A. M.; Novaes, F. P.; 2009. Micro-Raman spectroscopy and SEM/EDX applied to improve the zircon Fission Track Method used for dating geological formations. Journal of Raman Spectroscopy 40, 101-106.

Dias, A. N. C. **Método de traços de fissão em zircão: estudos geocronológicos no Grupo Bauru**. 2008. Dissertação (Mestrado em Ciências e Tecnologia de Materiais) – Unesp, Presidente Prudente, 2008, 78pp..

Fedo, C. M.; Sircombe, K. N.; Rainbird, R. H.; 2003. Detrital zircon analysis of sedimentary record. Reviews in Mineralogy & Geochemistry, 53, 277-303.

Fernandes, L.A., Coimbra, A.M., 1996. A Bacia Bauru (Cretáceo Superior, Brasil). Anais da Academia Brasileira de Ciências, 68 (2), 195–205.

Fleischer, R. L.; Price, P. B.; Walker, R. M. Nuclear tracks in solids: Principles and Applications. University of California Press, Berkeley, 1975.

Fleischer, R.L.; Price, P.B.; Walker, R. M.; 1965h. The ion explosion spike mechanism for formation of charger particles tracks in solids. Journal Appl. Phys.,36, 3645-3652.

Fleischer, R. L.; Price, P. B.; 1963a. Charged particle tracks in glass. J. Appl. Phys., 34,903−2904.

Fracalossi, C. P.; 2007. **Uso da termocronologia por traços de fissão em apatita no reconhecimento de áreas de recarga e análises isotópicas de $^{234}U/^{238}U$ em águas subterrâneas do Aquífero Itararé no município de Americana (SP)**, Dissertação de Mestrado, UNESP, Rio Claro, SP, 94p..

Franco, A. O. B., 2006. **Termocronologia por Traços de Fissão em apatitas na região do Arco de Ponta Grossa, entre os alinhamentos de Guapiara e São Jerônimo-Curiúva.** Tese de Doutorado, Unesp, Rio Claro-SP, 141p..

Galbraith, R. F.; Laslett, G. M.; 1997. Statistical modelling of thermal annealing of fission tracks in zircon. Chemical Geology, 140, 123-135.

Gallagher, K.; Brown, R.; Johnson, C.; 1998. Fission Track Analysis and its applications to geological problems. Annual Review Earth Planet. Science, 26, 519-572.

Garver, J. I., 2003. Etching zircon age standards for fission-track analysis. Radiation Measurements, 37, 47-53.

Garver, J.I.; Brandon, M.T.; Roden-Tice, M.K.; Kamp, P.J.J.; 1999. Exhumation history of orogenic highlands determined by detrital fission track thermochronology. In:Exhumation processes: Normal faulting, ductile flow, and erosion. Ring U, Brandon MT, Willett SD, Lister GS (eds) Geol. Soc. London Spec. Pub., 154, 283–304.

Garver, J. and Brandon, M.; 1994. Fission-track ages of detrital zircons from Cretaceous strata, southern British Columbia: Implications for the Baja BC hypothesis. Tectonics, 13 (2), 401-420.

Gleadow, A. J. W.; Duddy, I. R.; 1981. A natural long−term track annealing experiment for apatite. Nucl. Tracks. 5. pg. 169−174.

Gleadow, A. J. W., 1978. Comparison of Fission-track dating methods: effects of anisotropic etching and accumulated alpha-damage. In: R.E. Zartman (Ed.), Short Papers of the Fourth International Conference on Geochronology, Cosmochronology

and Isotope Geology, Snowmass Colorado,August 1978, US. Geological Survey, Open File Report 78-701.

Godoy, D. F., 2006. **Termotectônica por traços de fissão em apatitas dos altos estruturais de Pitanga, Pau d'Alho e Jiboia - Centro do estado de São Paulo.** Tese de Doutorado, Unesp, Rio Claro-SP, 141p..

Gray, M. B., and Zeitler, P. K.; 1997. Comparison of clastic wedge provenance in the Appalachian foreland using U/Pb ages of detrital zircons: Tectonics, 16, 151-160.

Green, P. F.; Laslett, G. M.; Duddy, I.R.; 1993. Mechanisms and kinetics of apatite fission track annealing - discussion. Am. Mineralog., 78, 441-445.

Green, P. F.; Duddy, I. R.; Gleadow, A. J. W.; Tingate, P. R. and Laslet, G. M.; 1986.Thermal annealing of fission tracks in apatite, 1. A qualitative description. Chem. Geol. (Isot. Geosci. Sect.), 59, 237-253.

Green, P. F., 1985. Comparation of Zeta Calibration baselines for Fission Track Dating of apatite, zircon and sphene. Chemical Geology, 58, 1-22.

Guadagnin, F.; Chemale Jr., F.; Dussin, I. A.; Jelinek, A. R.; Santos, M. N.; Borba, M. L.; Justino, D.; Bertotti, A. L.; Alessandretti, L.; 2010. Depositional age and provenance of the Itajaí Basin, Santa Catarina State, Brazil: Implications for SW Gondwana correlation. Precambrian Research, 180, 156-182.

Guedes, S., Iunes P. J.; Neto J. C. H.; Bigazzi G.; Tello C. A. S.; Alencar I.; Palissari R.; Curvo E. A.; Moreira P.; 2005b. Kinetic model for the relationship between mean diameter shortening and age reduction in glass samples. Radiat. Meas., 39, 647-652.

Guedes, S.; Hadler, J. C.; Iunes, P. J.; Oliveira, K. M. G.; Moreira, P. A. F. P.; Tello, C. A. S.; 2005a. Kinetic model for the annealing of fission tracks in zircon. Radiat. Meas., 40, 517-521.

Guedes, S.; Hadler, J. C.; Iunes, P. J.; Zuñiga, G.; Tello, C. A. S.; and Paulo, S. R.; 2003a. The use of the U(n,f) reaction dosimetry in the determination of the λ_f value

through fission-track techniques. Nuclear Instruments and Methods in Physics Reseach A, 496, 215-221.

Guedes, S.; Hadler, J. C.; Iunes, P. J.; Burke, A. K.; Kakazu, M. H.; Sarkis, J. E. S.; Paulo, S. R.; Tello S., C. A. 2001. Determination of the ^{238}U spontaneous fission decay constant without neutron irradiation. Journal of Radioanalytical and Nuclear Chemistry, 253 (1), 73-76.

Guedes, S.; 2001. **Duas novas determinações da constante de decaimento por fissão espontânea do ^{238}U, λ_F, utilizando-se técnicas de traços de fissão**. Tese de Doutorado , UNICAMP, Campinas – SP, 132 p.

Guedes, S.; Hadler N., J.C.; Iunes, P. J., Paulo, S. R.; Zuñiga, A.; 2000. The spontaneous fission decay constant of 238U using SSNTD. Journal of Radioanalytical and Nuclear Chemistry, 245 (2), 441-442.

Hadler, J.C.; Bigazzi, G.; Guedes, S.; Iunes, P. J.; Oddone, M.; Tello, C. A.; Paulo, S. R.; 2003. Spontaneous ^{238}U fission half-life measurements based on fission-track techniques. Journal of Radioanalytical and Nuclear Chemistry, 256 (1),155-157.

Hadler, J. C.; 1982. **Medida da constante de desintegração do ^{238}U por fissão espontânea**. Tese (Doutorado em Ciências) – UNICAMP, Campinas−SP.

Hadler, J.C.; Lattes, C. M. G.; Marques, A.; Marques, M. D. D.; Serra, D. A. B.; Bigazzi, G.; 1981. Measurement of the spontaneous-fission disintegration constant of ^{238}U.Nuclear Tracks, 5 (1-2), 45-52.

Hasebe, N.; Watanabe, H.; 2004. Heat influx and exhumation of the Shimanto accretionary complex: Miocene fission track ages from the Kii Peninsula, southwest Japan. Island Arc., 13, 533-543.

Hasebe, N.; Tagami T.; 2001. Exhumation of an accretionary prism; results from fission track thermochronology of the Shimanto Belt, Southwest Japan. Tectonophysics, 331, 247-267.

Heller, P.L.; Tabor, R. W.; O'Neil, J. R.; Pevear, D. R.; Shafiquillah, M.; Winslow, N.S.;1992. Isotopic provenance of Paleogene sandstones from the accretionary core of the Olympic Mountains, Washington: GSA Bull 104:140-153

Hurford, A.J.; 1998. Zeta: the ultimate solution or just an interim measure? In: Van den haute, P., De Corte, F. (Eds.), Advances in Fission-Track Geochronology. Kluwer Academic Publishers, Dordrecht: 19-32.

Hurford, A. J. & Carter, A.; 1991. The role of fission track dating in discrimination of provenance. Geological Society. Special Publication, 57, 67-68.

Hurford, A. J.; 1990. Standardization of fission track dating calibration: Recommendation by the Fission Track Working Group of the I.U.G.S. Subcommission on Geochronology. Chemical Geology (Isotope Geoscience Section), 80, 171-178.

Hurford, A. J., Green, P. F., 1981. A reappraisal of neutron dosimetry and uranium-238 λ_F values in fission track dating, Nuclear Tracks, 5 (1/2), 53-61.

Iunes, P.J., G. Bigazzi, J.C. Hadler N., M.A. Laurenzi, M.L. Balestrieri, P. Norelli, A. M. Osório A., S. Guedes C.A. Tello S. and S.R. Paulo, 2005. Fission-track dating of Jankov Moldavite using U and Th thin films neutron dosimetry. Radiation Measurements, 39 (6), 665-668.

Iunes, P. J.; Hadler N., J. C.; Bigazzi, G.; Guedes, S.; Zuñiga G., A.; Paulo, S. R.; Tello S., C. A.; 2004. Uranium and thorium thin film calibrations by particle track techniques. Journal of Radioanalytical and Nuclear Chemistry, 262, 2, 461-468.

Iunes, P. J.; Bigazzi, G.; Hadler N., J.C.; Tello, S., C. A.; Guedes, S.; Paulo, S. R.; Balestrieri, M. L.; Norelli, P.; Oddone, M.; Osório, A. M.; Zuñiga, A.; 2002b. The Th/U ratio in minerals by a fission-track technique: application to some reference samples in order to estimate the influence of Th in fission-track dating. Radiation measurements,35, 195-201.

Iunes, P. J.; Hadler N., J. C.; Bigazzi, G.; Tello, S., C. A.; Guedes, S.; Paulo, S.

R.; 2002a. Durango apatite fission-track dating using length-based age corrections and neutron fluencemeasurements by thorium thin films and natural U-doped glasses calibrated through natural uranium thin films. Chemical Geology, 187, 201-211.

Iunes, P. J.; 1999. **Aplicação da dosimetria de neutrons através de filmes finos de urânio natura e tório na datação pelo método dos traços de fissão.** Tese (Doutorado em Física) – 76p. Instituto de Física Gleb Wataghin, UNICAMP, Campinas, SP

Iunes, P. J.; 1990. **Datação com o método dos traços de fissão: estudo da dosimetria de nêutrons com filmes finos de urânio natural**. 1990. 101 f. Dissertação (Mestrado em Ciências) – Instituto de Física Gleb Wataghin, UNICAMP, Campinas, SP.

Iwano, H.; Danhara, T.; 1998. A re-investigation of the geometry factors for fission-track dating of apatite, sphene and zircon. In P. Van den Haute and F. De Corte (eds.). Advances in Fission-Track Geochronology, 47-66.

Jackson,,S. E., Pearsona, N. J., Griffina, W.L., Belousova, E. A. 2004. The application of laser ablation-inductively coupled plasma-mass spectrometry to in situ U–Pb zircon geochronology. Chemical Geology, 211, 47-69.

Jelinek, A. R.; Gomes, C. H.; Dias, A. N. C.; Guadagnin, F.; Chemale Jr., F.; Souza, I. A.; 2010. Termocronologia aplicada às Geociências: Análise por Traços de Fissão. Pesquisas em Geociências , 37 (3), 191-203.

Košler J., Fonneland, H., Sylvester, P., Tubrett, M., Pedersen, R.B. 2002. U-Pb dating of detrital zircons for sediment provenance studies - a comparison of laser ablation ICPMS and SIMS technique. Chem. Geol. 182:, 605-618.

Lederer, C. M. and Shirley, V. S.; 1978. Table of Isotopes, Seventh edition. John Wiley and Sons, Inc., New York, USA. 1523pp.

Li, W.; Wang, L.; Lang, M.; Trautmann, C.; Ewing, R. C.; 2011. Thermal annealing mechanisms of latent fission tracks: Apatite vs. zircon. Earth and Planetary Science Letters, 302, 227–235.

Lindsay, J. F.; 2002. Supersequences, superbasins, supercontinents – evidence from the Neoproterozoic-Early Palaeozoic basins of central Australia. Basin Research, 14, 207-223.

Liu, T. K.; Hseih, S.; Chen, Y. G.; Chen, W. S.; 2001. Thermo-kinematic evolution of the Taiwan oblique-collision mountain belt as revealed by zircon fission track dating. Earth and Planetary Science Letters, 186, 45–56.

Ludwig, K. R.; 1998. Isoplot: A Plotting and Regression Program for Radiogenic-Isotope Data.

Maas, R.; Kinny, P. D.; Williams, I. S.; Froude, D. O.; Compston, W.; 1992. The Earth's oldest known crust: A geochronological and geochemical study of 3900-4200 Ma detrital zircons from the Mt Narryer and Jack Hills, Western Australia: Geochimica et Cosmichimica Acta, 56, 1281-1300.

Moreira, P. A. F. P.; Guedes, S.; Iunes, P. J., Hadler, J. C.; 2010. Fission track chemical etching kinetic model. Radiation Measurements, 45,157-162.

Murakami, M.; Yamada, R. and Tagami, T.; 2006. Short-term annealing characteristics of spontaneous fission tracks in zircon. Chemical Geology, 227, 214–222.

Naeser, C. W.; Gleadow, A. J. W.; Wagner, G. A.; 1979b. Standardization of fission-track data reports. Nucl. Tracks. 3. pg. 133−136.

Osório, A., A. M.; P.J. Iunes; G. Bigazzi; J.C. Hadler; M.A. Laurenzi; ; P. Norelli; C.A. Tello; S. Guedes; S.R. Paulo; 2003. Fission-track dating of Macusanite glasses with Plateau and Size Correction methods. Radiation Measurements, 36.407-412.

Palissari, R.; 2007. **Calibração de modelos de *annealing* de traços de fissão em zircão a partir de dados geológicos**. PhD. Thesis, Instituto de Física "Gleb Wataghin", UNICAMP, Campinas, SP, Brasil, 86 pp.

Paula e Silva, F. P., Kiang, C. H. and Caeteno-Hang, M. R. 2009. Sedimentation of the Cretaceous Bauru Group in São Paulo, Paraná Basin, Brazil. Journal of South American Earth Sciences 28: 25–39.

Price, P. B.; Walker, R. M.; 1963a. Fossil tracks of charged particles in mica and the age of minerals. J. Geophys. Res., 68, 4847−4862.

Price, P. B.; Walker, R. M.; 1962a. A new detector for heavy particle studies. Phys. Lett., 3, 113-115.

Rabone, J. A. L.; Carter, A.; Hurford, A. J.; Leeuw, N. H.; 2008. Modelling the formation of fission tracks in apatite minerals using molecular dynamics simulations. Phys. Chem. Miner. 35, 583-596.

Ravenhurst, C. E.; Roden-Tice, M. K.; Miller, D.S.; 2003. Thermal annealing of fission tracks in fluorapatite, chlorapatite, manganoanapatite, and Durango apatite: experimental results. Canadian Journal of Earth Ciences, 40, 995-1007.

Reiners, P.W. & Shuster, D.L. 2009. Thermochronology and Landscape Evolution. Physics Today, 31-36.

Reiners, P. W.; 2005. Zircon (U-Th)/He thermochronometry. Reviews in Mineralogy & Geochemistry, 58, 151-179.

Shaw, R.; Etheridge, M.; Lambeck, K.; 1991. Development of the Late Proterozoic to Mid-Paleozoic intracratonic Amadeus Basin in Central Australia: a key to understanding tectonic forces in plate interiors. Tectonics, 10, 688-721.

Simon, E.; Jackson, S. E.; Pearsona, N. J.; Griffina, W. L.; Belousova, E. A.; 2004. The application of laser ablation-inductively coupled plasma-mass spectrometry to in situ U-Pb zircon geochronology. Chemical Geology, 211, 47-69.

Sloss, L. L.; 1963. Sequences in the Cratonic Interior of North America. Geological Society of America Bulletin 74, 93-114.

Spikings, R. A.; Winkler, W.; Seward, D.; Handler, R.; 2001. Along-strike variations in the thermal and tectonic response of the continental Ecuadorian Andes to the collision with heterogeneous oceanic crust. Earth Planetary Science Letters, 186, 57-73.

Stacey, J. S., Kramers, J. D., 1975. Approximation of terrestrial lead isotope evolution by a two-stage model. Earth and Planetary Science Letters 26, 207–221.

Storzer, D.; Wagner, G. A.; 1969. Correction of thermally lowered fission track ages of tektites. Earh. Planet. Sci. Lett., 5, 463-468.

Tagami, T. and O'Sullivan, P. B.; 2005. Fundamentals of Fission-Track Thermochronology. Reviews in Mineralogy and Geochemistry, 58 (1), 19-47.

Tagami, T., 2005. Zircon fission-track thermochronology and applications to fault studies. Reviews In Mineralogy & Geochemistry, 58, 95-122.

Tagami, T.; Galbraith, R.F.; Yamada, R. and Laslett, G. M.; 1998. Revised annealing kinetics of fission tracks in zircon and geological implications. In: P. Van den haute and F. De Corte, Editors, Advances in Fission-Track Geochronology, Kluwer Academic Publishers, Dordrecht, The Netherlands, 99-112.

Tagami, T.; Carter, A.; Hurford, J.; 1996a. Natural long-term annealing of the zircon fission- track system in Vienna Basin deep borehole samples: Constrains upon the partial annealing zone and closure temperatures. Chem. Geol. (Isot. Geosc. Sect.), 130, 147-157.

Tagami, T., Ito, H., Nishimura, S., 1990. Thermal annealing characteristics of spontaneus fission tracks in zircon. Chemical Geology (Isot. Geosc. Sect.) 80, 159-169.

Tello S., C. A.; Palissari, R. ; Hadler, J. C. ; Iunes, P. J. ; Guedes, S. ; Curvo, E. A. C.; S. R.; 2006. Annealing experiments on induced fission tracks in apatite: I. Measurements of horizontal-confined-track lengths and track densities in basal sections and randomly oriented grains. American Mineralogist, 91, 252-260.

Tello S. C. A; Hadler N., J. C..; Iunes, P. J.; Guedes, S.; Hackspacher, P. C.; Ribeiro B., L. F.; Paulo, S. R. ; Osorio A., A. M.; 2005. Thermochronology of the South American platform in the state of São Paulo, Brazil, through apatite fission tracks Radiation Measurements, 39, 635-640.

Twenhofel, W. H.; 1941. The frontiers of sedimentary mineralogy and petrology. Journal of Sedimentary Petrography, 11, 53-63.

Thomson, S. N. and Hervé, F.; 2002. New time constraints for the age of metamorphism at the ancestral Pacific Gondwana margin of southern Chile (42-52°S). Revista Geológica de Chile, 29(2), 151-165

Wagner, G. A. and P. Van Den Haute, Fission-track dating. Kluwer Acad., Norwell, Mass., 1992; 6, 285p.

Williams, I.S. 1998. U-Th-Pb geochronology by ion microprobe. In: McKibben, M.A., Shanks III,W.C., Rydley,W.I. (Eds.), Applications of Microanalytical Techniques to Understanding Mineralizing Processes. Rev. Econ. Geol. 7, 1-35.

Yamada, R.; Murakami, M.; Tagami, T.; 2007. Statistical modeling of annealing kinetics of fission tracks in zircon; Reassessment of laboratory experiments. Chemical Geology (Isotopic Geocience Section), 236, 75-91.

Yamada, K., Tagami, T., Shimobayashi, N., 2003. Experimental study on hydrothermal annealing of fission tracks in zircon. Chemical Geology (Isot. Geosci. Sect) 201, 351-357.

Yamada, R.; Yoshioka, T.; Watanabe, K.; Tagami, T., Nakamura, H.; Hashimoto, T., Nishimura, S.; 1998. Comparison of experimental techniques to increase the number of

measureable confined fission tracks in zircon. Chem. Geol. (Isot. Geosci. Sect), 149, 99-107.

Yamada, R.; Tagami, T.; Nishimura, S.; Ito, H.; 1995. Annealing kinetics of fission tracks in zircon: an experimental-study. Chem. Geol. (Isot. Geosci. Sect), 122, 249-258.

Youden, W.J. 1951 Statiscal methods for chemists. Journal of the Royal Stastical. New York, Wiley, 126 pp.

Zalán, P.V.; Wolff, S.; Astolfi, M.A.M.; Vieira, I.S.; Conceição, J.C.J.; Appi, V.T.; Neto, E.V.S.; Cerqucira, J.R.; Marques, A. 1990. The Paraná Basin, Brazil. In: M. W. Leighton; D. R. Kolata; D. F. Oltz; J. J. Eidel (eds). Interior cratonic hasins. Tulsa: American Association of Petroleum Geologists Memoir, 51, 681-708.

CAPITULO V

V. CORPO PRINCIPAL DA TESE

5.1. Artigo 1 (publicado)

Dias, A. N. C.; Tello, C. A.; Chemale Jr.; F., Iunes, P. J.; Soares, C. J.; Curvo, E. A.; Guedes, S.; Barra, B. C.; Constâncio Jr.; M. and Hadler, J.C.; 2010. Zircon fission track and U-Th-Pb in situ dating of Rio Paraná Formation, Parana Basin, Brazil. Revista Mexicana de Física, 56 (1), 16-21.

Zircon fission track and U-Th-Pb in situ dating of Rio Paraná Formation, Parana Basin, Brazil

A.N.C. Dias[a,b,*], C.A. Tello[b], F. Chemale Jr.[a], P.J. Iunes[c], C.J. Soares[d],
E.A. Curvo[c], S. Guedes[c], B.C. Barra[b], M. Constâncio Jr.[b], and J.C. Hadler[c]
[a] *Laboratório de Geologia Isotópica – CPGq/UFRGS,*
91501-970, Porto Alegre-RS, Brazil,
Phone: 55 51 3308-7288,
[*]e-mail: diasanc@bol.com.br
[b] *Dep. de Física, Química e Biologia – FCT/UNESP,*
19060-900, Presidente Prudente-SP, Brazil.
[c] *Instituto de Física Gleb Wataghin – DRCC/UNICAMP,*
13083-970, Campinas-SP, Brazil.
[d] *Instituto de Geociências e Ciências Exatas – IGCE/UNESP,*
13506-900, Rio Claro-SP, Brazil.

Ages of zircon from sedimentary samples of Rio Paraná Formation, belonging of Bauru Group, north of Paraná Basin, Brazil, has been determined by zircon Fission Track and U-Th-Pb in situ dating methods. The obtained ages are from same zircon grain that provided information on the source areas for the sediments and the morphotectonic events.

Keywords: Zircon, fission track method; U-Th-Pb *in situ* dating; Bauru Group; Rio Paraná Formation.

En este trabajo se hizo datación de zircones provenientes de rocas sedimentarias de la Formación Rio Paraná, Grupo Bauru, ubicada en la porción norte de la Cuenca Paraná, con uso del método de datación de huellas de fisión y U-Th-Pb in situ. Las edades obtenidas son de los mismos zircones ó granos y contribuyeran con dados de área fuente de las sedimentitas y de los eventos morfotectonicos.

Descriptores: Zircones; método huellas de fisión; U-Th-Pb *in situ* datación; Grupo Bauru; Formación Rio Paraná.

PACS: 25.85.Ca; 25.85.Ec

1. Introduction

In the last decade, the Fission Track Method (FTM) on zircon, where the fission track age and its thermal history can be determined, has seen rapid growth and widespread application in a number of disciplines in the earth sciences [1-3]. Natural zircon commonly contains U and Th as well as other rare earth elements in significant amount. This mineral is a common accessory that can be found in igneous, sedimentary and metamorphic rocks. However, zircon is also a very important mineral for absolute dating (high precise) of magmatic, metamorphic and sedimentary geological events, combining the acquisition of U, Th, and Pb isotopes plus in situ analyses using either ion microprobe [4] or laser microprobe [5]. The combination of two techniques applied to detrital zircons in sedimentary can bring very important information on the high temperature and also intermediate to low temperature geological events as the igneous and metamorphic crystallization of the zircons, the morphotectonic events (uplift, denudation, etc) as well as sedimentary provenance studies [6].

The main purpose of this work is to determine the apparent ages and igneous and metamorphic ages from zircons extracted of sedimentary rocks of the Rio Paraná Formation (Bauru Group, north of Paraná Basin), São Paulo state,

Brazil, using FTM analyses on zircon and U-Th-Pb in situ dating with LA-MC-ICP-MS.
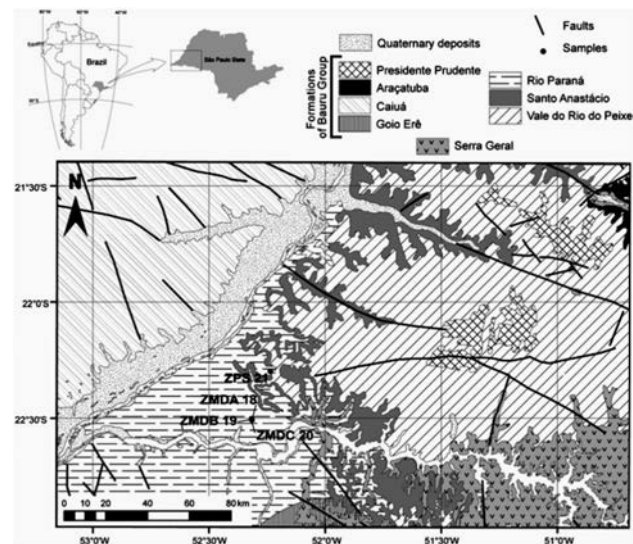
FIGURE 1. Geological map of the study area with sample location.

2. Material

The dated samples are from sedimentary rocks of the Rio Paraná Formation, Bauru Group, localized in the northern portion of Paraná Basin, São Paulo state, Brazil. The Fig. 1 shows the geological map of the study area with the location of collected samples. They are four samples of sedimentary rocks of Rio Paraná Formation, which is part of the Bauru Group. The stratigraphical age of this Group is estimated among 100 to 80 Ma formed after the widespread magmatism in South America, due to the separation of African and South American continents.

3. Experimental

The rock samples have been collected from different outcrops, where the samples ZMDA-18, ZMDB-19 and ZMDC-20 (UTM coordinate $364620E$, $7509633N$) were collected from the base, intermediate and top of Morro do Diabo (Diable Hill) and ZPS-21 (UTM coordinate $372705E$, $7532462N$) from the road margin (Fig. 1). Zircons have been separated from rock samples by conventional techniques as crushing, magnetic separation (isodynamic separator), heavy liquids and hand-picking.

The zircon Fission Track ages were obtained at the Departamento de Física, Química e Biologia of UNESP, Brazil, while the U-Pb zircon ages at the Isotope Geology Laboratory of Rio Grande University, Brazil.

3.1. Fission track method

The grains were incrusted in the Teflon®PFA sheets with a thermal plate. After the samples were grinded in three stages: 1200#, 2400# and 4000# sandpapers. In sequence, the samples were polished with diamond paste of 0.25 μm during 10 minutes using the polish machine. Finally, the zircon etching was made with NaOH:KOH (1:1), at $225 \pm 2°$C for 18h.

After that, the samples are juxtaposed to white mica, described as External Detector Method (EDM), previously etched with 48% HF at 15 °C for 90 minutes, and then sent to nuclear reactor of IPEN/CNEN (São Paulo, Brazil) for irradiation. The EDM is adjusted to the sedimentary basin study and samples with different populations. Besides the micas, in each irradiation assembly was used glasses doped with uranium, U (CNs) to obtain the value of R_M [see Eq. (1)] and thin films of Th to obtain the rate Th/U. The doped glass used in this work was CN-5 with calibration factor $N_U^v \varepsilon_U^v$=0.4169×10^{14} [7]. R_M is a value that varies for each reactor, and was determined experimentally through Eq. (1):

$$R_M = \frac{\rho_U^v}{N_U^v \varepsilon_U^v} \qquad (1)$$

Where, ρ_U^v is the density obtained in the mica and $N_U^v \varepsilon_U^v$ is a calibration factor. Then, the knowledge of the product and $N_U^v \varepsilon_U^v$ leads to R_M if ρ_U^v is measured. Finally, the R_M value obtained was 2.5×10^{-9}.

The ages were obtained using the Eq. (2), that it the methodology implemented by the Chronology Group of IFGW/UNICAMP [8,9]. This methodology uses the Absolute calibration and not the ζ-calibration. The interest in using the methodology developed by Iunes [10] it is in the fact that the obtained ages do not need necessarily be linked to other radioactive methods, *i.e.*, the age is obtained by independent way.

$$T = \frac{1}{\lambda} \ln \left[1 + \frac{\rho_S}{\rho_I} \left(\frac{\lambda}{\lambda_F} \right) \left(\frac{R_M}{C_{238}} \right) g \right]. \qquad (2)$$

Where λ is the alpha decay constant of ^{238}U; λ_F is the spontaneous fission decay constant of ^{238}U; ρ_S (or ρ_I) is the superficial density of spontaneous (or induced) tracks; $\mathbf{C}_{238}$ is the natural isotopic concentration of ^{238}U; $\mathbf{R}_M$ is the parameter that involves the nuclear reactor neutrons dosimetry and; $\mathbf{g}$ is geometry factor. The following values for the constants of Eq. (1) were adopted: $\mathbf{C}_{238}$= 0.99275, λ_F= 8.35×10^{-17} a^{-1}, λ = 1.55125×10^{-10} a^{-1}, g = 0.684.

3.2. U-Th-Pb *in situ* method

All zircon mountings that were incrusted on TEFLON®PFA used for FTM determination (ca. 1 cm ×1cm) were mounted in an epoxy, 2.5-cm-diameter circular mount. Images of zircons were obtained using the optical microscope (Leica MZ 12$_5$) and back-scatter electron microscope (Jeol JSM 5800). Zircon grains were dated with laser ablation microprobe (New Wave UP213) coupled to a MC-ICP-MS (Neptune) at the Isotope Geology Laboratory of UFRGS. Isotope data were acquired using static mode with spot size of 25 μm, in the same zircons dated by FTM and, in most of cases, in the same area where the tracks density was obtained. Laser-induced elemental fractional and instrumental mass discrimination were corrected by the reference zircon (GJ-1) [11], following the measurement of two GJ-1 analyses to every ten sample zircon spots. For common Pb correction, we assume that the ^{204}Pb values obtained from zircons have common Pb composition [12], assuming concordant age of ^{206}Pb/^{238}Pb and ^{207}Pb/^{206}Pb (as estimated age). The Table I shows the operating conditions of the lasers.

TABLE I. Laser operating conditions.

Laser type New Wave UP213:	Laser output power: 6 J/cm^2; Shot repetition rate: 10 Hz; Laser spot: 25 and 40 μm.
MC-ICP-MS Neptune:	Cup configuration: Faradays ^{206}Pb, ^{208}Pb, ^{232}Th, ^{238}U; MIC's ^{202}Hg, ^{204}Hg+^{204}Pb, ^{207}Pb;
	Gas input: Coolant flow (Ar) 15 l/min, Auxiliary flow (Ar) 0.8 l/min,
	Carrier flow 0.75 l/min (Ar) + 0.45 l/min (He); Acquisition 50 cycles of 1.048 s.

TABLE IIA. Zircon U-Pb and FTM data for ZMDA18 sample.

Grain number	U ^{232}Th/^{238}U	(ppm)	ICPMS-Laser Ablation DATA ^{207}Pb/^{235}U	±σ (%)	Ratios # ^{206}Pb/^{238}U	±σ (%)	^{207}Pb/^{206}Pb	±σ (%)	FTM DATA $\rho_S \times 10^7$ cm^{-2}	N_S	$\rho_i \times 10^6$ cm^{-2}	N_I	AGES (Ma) U-Pb in situ	(± 2σ)	FTM	(± 2σ)
4 [C3]	1.04	59	0.6827	4.59	0.0819	1.68	0.0604	4.27	2.96	116	1.222	44	619	52	376	78
6 [D4]	1.05	57	0.7997	3.94	0.0957	2.50	0.0606	3.04	1.50	66	0.792	95	591	27	295	57
8 [D6]	0.30	71	5.7608	3.43	0.3236	2.31	0.1291	2.54	2.96	29	1.563	25	2086	106	296	87
9 [D7]	0.44	77	0.6533	3.45	0.0812	2.22	0.0583	2.64	3.27	16	1.313	21	505	22	386	164
10 [D9]	0.42	62	0.6529	8.76	0.0820	4.50	0.0577	7.52	3.27	16	1.813	29	509	43	282	93
12 [E4]	0.50	120	6.8986	1.62	0.3848	0.50	0.1300	1.54	3.29	161	0.833	100	2099	18	602	100
14 [E7]	0.61	177	6.0578	2.70	0.3427	1.19	0.1282	2.42	2.86	98	0.875	14	2073	100	502	153
15 [E9]	0.38	44	0.8164	5.50	0.0951	2.17	0.0622	5.06	2.96	58	0.806	29	683	70	563	142
16 [E10]	0.40	67	0.7092	2.64	0.0862	1.73	0.0597	1.99	3.67	18	1.625	26	535	15	352	114
17 [F2]	0.35	58	0.7663	6.38	0.0940	1.91	0.0591	6.08	2.95	101	1.203	77	2036	70	380	71
18 [F3]	0.62	77	5.4563	2.01	0.3251	1.32	0.1217	1.52	3.27	32	0.889	32	1981	60	562	141
19 [F6]	0.47	139	0.7091	4.80	0.0849	1.30	0.0606	4.62	3.10	152	0.797	51	625	32	594	116
20 [F8]	0.74	45	1.2082	5.89	0.1313	1.47	0.0668	5.70	3.13	92	0.656	42	795	22	721	155
21 [F10]	0.77	45	0.8584	4.91	0.1030	1.56	0.0604	4.66	3.16	124	0.953	61	632	19	510	97
22 [G1]	1.53	62	6.4805	2.11	0.3638	1.41	0.1292	1.58	3.21	63	1.028	37	2087	66	482	113
23 [G2]	0.35	25	1.5237	5.38	0.1526	1.59	0.0724	5.14	2.83	97	1.306	47	917	27	587	117
24 [G3]	0.60	59	7.1491	2.15	0.3927	1.35	0.1320	1.67	2.96	29	1.028	37	2131	38	445	120
28 [G8]	0.42	61	0.6092	7.34	0.0777	1.92	0.0569	7.09	3.18	109	0.828	53	482	18	338	70
31 [H2]	0.46	63	0.7269	6.84	0.0901	1.77	0.0585	6.60	2.04	40	1.083	39	556	19	295	73
33 [H5]	1.66	54	0.5678	6.83	0.0734	2.62	0.0561	6.31	2.55	25	1.250	20	457	23	318	101
35 [H7]	0.83	66	1.1282	4.99	0.1192	1.48	0.0686	4.76	1.81	124	0.458	33	888	84	602	134
38 [H10]	0.38	103	0.6853	5.04	0.0827	2.65	0.0601	4.29	2.70	53	1.521	54	607	52	282	62
45 [I6]	0.52	136	0.8035	3.61	0.0971	1.06	0.0600	3.45	2.91	57	0.944	34	597	12	475	115
46 [I7]	0.32	93	2.6696	2.09	0.2165	1.12	0.0894	1.77	2.65	104	0.858	103	1413	50	477	84
47 [I8]	0.77	136	0.5011	7.39	0.0624	6.73	0.0583	3.06	2.59	38	1.417	51	540	34	286	68

Twenty five grains were dated; ρ_S (ρ_i), spontaneous (induced) track density; N_S (N_i), number of tracks counted to determine ρ_S (ρ_i); ρ_i, induced track density of sample measured that was obtained in a white mica. The FT ages were obtained using the Eq. (2).

Table IIB. Zircon U-Pb and FTM data for ZMDB19 sample.

| Grain number | ^{232}Th/^{238}U | U (ppm) | ICPMS-Laser Ablation DATA Ratios # | | | | | | FTM DATA | | | | AGES (Ma) | | | |
			^{207}Pb/^{235}U	±σ (%)	^{206}Pb/^{238}U	±σ (%)	^{207}Pb/^{206}Pb	±σ (%)	ρ_S X 10^7 cm^{-2}	N$_S$	ρ_i X 10^6 cm^{-2}	N$_I$	U-Pb in situ (± 2σ)		FTM (± 2σ)	
1 [A1]	1.09	129	0.6993	6.36	0.0844	2.68	0.0601	5.77	2.93	43	1.028	37	606	69	440	109
2 [A8]	0.32	122	0.7817	7.03	0.0951	1.49	0.0596	6.87	3.20	47	1.438	23	586	18	347	95
3 [A9]	0.59	97	0.7912	3.75	0.0959	1.69	0.0598	3.35	2.79	41	1.125	18	591	20	385	116
5 [B1]	0.72	95	0.8923	4.59	0.1057	1.73	0.0612	4.25	2.96	29	1.563	25	648	22	296	86
7 [B6]	0.81	39	0.8912	6.91	0.1062	3.68	0.0608	5.85	2.79	41	1.813	29	650	43	241	62
8 [B7]	0.59	131	0.7940	4.36	0.0968	1.54	0.0595	4.08	2.65	13	1.125	18	595	18	367	139
9 [B8]	0.76	61	1.9492	2.68	0.1907	0.98	0.0741	2.50	2.90	71	1.563	25	1122	20	290	74
10[C2]	0.57	42	1.6628	2.95	0.1656	2.19	0.0728	1.97	3.47	51	1.306	47	992	35	412	94
11 [C4]	1.19	140	0.7149	2.80	0.0896	1.50	0.0579	2.37	2.55	25	1.512	24	552	16	267	81
12 [C5]	0.90	90	0.8680	3.06	0.1038	1.27	0.0606	2.78	2.79	41	1.124	36	637	16	432	109
13 [C7]	0.42	47	1.1771	6.18	0.1304	1.21	0.0655	6.06	2.40	47	0.944	34	790	18	394	98
14 [D2]	0.61	80	2.4738	3.37	0.2176	1.77	0.0825	2.86	2.79	41	0.667	24	1268	37	637	177
15 [D10]	0.98	93	0.7202	4.00	0.0886	1.85	0.0589	3.54	2.45	36	1.752	28	548	20	220	60
16 [E4]	0.85	195	0.8846	4.67	0.1011	3.37	0.0635	3.23	2.65	130	0.813	78	627	37	503	90
17 [E6]	0.63	110	0.8016	4.97	0.0950	1.58	0.0612	4.71	2.60	102	0.917	132	585	18	439	75
19 [E10]	0.27	166	0.7681	3.94	0.0939	1.40	0.0593	3.69	3.06	15	1.438	23	578	16	332	116
20 [F1]	0.45	108	0.6736	3.58	0.0847	1.44	0.0577	3.28	2.70	53	1.563	25	524	14	271	72
21 [F8]	1.72	106	0.8627	3.67	0.1027	1.45	0.0609	3.37	2.74	67	1.028	37	630	18	412	95
22 [F9]	0.72	67	1.2053	3.26	0.1324	1.42	0.0660	2.93	2.45	48	0.875	14	802	22	433	139
23 [F10]	0.65	154	0.7474	3.62	0.0915	1.33	0.0593	3.36	3.11	61	1.063	17	564	14	453	133

Twenty grains were dated; ρ_S (ρ_i), spontaneous (induced) track density; N$_S$ (N$_i$), number of tracks counted to determine ρ_S (ρ_i); ρ_i, induced track density of sample measured that was obtained in a white mica. The FT ages were obtained using the Eq. (2).

TABLE III. Zircon FTM data for ZMDC20 and ZPS21 samples.

	ZMDC20							ZPS21					
	FTM DATA				**AGES (Ma)**			**FTM DATA**				**AGES (Ma)**	
Grain number	ρ_S**X** 10^7 **cm**$^{-2}$	**N**$_S$	ρ_i**X** 10^6 **cm**$^{-2}$	**N**$_I$		**($\pm$ 2σ)**	**Grain number**	ρ_S**X** 10^7 **cm**$^{-2}$	**N**$_S$	ρ_i**X** 10^6 **cm**$^{-2}$	**N**$_I$		**($\pm$ 2σ)**
1	3.27	32	1.389	50	366	91	1	2.19	43	0.889	32	383	98
2	3.47	68	1.083	39	493	112	2	2.49	61	1.208	29	322	80
3	2.79	41	1.125	18	385	116	3	2.55	50	0.889	32	444	111
4	2.45	48	0.844	54	449	101	4	1.68	33	1.000	36	264	70
5	3.06	60	1.889	68	254	52	5	2.25	33	1.252	20	281	85
6	3.47	51	1.361	49	396	90							

Grain number is the amount of the grain dated; ρ_S (ρ_i), spontaneous (induced) track density; N$_S$ (N$_i$), number of tracks counted to determine ρ_S (ρ_i); ρ_i, induced track density of sample measured that was obtained in a white mica. The FT ages were obtained using the Eq. (2).
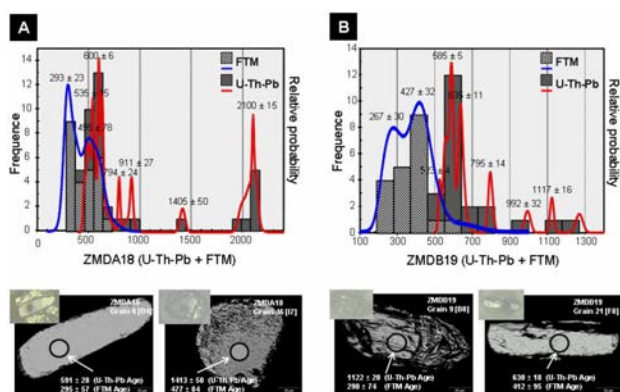

FIGURE 2. FT and U-Th-Pb ages distribution for ZMDA18 (A) and ZMDB19 (B) samples. Below is shown the Back Scattering images with optical microscopy (inset) that show the laser spot in each sample.

4. Results and discussion

The results of the FTM analyses and U-Th-Pb ages are shown in Tables IIa, IIb and III. The obtained U-Th-Pb ages of the detrital zircon are interpreted to be magmatic one, since the Th/U ratios are higher than 0.2 which the limit for igneous versus metamorphic zircons (Th/U data for the analyzed zircons are from 0.32 to 1.79). On other side, the analyzed zircons show a clear source area of Brasiliano orogeny, ranging from 523 $\pm$ 4 to 795 $\pm$ 14 (Figs. 2a and 2b), as main group of obtained ages, but there also in minor occurrence Lower Neoproterozoic to Mesoproterozoic ages (911 $\pm$ 27 and 1405 $\pm$ 50) on Fig. 2a, 992 $\pm$ 32 and 1117 $\pm$ 16 on Fig. 2b as well some Paleoproterozoic ages in the sample ZMDA 18 (mean value of 2100 $\pm$ 15 Ma). The data reproduce very well the main source for the region, the Brasiliano and Paleoproterozoic ages, and point to a western source area for the Mesoproterozoic ages.

On other side the FT zircon data yield distinct apparent ages for both samples. However we can distinguish three main groups of ages, as follow:

i) 495 $\pm$ 98 Ma (ZMDA 18);

ii) 427 $\pm$ 32 Ma (ZMDB 19);

iii) 293 $\pm$ 23 Ma (ZMDA-18) to 267 $\pm$ 30 Ma.

It is noteworthy to emphasize that mostly of analyzed zircons have FT apparent ages than those obtained at same grain by the U-Th-Pb method. It is well illustrated on Fig 2, where we observe the dated zircon grains with the information of the obtained ages by both methods, where the FT ages are always younger than crystallization ages. Of course, it is supported by the crystallization zircon formation (ca. 850°C) versus the formation of tracks in the zircon with the estimated temperature at 220°C.

The integration of both set of data allows us to distinguish different source areas for the 90-100 Ma old sediments of the Rio Paraná Formation. (Brasiliano, Mesoproterozoic and Paleoproterozoic rocks) but also recycled zircon or denudation processes which pass the total annealing zone to the partial annealing zone at two different events of the South American Plate, namely Devonian orogeny and the Gondwanides orogeny (Permian-Carboniferous event related to the assembling of the Pangea).

5. Conclusions

The combination of two thermochronometer techniques, namely high temperature (U-Th-Pb) and intermediate to low temperature (FT on zircon) ones, applied in the same detrital zircon grains of the Rio Paraná Formation confirmed as a powerful tool to unravel the provenance of the rocks as the morphotectonic events.

FTM data of four analyzed samples produced at least three main group of apparent ages: the Brasiliano ages (800 to 480 Ma) with main grouping at the end of the cycle (480-500 Ma), Devonian ages which can correspond to main uplift in the South Platform during the formation of Paraná Basin; the third group with Permian-Caborniferous ages (293

to 267 Ma) that is linked with the Pangea Formation or the Gondwanides orogeny.

The U-Th-Pb method provided consistent information on the main source areas for the sediments of the Rio Paraná Formation, formed between 90 to 100 Ma old before present, where there were recognized one major source area, the Brasiliano rocks (795 to 485 Ma) and subordinate sources as the Mesoproterozoic (or Greenvilian coeval material) and Paleoproterozoic (Transamazonian material).

We still need to investigate the behavior of FT zircon data versus U-Th-Pb data since we have mostly older ages of FT zircon (the Brasiliano ages obtained by this method) when the U-Th-Pb zircon age is also older than Neoproterozoic.

1. K. Yamada, T. Tagami, and N. Shimobayashi, *Chem. Geol.* **201** (2003) 351.

2. J.I. Garver, *Radiation Measurements* **37** (2003) 47.

3. A.N.C. Dias *et al.*, *J. of Raman Spectroscopy* **40** (2009) 101.

4. I.S. Williams, *Rev. Econ. Geol.* **7** (1998) 1.

5. S.E. Jackson, N.J. Pearson, W.L. Griffin, and E.A. Belousova, *Chem. Geol.* **211** (2004) 47.

6. J. Koesler, H. Fonneland, P. Sylvester, M. Tubrett, and R.B. Pedersen, *Chem. Geol.* **182** (2002) 605.

7. P.J. Iunes *et al.*, *Chem.Geol.* **187** (2002) 201.

8. G. Bigazzi *et al.*, *9th International Conference on Fission Track Dating and Thermocronology* (Book of Extend abstracts. Lorne, Australia, 2000) p. 33.

9. P.J. Iunes *et al.*, *J. of Radioanalytical and Nuclear Chemistry* **262** (2004) 461.

10. P.J. Iunes, *PhD Thesis* (IFGW/UNICAMP, São Paulo state, Brazil, 1999).

11. E. Simon, S.E. Jackson, N.J. Pearsona, W.L. Griffina, and E.A. Belousova, *Chem. Geol.* **211**(2004) 47.

12. J.S. Stacey and J.D. Kramers, *Earth and Planetary Science Letters* **26** (1975) 207.

5.2. Artigo 2 (publicado)

Dias, A. N. C.; Tello, C. A. S.; Chemale Jr., F.; Godoy, M. C. T. F.; Guadagnin, F.; Iunes, P. J.; Soares, C. J.; Osório, A. M. A.; Bruckmann, M. P.; 2011. Fission track and U-Pb in situ dating applied to detrital zircon from the Vale do Rio do Peixe Formation, Bauru Group, Brazil. Journal of South American Earth Sciences, 31, 298-305.

Fission track and U–Pb *in situ* dating applied to detrital zircon from the Vale do Rio do Peixe Formation, Bauru Group, Brazil

A.N.C. Dias [a], C.A.S. Tello [a,*], F. Chemale Jr. [b], M.C.T.F. de Godoy [a], F. Guadagnin [b], P.J. Iunes [c], C.J. Soares [d], A.M.A. Osório [a], M.P. Bruckmann [b]

[a] Dep. de Física, Química e Biologia – FCT/UNESP, 19060-900 Presidente Prudente-SP, Brazil
[b] Laboratório de Geocronologia,IG-UnB, 70904-970 Brasilia-DF, Brazil
[c] Instituto de Física Gleb Wataghin – DRCC/UNICAMP, 13083-970 Campinas-SP, Brazil
[d] Instituto de Geociências e Ciências Exatas – IGCE/UNESP, 13506-900 Rio Claro-SP, Brazil

A B S T R A C T

Combined methods of fission track (FTM) and U–Pb *in situ* zircon dating were applied to sedimentary samples from the Vale do Rio do Peixe Formation, Bauru Basin, Brazil. Detrital zircons of nine samples were determined by the FTM, and the obtained ages varied from 239 Ma–825 Ma, which can be grouped into four main populations as the 230–300 Ma, 460–490 Ma, 500–650 Ma and 696–825 Ma groups. The U–Pb data show two clear source areas: the Early Paleozoic to Neoproterozoic zircons, ranging from 445 ± 14 to 708 ± 18 Ma, and the Paleoproterozoic zircons, ranging from 1879 ± 23 to 2085 ± 27 Ma. Subordinate occurrences of Early Neoproterozoic to Mesoproterozoic zircons (836 ± 15 and 1780 ± 38 Ma) were identified. The combined information allows us to characterize Early Brazilian, Brazilian and Rhyacian material as the main source for the zircons, which are areas situated to west of the Bauru Basin (e.g., Goiás Massif) that have been incorporated into the sedimentary cycles in the Phanerozoic (mainly in the Paraná Basin). FT zircon ages reflect the main denudation processes of the South American Plate from Neoproterozoic to Early Triassic as those related to orogenic cycles of Early Brazilian, Brazilian, Famatinian/Cuyanian and Gondwanide.

© 2011 Elsevier Ltd. All rights reserved.

1. Introduction

In the last decade, the fission track method (FTM) in zircon, in which the fission track age and its thermal history can be determined, has experienced rapid growth and widespread application in the Earth Sciences (Yamada et al., 2003; Hasebe and Watanabe, 2004; Garver, 2003; Dias et al., 2009). Some of the most exciting advances in geochronology have been driven by Laser Ablation Multicollector Inductively Coupled Plasma Mass Spectrometers (LA-MC-ICP-MS). The LA-MC-ICP-MS is well accepted as a reliable and convenient method for dating detrital zircons (provenance information applied to sedimentary basin evolution), mainly after the introduction of Laser Microprobe with 213 nm laser wavelength.

Similar to the FTM, U–Th–Pb geochronology is becoming an increasingly important tool in Earth Science research because it provides improved precision and accuracy, finer spatial resolution,

and more efficient data acquisition (Gehrels and Juiz, in press). Analysis of the heavy mineral fraction of clastic sediments has proven to be a useful tool for stratigraphic correlations, especially in sedimentary sequences lacking biostratigraphical markers, stratigraphically distinct horizons or other time constraints such as cross-cutting dykes or sills. In addition, heavy mineral assemblages present in clastic sediments may record sediment sources and/or transport and depositional histories. Age dating of clastic heavy minerals, particularly zircon and monazite, is therefore a powerful tool in sedimentary provenance studies (Kösler et al., 2002). The combination of the two techniques applied to detrital zircons in sediment can provide important information on high-temperature as well as intermediate- to low-temperature geologic events such as the igneous and metamorphic crystallization of zircons and morphotectonic events (e.g., uplift and denudation) as well as the abovementioned sedimentary provenance studies.

The zircon mineral is a common accessory that can be found in igneous, sedimentary and metamorphic rocks and is considered to be the most resistant mineral to weathering and dissolution (Morton and Hallsworth, 1999). Studies about this mineral have

* Corresponding author. Tel.: +55 18 32295355x218.
  E-mail address: tello@fct.unesp.br (C.A.S. Tello).

been conducted in several geological applications (Tagami, 2005; Watson and Harrison, 2007; Menneken et al., 2007; Tagami and Murakami, 2007; Yamada et al., 2007, 2009).

The main purpose of this work is to determine the apparent and absolute zircon ages extracted from sedimentary rocks from the Vale do Rio do Peixe Formation (Bauru Basin), São Paulo, Brazil, using FTM analysis and U–Th–Pb *in situ* dating with LA-MC-ICP-MS. Because the zircon grains are detrital, they may reveal something about the thermal evolution of their sources. The U–Th–Pb ages may be related to the formation of these minerals, usually as a result of a magmatic crystallization episode, and FTM ages are related to later events of regional cooling, such as the exhumation of the rock units. These apparent ages could be used in provenance studies by correlating them with known geological domains within the regional context.

2. Geological setting

The dated samples are from the Vale do Rio do Peixe Formation, which belongs to Bauru Basin in the North of Parana Basin, São Paulo, Brazil. Fig. 1 shows the geological map of the study area and the location of the samples analyzed in this work. Nine samples (six in Table 2 and three in Table 3) of sedimentary rocks were dated by FTM (reported in the Fig. 3), and three of these samples were analyzed by U–Th–Pb dating (samples ZPI23, ZEM11 and ZCG7 – see Fig. 5).

The Bauru Basin is a Coniacian–Maastrichtian intracratonic continental basin that developed on the central southern part of the South American Platform after the dissolution of Gondwanaland

(Fernandes and Coimbra, 1996). The basin substrate consists of basalts of the Eocretaceous Serra Geral Formation (Renne et al., 1992), from which the sedimentary sequence is separated by a regional erosive unconformity (Fig. 2). The Vale do Rio do Peixe Formation (VPF) comprises the largest extension in the basin and constitutes the substratum of most of the West of São Paulo state and Triângulo Mineiro (Minas Gerais). The VPF is deposited above the Serra Geral Formation on the eastern Bauru Basin, whereas in the central part, it covers the Araçatuba Formation. In Fig. 2, different sedimentary stratigraphic units of the Bauru Basin proposed by Fernandes et al. (2003), are shown.

3. Analytical procedures

3.1. Materials and methods

The zircon fission track (FT) ages were obtained using a Leica DMRX microscope at the Departamento de Física, Química e Biologia of UNESP, Brazil. The irradiations for FT analyses were made in the nuclear reactor of IPEN/CNEN in São Paulo state with a neutron fluence of 5×10^{14} neutrons/cm^2. U–Pb zircon dating was carried out at the Isotope Geology Laboratory of Rio Grande University with a laser microprobe (New Wave UP213) coupled to an MC-ICP-MS (Neptune).

3.2. Fission track method

The sample separations were accomplished by conventional techniques of crushing, magnetic separation, and heavy liquids.
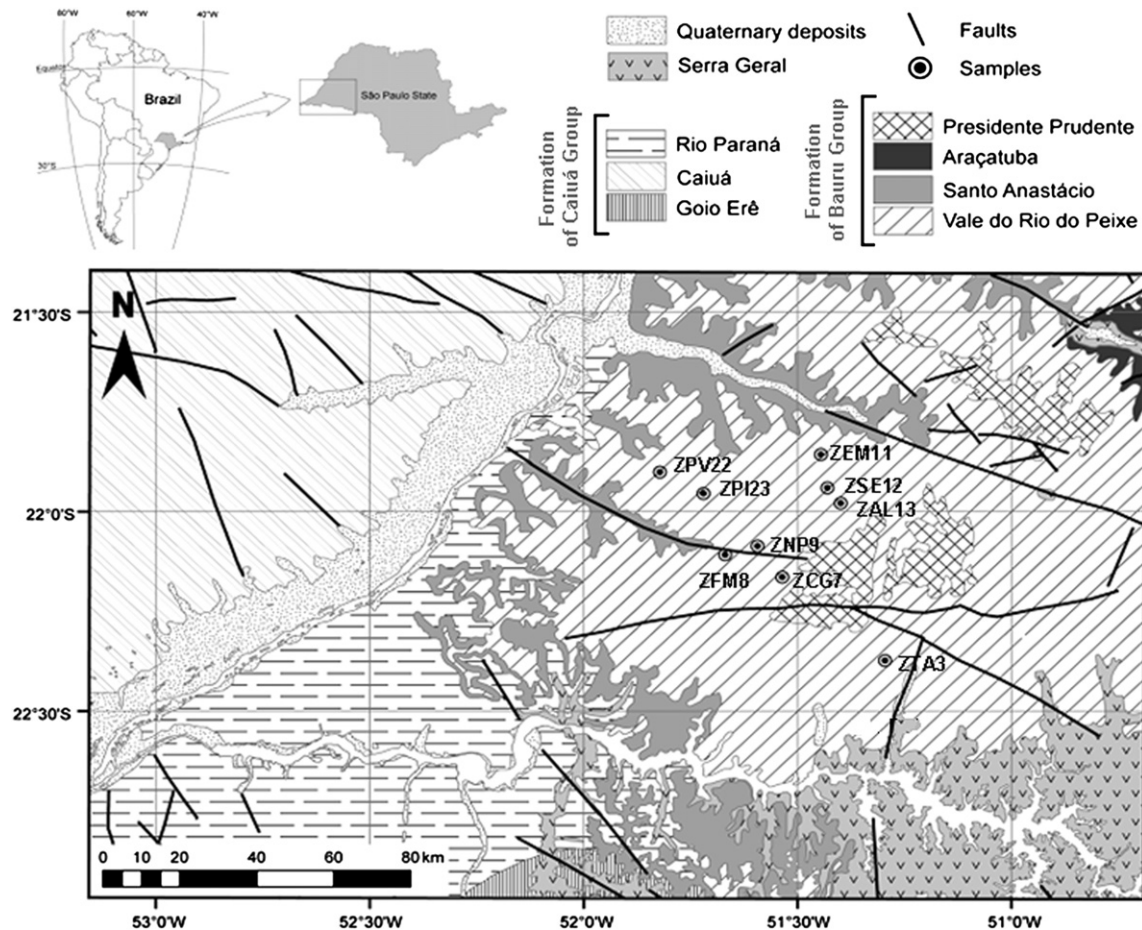

Fig. 1. Geological map of the Bauru Group with location of analyzed samples.
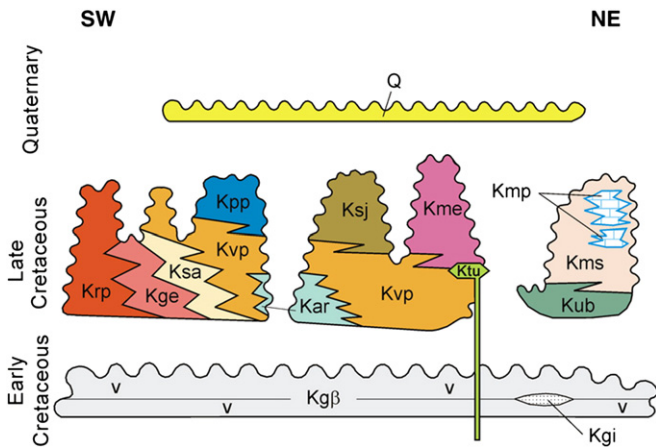
Fig. 2. Stratigraphy of the Bauru Basin (modified of Fernandes and Basilici, 2009). Key: *São Bento Group*: Kg = Serra Geral Fm., β = basalt rock, i = inter-trap sandstone. *Caiuá Group*: Krp = Rio Paraná Fm.; Kge = Goio Erê Fm.; Ksa = Santo Anastácio Fm.; *Bauru Group*: Kvp = Vale do Rio do Peixe Fm. (study area); Ktu = Taiúva Analcimites; Kar = Araçatuba Fm.; Kpp = Presidente Prudente Fm.; Ksj = São José do Rio Preto Fm.; Kub = Uberaba Fm.; Km = Marília Fm. (e = Echaporã Member, s = Serra da Galga Member and p = Ponte Alta Member). Q = Quaternary sediments.

Later, the grains were mounted in Teflon® PFA sheets, grinded, and polished. In the assembly process, the zircon grains are selected with a sharp tip and a binocular magnifying glass and then put in an aluminum sheet with the *C*-axis crystallography face parallel to the sheet. The grains were incrusted in the Teflon with a thermal plate. After assembly, the mounting was sanded in three stages: sandpaper 1200 (~10 μm) manually, sandpaper 2400 (~5 μm) manually for 2 min, and sandpaper 4000 (~3 μm) for 5 min using a polish machine at 60 rpm. The sample was then polished with ¼ μm diamond paste for 10 min at 60 rpm. Finally, the zircon etching was made with NaOH:KOH (1:1) at $225 \pm 2\,°C$ (Tagami et al. 1990) in periods varying from 4 to 72 h (Garver, 2003). The time of the adequate etching can be different for each sample, and all samples were etched for 16 h.

The ages were obtained using Equation (1), according to the method implemented by the Chronology Group of IFGW/UNICAMP, Brazil (Iunes, 1999; Bigazzi et al., 2000; Iunes et al., 2004). This method uses the absolute.

$$T = \frac{1}{\lambda}\ln\left[1 + \frac{\rho_S}{\rho_I}\left(\frac{\lambda}{\lambda_F}\right)\left(\frac{R_M}{C_{238}}\right)g\right] \tag{1}$$

where λ is the alpha decay constant of ^{238}U; λ_F is the spontaneous fission decay constant of ^{238}U; ρ_S (or ρ_I) is the superficial density of spontaneous (or induced) tracks; C_{238} is the natural isotopic concentration of ^{238}U; R_M is the parameter that involves the nuclear reactor neutrons dosimetry (for more information, see Iunes et al., 2002); and g is the geometry factor. The following values for the constants of Equation (1) were adopted: $C_{238} = 0.99275$ (Lederer and Shirley, 1978), $\lambda_F = 8.35 \times 10^{-17}$ a^{-1} (Guedes et al., 2003), $\lambda = 1.55125 \times 10^{-10}$ a^{-1} (Lederer and Shirley, 1978), and $g = 0.684$ (Iwano and Danhara, 1998).

3.3. U–Pb in situ dating

All zircon mountings used for FTM determination (ca. 1 cm × 1 cm) were mounted in an epoxy, 2.5-cm-diameter circular mount, requiring no further repetition for assembly, grinding, and polishing. Zircon images were obtained using an optical microscope (Leica MZ 125) and a back-scatter electron microscope (Jeol JSM 5800).

Table 1
Laser operating conditions.

Laser type New Wave UP213:	Laser output power: 6 J/cm^2; Shot repetition rate: 10 Hz; Laser spot: 25 μm.
MC-ICP-MS Neptune:	Forward power 1200 W; Reflected power <5 W; Cup configuration: Faradays ^{206}Pb, ^{208}Pb, ^{232}Th, ^{238}U; MIC's ^{202}Hg, ^{204}Hg + ^{204}Pb, ^{207}Pb; Gas input: Coolant flow (Ar) 15 l/min; Auxiliary flow (Ar) 0.8 l/min; Carrier flow 0.75 l/min (Ar) + 0.45 l/min (He); Acquisition 50 cycles of 1.048 s.

Table 2
Zircon FTM data for samples of VRP formation.

$\rho_S \times 10^7$ cm^{-2}	N_S	$\rho_I \times 10^6$ cm^{-2}	N_I	Age (Ma) $\pm 2\sigma$
ZFM8 sample				
3.32	65	1.028	37	497 ± 116
3.27	48	0.861	31	580 ± 148
3.57	35	1.472	53	377 ± 92
3.27	32	1.389	50	366 ± 92
3.57	35	0.944	34	579 ± 153
3.33	49	1.222	44	422 ± 99
3.56	122	0.775	93	696 ± 122
3.52	69	0.9722	35	555 ± 130
ZTA3 sample				
2.90	71	0.750	27	591 ± 148
2.96	29	0.694	25	648 ± 190
2.04	40	1.310	21	244 ± 71
1.73	17	1.063	17	256 ± 92
2.18	32	0.937	15	361 ± 120
1.94	19	0.500	18	593 ± 205
2.11	31	0.722	26	451 ± 130
1.70	25	0.812	13	327 ± 117
2.59	38	0.937	15	427 ± 138
2.55	25	0.937	15	422 ± 145
ZPV22 sample				
3.06	45	0.687	11	676 ± 239
2.76	27	0.812	13	521 ± 185
ZAL13 sample				
3.81	112	1.063	68	550 ± 103
4.69	23	2.194	79	334 ± 87
3.37	66	0.833	30	616 ± 151
4.08	20	2.688	43	239 ± 70
3.37	33	1.188	19	439 ± 135
3.20	47	1.125	18	440 ± 131
4.49	44	2.188	35	320 ± 80
ZNP9 sample				
2.65	26	1.500	24	277 ± 84
3.27	16	1.688	27	303 ± 101
2.54	87	0.765	49	510 ± 106
3.06	45	1.056	38	448 ± 110
2.47	121	0.631	53	598 ± 118
3.06	15	1.125	18	422 ± 154
2.93	43	1.563	25	293 ± 80
ZSE12 sample				
3.21	32	1.375	22	369 ± 110
3.16	31	0.833	30	581 ± 161
3.54	52	1.563	25	353 ± 94
3.47	51	1.688	27	321 ± 84
4.18	41	1.000	36	637 ± 161
3.06	45	1.694	61	283 ± 63
4.08	20	1.875	30	339 ± 105
3.40	100	1.806	65	295 ± 57

The FTM ages were obtained using the Equation (1); ρ_S (ρ_i), spontaneous (induced) track density; N_S (N_i), number of tracks counted to determine ρ_S (ρ_i); ρ_i, induced track density of sample measured that was obtained in a white mica. The data of samples ZCG7, ZEM11 and ZPI23 are reported in the Table 3 together with U–Pb data.

Table 3
Zircon U–Th–Pb and FTM data for samples of VRP formation.

Grain #	LA-MC-ICP-MS DATA							FTM DATA				AGES (Ma)				
	Th/U	U ppm	Isotope ratios					$\rho_S \times 10^7$ cm^{-2}	N_S	$\rho_I \times 10^6$ cm^{-2}	N_I	U–Pb in situ			FTM	
			^{207}Pb/^{235}U	$\pm\sigma$ (%)	^{206}Pb/^{238}U	$\pm\sigma$ (%)	^{207}Pb/^{206}Pb	$\pm\sigma$ (%)					Age	($\pm2\sigma$)	% Conc	Age	($\pm2\sigma$)
ZPI23 sample																
2 [A2]	0.91	79	6.811	0.97	0.3870	0.36	0.1276	0.91	2.96	29	0.750	12	2066	67	102	603	216
4 [A5]	0.57	88	1.005	3.82	0.1160	1.34	0.0628	3.58	2.45	24	0.938	15	708	18	101	585	140
5 [A6]	0.23	142	0.926	2.82	0.1093	1.18	0.0615	2.56	2.97	102	0.778	28	668	14	102	400	118
6 [B2]	0.48	103	4.706	1.94	0.3174	0.43	0.1075	1.89	3.06	45	1.188	19	1776	14	101	605	228
8 [B6]	0.20	179	1.430	2.95	0.1461	1.45	0.0710	2.57	3.47	17	0.875	14	882	24	92	331	123
9 [B8]	1.37	90	1.828	2.63	0.1809	0.81	0.0733	2.5	2.65	13	1.250	20	1070	16	105	460	135
10 [B10]	0.58	147	1.674	2.63	0.1675	1.1	0.0725	2.38	3.16	62	1.061	17	998	20	100	319	94
11 [C2]	0.68	52	2.417	3.28	0.2116	1.54	0.0828	2.9	3.06	30	1.502	24	1240	33	98	558	196
12 [C3]	0.92	125	6.192	1.5	0.3689	0.44	0.1217	1.43	2.96	29	0.813	13	2021	14	102	583	143
13 [C7]	0.75	62	6.119	1.69	0.3579	1.01	0.1240	1.35	2.86	84	0.750	27	1986	27	98	605	279
14 [C9]	1.07	66	0.657	5.39	0.0830	1.59	0.0574	5.15	1.74	17	0.438	7	514	16	101	505	116
16 [D2]	0.84	58	1.893	3.39	0.1846	1.33	0.0744	3.12	2.92	100	0.889	32	1090	25	104	444	140
17 [D7]	0.81	38	11.389	2.53	0.4602	2.33	0.1795	0.99	2.04	10	0.438	7	2648	61	92	640	167
18 [E3]	0.49	57	4.651	2.5	0.3136	1.34	0.1076	2.12	2.55	49	1.042	15	1758	35	100	461	122
19 [E4]	0.53	57	0.788	5.68	0.0956	2.66	0.0598	5.02	2.69	79	0.639	23	589	29	99	454	154
20 [E6]	0.85	45	1.991	3.01	0.1907	1.17	0.0758	2.77	3.71	95	0.722	21	1123	24	103	521	125
22 [E8]	1.16	37	1.476	4.27	0.1565	1.51	0.0684	4	2.76	27	1.662	15	936	25	106	280	73
23 [E10]	0.99	58	7.484	1.96	0.4010	1.53	0.1354	1.23	2.45	132	0.687	26	1170	33	102	546	197
25 [F6]	0.89	182	0.768	3.05	0.0939	1.36	0.0593	2.74	2.54	65	0.805	24	579	14	100	532	131
23 [G3]	0.80	283	0.779	2.73	0.0950	1.11	0.0595	2.5	2.45	36	1.313	11	585	12	100	316	117
27 [G9]	1.06	77	0.725	5.77	0.0899	1.9	0.0585	5.44	2.79	41	0.812	29	555	20	101	402	140
28 [H6]	1.16	111	0.665	4.64	0.0832	1.43	0.0579	4.42	2.65	13	1.139	21	515	14	98	328	78
30 [H9]	0.84	65	0.876	4.33	0.1037	1.53	0.0613	4.06	2.11	31	1.188	13	636	18	98	318	89
ZEM11 sample																
1 [C1]	1.04	292	6.3029	1.02	0.3625	0.46	0.1261	0.92	3.24	83	1.591	23	2045	32	98	370	96
2 [D1]	0.88	125	4.6548	1.70	0.3142	0.96	0.1074	1.4	2.85	73	0.923	30	1760	26	100	554	134
4 [E2]	0.50	58	0.6934	8.00	0.0855	3.49	0.0588	7.2	3.39	130	1.323	43	529	35	94	462	95
7 [J2]	0.64	119	6.2068	1.66	0.3597	1.16	0.1252	1.18	1.72	33	0.969	14	2004	29	98	324	109
9 [I3]	0.39	140	0.5507	2.81	0.0715	1.61	0.0559	2.31	2.77	71	0.954	31	445	14	99	523	126
10 [E4]	0.38	81	1.7553	3.08	0.1712	1.64	0.0744	2.61	2.71	104	1.352	44	1021	30	97	364	76
12 [I4]	0.58	122	0.7282	4.36	0.0900	1.72	0.0587	4.01	2.63	118	1.931	63	555	18	100	250	47
13 [F5]	0.66	25	5.5327	2.35	0.3434	0.99	0.1169	2.13	2.11	27	1.317	19	1904	30	100	293	93
14 [I5]	0.79	100	3.7873	1.37	0.2663	0.59	0.1031	1.23	2.38	61	0.554	10	1681	46	91	614	219
15 [A6]	0.33	75	1.3797	4.03	0.1383	0.94	0.0724	3.92	2.75	123	1.501	49	836	15	84	332	67
16 [D6]	0.27	111	1.4931	2.21	0.1497	1.31	0.0724	1.78	3.56	114	1.204	39	996	75	90	533	114
17 [E6]	0.39	165	0.6707	2.99	0.0842	1.37	0.0578	2.66	3.03	97	1.441	47	521	14	100	381	79
20 [B8]	1.05	126	0.7827	3.29	0.0952	1.55	0.0597	2.9	2.55	98	1.268	41	586	17	99	368	79
21 [C8]	0.61	74	4.5179	1.34	0.2818	1.06	0.1163	0.82	1.84	47	1.243	18	1899	32	84	270	80
22 [D8]	0.45	89	0.9505	3.74	0.1110	1.76	0.0621	3.3	2.53	81	1.591	23	679	22	100	291	76
23 [F8]	0.70	120	4.7828	2.27	0.3168	1.53	0.1095	1.67	2.32	89	1.174	17	1780	38	99	359	102
24 [A9]	0.54	131	5.9859	1.05	0.3364	0.72	0.1290	0.76	2.92	112	2.002	29	2085	27	90	266	62
25 [H9]	0.81	62	5.8110	2.56	0.3512	1.79	0.1200	1.83	2.31	59	1.451	21	1948	44	99	290	80
26 [A10]	0.92	21	0.7470	8.08	0.0917	2.5	0.0591	7.68	2.53	81	1.077	35	565	27	99	426	97
27 [D10]	1.02	86	0.6554	4.62	0.0826	2.23	0.0576	4.04	2.11	54	1.522	22	512	22	100	254	70
ZCG7 sample																
1 [A2]	0.66	145	0.8612	3.50	0.1016	1.59	0.0615	3.11	1.91	28	0.861	31	624	20	95	345	97
2 [A7]	0.54	268	4.0127	3.83	0.2873	1.61	0.1013	3.47	2.96	29	0.583	21	1630	43	99	764	234
8 [C4]	1.56	134	0.6605	4.18	0.0827	1.78	0.0579	3.78	2.86	28	1.052	38	512	18	100	419	113
11 [B10]	0.62	175	5.3682	1.67	0.3379	1.08	0.1152	1.27	2.86	56	0.583	35	1879	27	100	739	178
16 [D6]	0.55	110	2.4029	3.78	0.2115	1.62	0.0824	3.42	3.22	79	0.625	40	1238	35	99	825	200
17 [D7]	0.51	127	0.7120	5.77	0.0888	2.65	0.0581	5.12	2.72	40	0.578	37	548	27	97	501	118
18 [D8]	0.80	170	0.7366	5.83	0.0907	2.99	0.0589	5.01	3.27	48	0.593	38	560	31	100	501	107
20 [F5]	0.56	39	1.7289	2.97	0.1709	1.65	0.0734	2.47	3.18	78	0.781	50	1018	29	99	439	108

For U–Th–Pb zircon analyses: (i) Sample and standard are corrected after Pb and Hg blanks; (ii) ^{206}Pb/^{207}Pb and ^{206}Pb/^{238}U are corrected after common Pb presence; (iii) Common Pb assuming ^{206}Pb/^{238}U concordant age; (iv) ^{235}U = 1/137.88 × U$_{total}$; (v) Standard GJ-1; Th/U = ^{232}Th/^{238}U × 0.992743; (vi) the isotope ratios errors in the table are calculated 1 sigma and the ^{206}Pb/^{238}U concordant age with 2 sigma error. (vii) degree of concordance = (^{206}Pb/^{238}U age × 100/^{207}Pb/^{206}U age).The FTM ages were obtained using the Equation (1); ρ_S (ρ_I), spontaneous (induced) track density; N_S (N_I), number of tracks counted to determine ρ_S (ρ_I); ρ_I, induced track density of sample measured that was obtained in a white mica.

Zircon grains were dated with a laser ablation microprobe (New Wave UP213) coupled to an MC-ICP-MS (Neptune) at the Isotope Geology Laboratory of UFRGS (see Table 1). Isotope data were acquired using static mode with a spot size of 25 μm in the same zircons dated by FTM and largely in the same region of the zircon grain. Laser-induced elemental fractional and instrumental mass discrimination were corrected by the reference zircon (GJ-1)

(Simon et al., 2004), following two GJ-1 analyses for every ten samples. For common Pb correction, we assumed that the ^{204}Pb values obtained from zircons have a common Pb composition (Stacey and Kramers, 1975), assuming a concordant age of ^{206}Pb/^{238}Pb and ^{207}Pb/^{206}Pb as estimated age. Table 1 shows the operating conditions of the lasers. Detailed analytical methods and data treatment can be found elsewhere (Guadagnin et al., 2010).

4. Combining FT and U–Pb analysis applied to detrital zircon

The pioneering work that combined both FT and U–Pb analysis in detrital zircons was made by Carter and Moss (1999). While each detrital zircon dating technique may provide unique source information, in any study, there invariably remain questions about each method's limitations. For example, U–Th–Pb dates are characterized by a high resistance to thermal overprinting and may therefore not represent an immediate terrane, instead deriving from more geographically and temporally distal sources due to polycyclic history. Similarly, it remains unclear whether a measured FTM age relates to source cooling and/or zircon formation. Detrital zircon data derived from either the FTM or U–Th–Pb methods are thus inherently ambiguous, and their separate use may result in a biased or misleading provenance interpretation. By adopting a dual zircon dating approach, combining both FT and U–Th–Pb analyses on the same samples and/or grains, such limitations can be overcome, and the optimum amount of provenance information that relates to the age structure and thermal evolution of the immediate source terranes can be extracted (Carter and Bristow, 2000).

This work improved the methodology described in Carter and Moss (1999). The ages found in both methods (detailed in the Tables 2 and 3) were obtained in the same grains and, more specifically, in the same areas of the grains. Initially, each sample was mapped by optical microscopy and dated. Then the grains were dated by the FTM and the U–Th–Pb method. The etching applied in the FTM helped to indicate at which specific area of grain the spot laser should be applied. This area presented uniform FT distribution.

5. Results

5.1. Fission track methodology

In Table 2 are the fission track data ages and Fig. 3 shows the FT age distribution of 96 grains distributed in nine samples from the Vale do Rio do Peixe formation. In Fig. 3, we present all FT zircon data in a frequency *versus* age (Ma) histogram, showing two main peaks at 525 ± 15 Ma and 354 ± 6 Ma. The present diagram shows an asymptotic curve, suggesting three or more populations of age groups.

To distinguish among different age populations, we plotted the nine samples in a normalized age *versus* FT zircon age (Ma)

probability diagram (Fig. 4). The process recognized three main histogram groups: (i) red lines represent populations in the primary age range (from ca. 300 to 239 Ma), (ii) green lines represent those from 500 to 650 Ma, and (iii) blue lines represent multiple populations, such as sample ZGC7 with two age populations from 490–460 Ma to 720–860 Ma.

The first group of samples (red lines in Fig. 4) had zircon ages from ca. 239 to 339, 353 to 369 and 581 to 637 Ma (ZSE12), from 277 to 303 Ma, 422 to 448 Ma and 510 to 598 Ma (ZNP9), from 239 to 334 Ma, 439 to 440 Ma and 550 to 616 Ma (ZAL13) and from 250 to 332 Ma, 359 to 462 Ma and 554 to 614 Ma (ZEM11). These samples present dominant ages from 239 Ma to 339 Ma and two subordinate older zircon age populations.

The second group of samples (blue lines in Fig. 4) has a normalized age probability histogram ranging from 345–501 to 739–825 Ma (Sample ZGC7) and from 244 to 327, 422 to 451 and 591 to 648 Ma. The third group of samples (green lines in Fig. 4) is dominated by zircon ages from 497 to 696 Ma (samples ZPV22, ZFM8 and ZPI23) but also includes ages from 280 to 461 Ma (samples ZFM8 and ZPI23).


Fig. 3. FT ages distribution for all dated zircon grains of Vale do Rio do Peixe Formation. The solid line represents the relative probability.
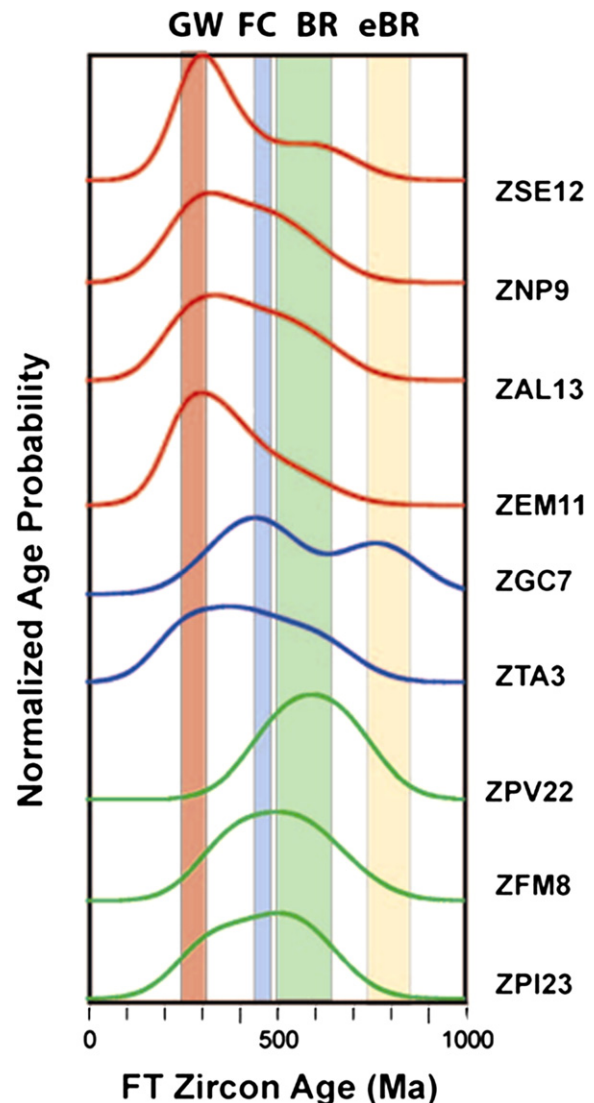
Fig. 4. Normalized ages probability *versus* FT ages for all dated zircon grains.

5.2. U–Pb in situ zircon data

Because the Th/U ratios vary from 0.20 to 1.57, the zircon grain U–Pb ages obtained are magmatic. A Th/U ratio greater than 0.2 indicates igneous zircons as opposed to metamorphic zircons, which usually have very low values (10^{-2} to 10^{-3}) (Cates and Mojzsis, 2009). In Fig. 5A, the distribution of all dated zircons distinguishes major age populations with main peaks at 513 ± 23 Ma, 1007 ± 15 Ma, 1776 ± 24 Ma, and 2024 ± 30 Ma and one zircon at 2658 ± 66 Ma. The same figure shows the distribution of FT zircon ages for comparison.

For individual samples, the three analyzed samples represent very important Brazilian zircons formed from 514 to 668 Ma (sample ZPI23), 512 to 679 Ma (ZEM11) and 512 to 624 Ma (ZGC7), respectively. The second important population of zircon ages comprise the Paleoproterozoic zircons, which were formed from 1758 to 2066 Ma (ZPI23), 1681 to 2085 Ma (ZEM11) and 1630 to 1879 Ma (ZGC7). Both populations can be recognized as Fields I and III in Fig. 6, and a subordinate population is represented by the zircon aged from ∼1.0 to 1.2 Ga, as Field II in Fig. 6. We also recognized one Archean and three early Neoproterozoic zircon local occurrences.

5.3. Discussion of results

FT zircon data are usually younger than those ages obtained by the LA-MC-ICP-MS (Fig. 5), range from 239 to 825 Ma, and can be related to the four main orogenic cycles of the South American plate: the Gondwanide (GW, 230–300 Ma), Famatinian and Cuyania (FC, 460–490 Ma), Brazilian (BR, 500–650 Ma) and early Brazilian (eBR, 696–825 Ma).

The Neoproterozoic orogenic cycles are well distributed and documented in the South America. Accretion of Famatinian Terrane and Cuyana Terrane in Central Andes occurred at 460 Ma Famatinian cycle in northern Chile and the Argentine Puna formed mainly from 490 to 470 Ma early to middle Ordovician arcs. In the Late Paleozoic (300–230 Ma) took place a very important orogenic event at the margin of the pan-Pacific Gondwana, that is described as Gondwanides Orogeny. These are very well documented at the western South America margin in the Andean Mountains (e.g., Ramos, 2009; Ramos and Alemán, 2000), and responsible by the

input of the zircons aged from ∼300 Ma to 250 Ma in the sedimentary cycle of the South American Platform.

These cycles appear in Fig. 4 as red, blue, green and pink, respectively. This information suggests provenance of at least four different sources in terms of age grouping in the Bauru Basin. However, most zircons are recycled because the main source area for the sediments was likely the Paleozoic Paraná Basin. We speculate that these zircons reached 220 °C during the main exhumation processes of the South American Plate, especially during orogenic processes that affected the plate as well. Fig. 5 presents ages obtained by both methods. Even when in the same grain, most zircon ages derived via FTM analysis are younger than those derived using the U–Th–Pb method. This suggests that zircon crystallization occurs at approximately 850 °C, the temperature associated with U–Th–Pb dating, while the zircon tracks form at approximately 220 °C.

To understand the obtained ages with combined zircon methods, we plotted the three samples against both U–Pb and FTM zircon ages. The integration of both sets of data allows us to distinguish different source areas for the 90- to 100-Ma-old sediments of the Vale do Rio do Peixe Formation, which is composed of Brazilian, Early Neoproterozoic, Mesoproterozoic and Paleoproterozoic source rocks (in declining order of age) (Figs. 5A and 6). The analyzed zircons show a clear provenance of Brazilian aged zircons, ranging from 445 ± 14 to 708 ± 18 Ma. The second important group is the Paleoproterozoic zircons formed from 1879 ± 23 to 2085 ± 27 Ma. Minor occurrences of Early Neoproterozoic and Mesoproterozoic zircons formed from 836 ± 15 to 1780 ± 38 Ma provide additional information on sedimentary input in the Bauru Basin. These zircons are incorporated from the source areas of Brazilian Belts, such as those situated west of Bauru Basin in the Tocatins Province and Paleoproterozoic Rhyacian Terranes located in the northern, western or eastern Bauru Basin. The Mesoproterozoic zircons are sourced from areas situated to the west (e.g., the mafic–ultramafic complexes of the Goiás Massif, as discussed by Ferreira Filho et al., 2010) or to the north (from the Mesoproterozoic basin of the Espinhaço region). A detailed comparison of FTM apparent ages and U–Pb crystallization ages for samples ZCG7, ZEM11 and ZPI23 provide the following conclusions. First, the three analyzed samples contain grains with Neoproterozoic ages (500–700 Ma) and Early Neo to Mesoproterozoic ages (800–996 Ma) that were exhumed at
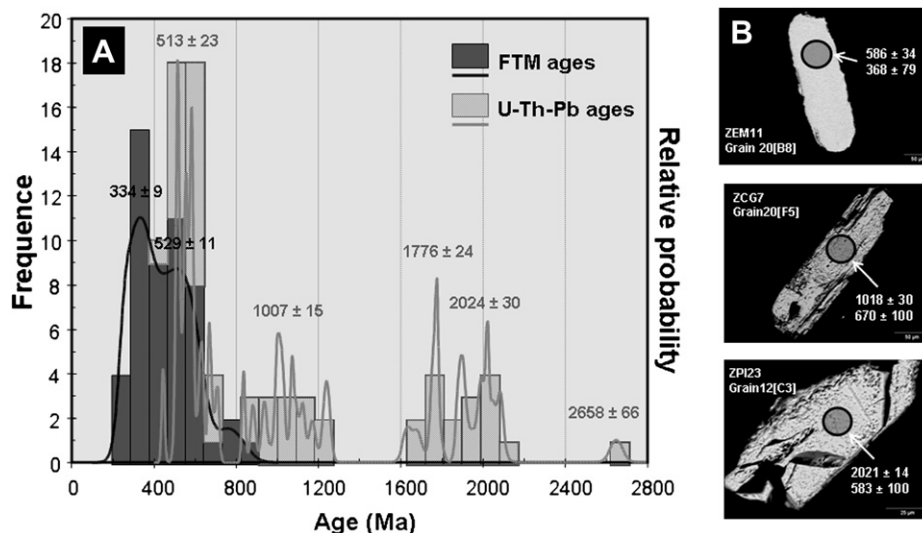

Fig. 5. (A) FT and U–Pb zircon ages distribution of sedimentary samples from the Vale do Rio do Peixe Formation. (B) Back Scattering images with U–Pb (upper) and FT (lower) ages. The circle represents the laser spot area obtained during the laser ablation U–Pb method.
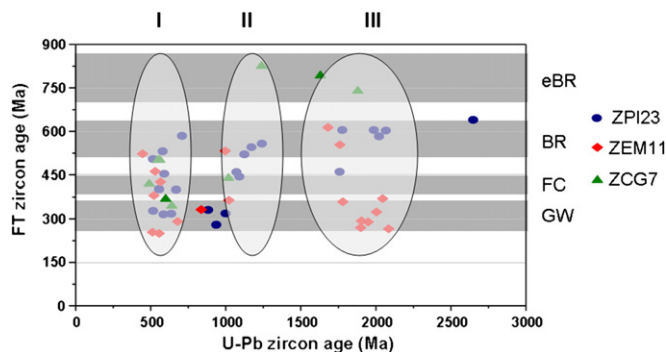
Fig. 6. FT *versus* U–Pb zircon ages for the samples from the Vale do Rio do Peixe Formation. The I, II and III fields are related to the U–Pb zircon ages, whereas eBR, BR, FC and GW fields to the FT zircon ages (see text for further explanation).

different times and possibly from different places, suggesting origins in a reworked source (e.g., Paleozoic Paraná rocks). Second, ZPI23 contained Paleoproterozoic or Archean zircons that were exhumed around 600 Ma (A2, B2, C3, C7 and D7), possibly from a basement inlier within the mobile Brazilian Belt located either in the Goiás Massif or the São Francisco Craton. Additionally, ZCG7 contains three grains with Mesoproterozoic ages that were exhumed during Early Neoproterozoic from 739 to 825 Ma. These zircons may be related to the mafic–ultramafic complexes of the Goiás Massif, which were incorporated by metamorphic and deformational processes during the Mara Rosa orogeny, a 700–800 Ma orogenic process in the Brazilian Shield, similar to the Goiás Massif and situated west of Bauru Basin. Finally, ZEM11 shows a cluster of zircons with Paleoproterozoic age (1800–2100 Ma) that were exhumed from late Devonian to Permian time (C1, J2, F5, C8, F8, A9 and H9) and range from 370 to 250 Ma. Zircons I4, E6, B8, A9 and D10 crystallized during the late stages of the Brazilian Cycle (586–512 Ma) and were exhumed from 381 to 250 Ma. Both zircon sets provide important information about exhumation time in the South American Plate related to the Gondwanide orogeny.

The Bauru Group zircons analyzed here were reworked sediments from the Paleozoic to Triassic Paraná Basin and from inlier basement rocks formed during the Precambrian. Additionally, the FTM zircon ages may reflect denudation processes extending from the total to partial annealing zones at different orogenic cycles of the South American Plate from the Neoproterozoic to the Triassic, in particular the Early Brazilian, Brazilian and Famatinian/Cuyania (Ordovician to Silurian) and the Gondwanide (Carboniferous to Early Triassic) orogenies. Those FT zircon ages close to 250 Ma are interpreted as belonging to the late Gondwanide orogeny, as recorded in the Permian sediments of the Paraná Basin.

6. Conclusions

The combination of high-temperature U–Pb zircon dating and intermediate- to low-temperature FTM zircon dating provided a powerful tool for unraveling the origin of the rocks and morphotectonic events in the geological evolution of the South American Plate. The U–Th–Pb method provided consistent information about the main source areas of the Vale do Rio do Peixe Formation sediments, formed between 90 and 100 Ma and dominated by Brazilian and Rhyacian zircons with additional Early Neoproterozoic and Mesoproterozoic (or Greenvilian coeval material) sources. The main sedimentary source for this basin originated in the Paraná Basin sediments containing reworked zircons of the Paleoproterozoic to Eopaleozoic crystalline basement or in the

western and northern Bauru Basin basement rocks. The early Neoproterozoic zircons could have been transported from the Goiás Massif region, a region west of the Bauru Basin containing a Mara Rosa orogenic belt, which formed at that time. The FTM data can be grouped in four distinct age groups: the early Neoproterozoic, Brazilian, Ordovician–Silurian and Carboniferous–Early Triassic. The exhumation processes of the early Neoproterozoic and Brazilian are related to basement inliers situated to the west of the Bauru Group units (e.g., the Goiás Central Massif). The Paleozoic ages analyzed here are grouped in the two main mountain formations of the western South American Platform: the Famatinian and Gondwanide orogenies. The latter is well represented by FTM apparent ages from ∼370 to 250 Ma and indicates the passage of zircon from the total to partial annealing zone during the Gondwanide Cycle. Continued comparative analyses of FTM and U–Th–Pb data are needed, but the combination of the two techniques is promising. FTM applications in zircon dating remain coherent with known geological data.

References

Bigazzi, G., Guedes, S., Hadler N, J.C., Iunes, P.J., Paulo, S.R., Tello S, C.A., 2000. Application of neutron dosimetry by natural uranium and thorium thin films in fission track dating. In: 9th International Conference on Fission Track Dating and Thermochronology. Book of Extend Abstracts. Lorne, Australia, pp. 33–35.

Carter, A., Bristow, C.S., 2000. Detrital zircon geochronology: enhancing the quality of sedimentary source information through improved methodology and combined U–Pb and fission-track techniques. Basin Research 12, 47–57.

Carter, A., Moss, S.J., 1999. Combined detrital-zircon fission-track and U–Pb dating: a new approach to understanding hinterland evolution. Geology 27 (3), 235–238.

Cates, N.L., Mojzsis, S.J., 2009. Metamorphic zircon, trace elements and Neoarchean metamorphism in the ca. 3.75 Ga Nuvvuagittuq supracrustal belt, Québec (Canada). Chemical Geology 261 (1–2), 99–114.

Dias, A.N.C., Tello S, C.A., Constantino, C.J.L., Soares, C.J., Osório, A.M., Novaes, F.P., 2009. Micro-Raman spectroscopy and SEM/EDX applied to improve the zircon fission track method used for dating geological formations. Journal of Raman Spectroscopy 40, 101–106.

Fernandes, L.A., Basilici, G., 2009. Transition of ephemeral palustrine to aeolian deposits in a continental arid – semi-arid environment (Upper Cretaceous Bauru Basin, Brazil). Cretaceous Research 30, 605–614.

Fernandes, L.A., Coimbra, A.M., 1996. A Bacia Bauru (Cretáceo Superior, Brasil). Anais da Academia Brasileira de Ciências 68 (2), 195–205.

Fernandes, L.A., Giannini, P.C.E., Góes, A.M., 2003. Araçatuba formation: Palustrine deposits from initial sedimentation phase of the Bauru Basin. Anais da Academia Brasileira de Ciências 75 (2), 173–187.

Ferreira Filho, C.F., Pimentel, M.M., Araújo, S.M., Laux, J.H., 2010. Layered intrusions and volcanic sequences in Central Brazil: geological and geochronological constraints for Mesoproterozoic (1.25 Ga) and Neoproterozoic (0.79 Ga) igneous association. Precambrian Research 183 (3), 617–634.

Garver, J.I., 2003. Etching zircon age standards for fission-track analysis. Radiation Measurements 37, 47–53.

Gehrels, G.E., Juiz J. U–Th–Pb geochronology of zircon by laser-ablation multi-collector ICP mass spectrometry at the Arizona LaserChron Center. Journal of Analytical Atomic Spectrometry, in press.

Guadagnin, Felipe, Chemale Jr., F., Dussin, Ivo A., Jelinek, Andréa R., dos Santos, Marcelo N., Borba, Maurício L., Justino, Dayvisson, Bertotti, Anelise L., Alessandretti, Luciano, 2010. Depositional age and provenance of the Itajaí Basin, Santa Catarina State, Brazil: implications for SW Gondwana correlation. Precambrian Research 180, 156–182.

Guedes, S., Hadler N, J.C., Iunes, P.J., Zuñiga, A., Tello S, C.A., Paulo, S.R., 2003. The use of the U(n, f) reaction dosimetry in the determination of the λ_f value through fission-track techniques. Nuclear Instruments and Methods in Physics Reseach A 496, 215–221.

Hasebe, N., Watanabe, H., 2004. Heat influx and exhumation of the Shimanto accretionary complex: Miocene fission track ages from the Kii Peninsula, southwest Japan. Island Arc 13, 533–543.

Iunes, P.J., 1999. Utilização da dosimetria de nêutrons através de filmes finos de urânio e de tório naturais na datação de minerais com o método dos traços de fissão. Ph.D. thesis, IFGW/Unicamp, 68 p.

Iunes, P.J., Hadler N, J.C., Bigazzi, G., Tello S, C.A., Guedes O, S., Paulo, S.R., 2002. Durango apatite fission-track dating using length-based age corrections and neutron fluence measurements by thorium thin films and natural U-doped glasses calibrated through natural uranium thin films. Chemical Geology 187, 201–211.

Iunes, P.J., Hadler N, J.C., Bigazzi, G., Guedes O, S., Zuñiga G, A., Paulo, S.R., Tello S, C.A., 2004. Uranium and thorium film calibrations by particle track techniques. Journal of Radioanalytical and Nuclear Chemistry 262, 461–468.

Iwano, H., Danhara, T., 1998. A re-investigation of the geometry factors for fission-track dating of apatite, sphene and zircon. In: Van den Haute, P., De Corte, F. (Eds.), Advances in Fission-Track Geochronology, pp. 47–66.

Kŏsler, J., Fonneland, H., Sylvester, P., Tubrett, M., Pedersen, R., 2002. U–Pb dating of detrital zircons for sediment provenance studies: a comparison of laser ablation ICPMS and SIMS techniques. Chemical Geology 182, 605–618.

Lederer, C.M., Shirley, V.S., 1978. Table of Isotopes, seventh ed. John Wiley and Sons, Inc., New York, USA, 1523 p.

Menneken, M., Nemchin, A.A., Geisler, T., Pidgeon, R.T., Wilde, S.A., 2007. Hadean diamonds in zircon from Jack Hills, Western Australia. Nature 448, 917–921.

Morton, A.C., Hallsworth, C.R., 1999. Process controlling the composition of heavy mineral assemblages in sandstones. Sedimentary Geology 124, 3–29.

Ramos, V., 2009. Anatomy and global context of the Andes: main geologic features and the Andean orogenic cycle. In: Kay, S.M., Ramos, V.A., Dickinson, W.R. (Eds.), Backbone of the Americas. Shallow Subduction, Plateau Uplift, and Ridge and Terrane Collision. The Geol. Soc. of America, Memori, 204, pp. 31–67.

Ramos, V.A., Alemán, A., 2000. Tectonic evolution of the Andes. In: Cordani, E.U.J., Milani, E.J., Thomaz Filho, A., Campos, D.A. (Eds.), Tectonic Evolution of South America: Río de Janeiro, 31st International Geological Congress, pp. 635–685.

Renne, P.R., Ernesto, M., Pacca, I.G., Coe, R.S., Glen, J.M., Prévot, M., Perrin, M., 1992. The age of the Paraná flood volcanism, rifting of Gondwanaland, and the Jurassic–Cretaceous boundary. Science 258, 975–979.

Simon, E., Jackson, S.E., Pearsona, N.J., Griffina, W.L., Belousova, E.A., 2004. The application of laser ablation-inductively coupled plasma-mass spectrometry to in situ U–Pb zircon geochronology. Chemical Geology 211, 47–69.

Stacey, J.S., Kramers, J.D., 1975. Approximation of terrestrial lead isotope evolution by a two-stage model. Earth and Planetary Science Letters 26, 207–221.

Tagami, T., 2005. Zircon fission-track thermochronology and applications to fault studies. Reviews in Mineralogy & Geochemistry 58, 95–122.

Tagami, T., Murakami, M., 2007. Probing fault zone heterogeneity on the Nojima fault: constraints from zircon fission-track analysis of borehole samples. Tectonophysics 443, 139–152.

Tagami, T., Ito, H., Nishimura, S., 1990. Thermal annealing characteristics of spontaneous fission tracks in zircon. Chemical Geology: Isotope Geoscience Section 80, 159–169.

Watson, E.B., Harrison, T.M., 2007. Zircon thermometer reveals minimum melting conditions on earliest Earth. Science 308, 841–844.

Yamada, K., Tagami, T., Shimobayashi, N., 2003. Experimental study on hydrothermal annealing of fission tracks in zircon. Chemical Geology: Isotope Geoscience Section 201, 351–357.

Yamada, R., Murakami, M., Tagami, T., 2007. Statistical modelling of annealing kinetics of fission tracks in zircon; Reassessment of laboratory experiments. Chemical Geology 236, 75–91.

Yamada, K., Hanamuro, T., Tagami, T., Shimada, K., Takagi, H., Iwano, H., Danhara, T., Umeda, K., 2009. (U–Th)/He thermochronologic analysis of the median tectonic line and associated pseudotachylyte. Geochimica et Cosmochimica Acta 73 (13), A1468.

5.2. Artigo 3 (submetido)

BOL MAIL

◎ Submission Confirmation

De:	**Earth and Planetary Science Letters**
Para:	**diasanc@bol.com.br**
Assunto:	Submission Confirmation
Data:	01/05/2012 21:58

Dear M.Sc. Dias,

Your submission entitled "RECOGNITION OF MAIN TECTONIC EVENTS OF THE SOUTH AMERICAN PLATFORM BY DETRITAL ZIRCON FISSION TRACK AND U-Pb DATING OF THE INTRACRATONIC MESOZOIC BAURU BASIN, BRAZIL" has been received by Earth and Planetary Science Letters

You may check on the progress of your paper by logging on to the Elsevier Editorial System as an author. The URL is http://ees.elsevier.com/epsl/.

Your manuscript will be given a reference number once an Editor has been assigned.

Thank you for submitting your work to this journal.

Kind regards,

Editorial Office
Earth and Planetary Science Letters

Title: RECOGNITION OF MAIN TECTONIC EVENTS OF THE SOUTH AMERICAN PLATFORM BY DETRITAL ZIRCON FISSION TRACK AND U-Pb DATING OF THE INTRACRATONIC MESOZOIC BAURU BASIN, BRAZIL

Corresponding Author: M.Sc. Airton Natanael Coelho Dias, M.D.

Corresponding Author's Institution: Faculdade de Ciências e Tecnologia/UNESP

First Author: Airton N Dias, PhD.

Order of Authors: Airton N Dias, PhD.; Farid Chemale Jr, PhD.; Carlos A Tello S., PhD.; Peter C Hackspacher, PhD.; Cleber J Soares, PhD.; Camilo I Aristizábal, MSc; Sandro Guedes, PhD.

Abstract: Intracratonic basins usually record the polyhistory of cratons or plates during the deposition time as well as the remote geological time. Fission-track (FT) combined with U-Pb in situ analyses of detrital zircons thus reveals the polyhistory of this type of basin. To distinguish the crustal accretion of the South American Platform, 29 sandstone samples of the depositional sequences of the intracratonic Bauru Basin, formed between 90 and 73 Ma, were dated. The results of U-Pb zircon dating integrated with paleocurrent information and potential source areas suggest that the Rhyacian (Transmazonian Cycle, 2.2-1.9 Ga), Statherian (1.8-1.68 Ga), Sunsás-Grenvile (1.2-0.9 Ga), Tonian (Early Brasiliano, 0.9 to 0.75 Ga) and Brasiliano (0.65 to 0.50 Ga) are the main source areas. The FT data provide important evidence of rapid uplift during the Early Brasiliano and Brasiliano and yield two main Paleozoic age populations, one between 500 and 360 Ma and other between 345 and 230 Ma. These age populations are interpreted to reflect the main tectonic event along the western margin of the South American Platform that affected the platform's internal composition by uplift and exhumation. These materials have been recycled by sedimentary processes in a continental intraplate environment without attaining the necessary temperature to reset the FT isotopic system of the studied zircons and thereby depositing during the Upper Cretaceous.

Julio Hadler PhD.
Instituto de Física Gleb Wataghin, Universidade de Campinas - UNICAMP - 13083-970 - Campinas, SP - Brasil. Phone: +55 19 35215317
hadler@ifi.unicamp.br
He and his research group worked in the last decades on the Fission Track analytical procedures on apatite, mainly on the physical aspects.

João Orestes Santos PhD.
Centre for Exploration Targeting, University of Western Australia, 35 Stirling Highway, Crawley, 6009 Perth, WA, Australia.
orestes.santos@bigpond.com
He worked for several decades mainly with in situ geochronology of U-Pb on minerals to unravel the tectonic history of magmatic, metamorphic and sedimentary rocks from South American Platform.

Victor Alberto Ramos PhD.
Instituto de Estudios Andinos "Don Pablo Groeber", Universidad de Buenos Aires - CONICET - Buenos Aires – BS, Argentina
andes@gl.fcen.uba.ar
Victor Ramos is on of the main researcher worldwide on the Paleozoic Evolution of those rocks found in the Andean Mountains, like the Famatinain and Gondwanides related rocks.

Opposed Reviewers:

TO:

T.M. Harrison
Managing Editor
Earth and Planetary Science Letters   April 30, 2012.

JOURNAL TITLE : Earth and Planetary Science Letters
MANUSCRIPT TITLE: RECOGNITION OF MAIN TECTONIC EVENTS OF THE SOUTH AMERICAN PLATFORM BY DETRITAL ZIRCON FISSION TRACK AND U-Pb DATING OF THE INTRACRATONIC MESOZOIC BAURU BASIN, BRAZIL
CORRESPONDING AUTHOR: Airton Natanael Coelho Dias

Dear editor,

Enclosed please you find the manuscript on "**RECOGNITION OF MAIN TECTONIC EVENTS OF THE SOUTH AMERICAN PLATFORM BY DETRITAL ZIRCON FISSION TRACK AND U-Pb DATING OF THE INTRACRATONIC MESOZOIC BAURU BASIN, BRAZIL** " by Dias et al., which I would like to submit it to the Earth and Planetary Science Letter for peer review process. This manuscript has not been previously published, is not currently submitted for review to any other journal, and will not be submitted elsewhere before one decision is made.

The present manuscript has as main propose the use of double dating methods in zircon (U-Pb in situ and FT method) applied to sedimentary rocks from the Bauru Basin, Brazil, formed in an intracratonic tectonic setting. The obtained results were the integration of sedimentary flow during the deposition of the Bauru Basin with the potential source areas and of U-Pb and FT zircon dating to distinguish the main source areas as well as the main tectonic events in the South America Platform.

If you need additional information, please do not hesitate to contact me.

Sincerely,

Airton Natanael Coelho Dias

Instituto de Física - UFU - Av. João Naves de Avila 2121 - Uberlândia-MG, Brazil.
Phone: +55 (34) 3239-4607. e-mail: diasanc@bol.com.br

1   **RECOGNITION OF MAIN TECTONIC EVENTS OF THE SOUTH AMERICAN PLATFORM**

2   **BY DETRITAL ZIRCON FISSION TRACK AND U-Pb DATING OF THE INTRACRATONIC**

3   **MESOZOIC BAURU BASIN, BRAZIL**

4   A. N. C. Dias [1,*], F. Chemale Jr.[2], C. A. Tello S. [3], P. C. Hackspacher [5], C. J. Soares [4], C. I.

5   Aristizabal [6], S. Guedes[4]

6

7   [1] Instituto de Física, UFU – 38400-902, Uberlândia-MG, Brazil

8   [2] Universidade de Brasília, Instituto de Geociências, IG-UnB, 70910-900, Brasília, DF, Brazil

9   [3] Dep. de Física, Química e Biologia, UNESP, 19060-900, Presidente Prudente, SP, Brazil

10   [4] Instituto de Física "Gleb Wataghin", UNICAMP, 13083-970, Campinas, SP, Brazil

11   [5] Instituto de Geociências e Ciências Exatas, UNESP, 13506-900, Rio Claro, SP, Brazil

12   [6] Laboratório de Geologia e Geofísica Marinha – LAGEMAR, UFF, 24210-346, Niterói, RJ,

13   Brazil

14

15   *Corresponding Author: Instituto de Física -UFU - Av. João Naves de Avila 2121 - Uberlândia-

16   MG, Brazil. Phone: +55 (34) 3239-4607. e-mail: diasanc@bol.com.br

17

18   **Abstract**

19   Intracratonic basins usually record the polyhistory of cratons or plates during the deposition

20   time as well as the remote geological time. Fission-track (FT) combined with U-Pb in situ

21   analyses of detrital zircons thus reveals the polyhistory of this type of basin. To distinguish the

22   crustal accretion of the South American Platform, 29 sandstone samples of the depositional

23   sequences of the intracratonic Bauru Basin, formed between 90 and 73 Ma, were dated. The

24   results of U-Pb zircon dating integrated with paleocurrent information and potential source

25   areas suggest that the Rhyacian (Transmazonian Cycle, 2.2-1.9 Ga), Statherian (1.8-1.68

26   Ga), Sunsás-Grenvile (1.2-0.9 Ga), Tonian (Early Brasiliano, 0.9 to 0.75 Ga) and Brasiliano

27   (0.65 to 0.50 Ga) are the main source areas. The FT data provide important evidence of rapid

28   uplift during the Early Brasiliano and Brasiliano and yield two main Paleozoic age populations,

29   one between 500 and 360 Ma and other between 345 and 230 Ma. These age populations

30   are interpreted to reflect the main tectonic event along the western margin of the South

31   American Platform that affected the platform's internal composition by uplift and exhumation.

32   These materials have been recycled by sedimentary processes in a continental intraplate

33   environment without attaining the necessary temperature to reset the FT isotopic system of

34   the studied zircons and thereby depositing during the Upper Cretaceous.

35

38

39

40   **1. Introduction**

41

42   Zircon has become one the most important minerals for studying the evolution of

43   sedimentary basins. U-Pb detrital zircon studies are applied to different types of basins to

44   reveal their provenance or sedimentary source and to correlate sedimentary sequences,

45   maximum depositional ages and the tectonic environment. On the other hand, the FT zircon

46   methodology reveals the low-temperature history of zircon from 200 to 320°C (Garver and

47   Brandon 1994; Tagami, 1998; Carter and Moss, 1999; Liu et al., 2001; Bernet et al., 2001),

48   which can provide much information regarding the denudation process in different tectonic

49   situations and an estimation of the maximum depositional age. The combination of the two

50   techniques, applied to detrital zircons in sedimentary rocks, can therefore provide very

51   important information regarding high-temperature and intermediate- to low-temperature

52   geologic events such as the igneous and metamorphic crystallization of zircons,

morphotectonic events (uplift, denudation, etc.) and sedimentary provenance, as described above. The best samples for performing FT thermochronology on detrital zircon are from synorogenic sediments formed during the Cenozoic, such as those in Himalayas and Andes, where it is a well-established tool for examining the cooling and exhumation history of convergent mountain belts (Garver et al., 1999; Bernet et al., 2006). In this area of rapid exhumation rates, low-temperature thermochronological systems, such as FT and U-Th/He on zircon and apatite and 40Ar/39Ar on mica or feldspar, have recorded the recent history without the memory of earlier events (Stuart, 2002; Bernet et al., 2006; Carrapal et al., 2009).

Combined FTM and U-Pb detrital zircon analyses are also used in different types of basins, to better understand the relationship between sedimentary sources and the infilling of a basin (Carter & Moss, 1999). In some cases, it is possible to determine the deposition, accretional events and metamorphism of metamorphic complexes along the ancestral margin, such as that of the ancestral Pacific margin of Gondwana, Chile during the Mesozoic (Thomson & Hervé, 2002). (U-Th)/He and U/Pb analyses are also integrated and applied to detrital zircons from the Lower Jurassic Navajo Sandstone, which is made up of erg deposits and situated close to a convergent margin but in a more stable platform. A large fraction of zircons formed between 1200 and 950 Ma but cooled below ~180 °C ca. 500–250 Ma, recording the formation of the Rodinia Supercontinent and later crustal convergence related to the Appalachian orogenesis situated to the east of the Navarro Basin (Rahl et al., 2003).

Intracratonic basins, which are the focus of this study, are located on the stable continental lithosphere (Sloss and Speed, 1974), located some distance from stretched or convergent margins (Allen & Armitage, 2012). These basins are characterized by low-rate sedimentation over a period of one hundred million years, a thickness of no more than 5 km and a widely superficial distribution (over one million square kilometers). The sedimentation may extend back more than 600 Ma, such as for the Central Australian or Espinhaço Basins

78 (Shaw et al. 1991, Chemale et al., 2012), or less than 400 Ma, as for the Phanerozoic

79 Michigan and Paraná Basins (Sloss, 1963, Zalan et al., 1990). Their sediments can thus

80 register a multifarious history of the cratonic areas that can be associated with geological

81 events of extensional or convergent margins situated at distances as large as one thousand

82 kilometers. Many important records of these events may be found in the intraplate continental

83 environment, as described for the Phanerozoic intracratonic basins (Lindsay, 2002).

84   The main purpose of this study was to understand the geological history of the

85 intracratonic Bauru Basin, formed during the Mesozoic at the center of the South American

86 Platform, and to determine its main source areas and maximum depositional age based on

87 the apparent and absolute ages obtained from the zircon of sedimentary rocks by FTM and U-

88 Pb *in situ* via LA-MC-ICP-MS analysis, respectively. Furthermore, the combination of both

89 zircon ages is applied to reveal the main crustal formation and denudation events of the

90 South American Platform.

91

92

93 **2. Geological setting**

94

95   The study area is located in the middle of the South America Platform (Fig. 1),

96 where the Paleozoic to Triassic sedimentary sequence of the Paraná Basin, the lava flows

97 (Paraná Basalts) and associated aeolian sediments (Botucatu Fm.) of the Lower Cretaceous

98 São Bento Group and the Upper Cretaceous sedimentary sequence of the Bauru Basin are

99 distributed, all of which formed in an intracratonic environment. The average crustal thickness

100 is ca. 40 km, and the area is located ca. 500 km away from the eastern Brazilian passive

101 margin and 1500 km from the Andean Mountains.

102

2.1. Bauru Basin

The Bauru Basin occurs as a continental sequence up to 320 m thick (Paula e Silva et al., 2009) in southeastern and central Brazil, which unconformably overlies the Lower Cretaceous Serra Geral magmatic units (or Paraná Basalts and related rocks) and sediments of the São Bento Group (Suguio, 1997). These continental sediments represent the last important sedimentation in the intraplate (or intracratonic) position of the South America Platform, widespread over approximately 370,000 km^2 in the states of Paraná, São Paulo, Minas Gerais and Goiás, Brazil (Fernandes and Coimbra, 1996; Paula e Silva et al., 2009). The age of the Bauru Group is still a subject of debate but is generally accepted to be the Upper Cretaceous, as evidenced by the vertebrate fossiliferous content and upper alkaline rocks (Fernandes and Coimbra, 1996, Paula e Silva et al., 2009), and correlated to the evolution stages of the Santos Basin, at the Brazilian passive margin (Pereira et al., 1986). A regional unconformity is also marked at the top of Bauru sedimentary units, which is described as the Sul-Americana (King, 1956) or Japi (Almeida, 1964) surface. The age of this regional surface is estimated to be between 78 and 73 Ma (Almeida & Carneiro, 1998). During the deposition of the Bauru Basin, between 90 Ma and 73 Ma, the basin was marked by arid to semi-arid conditions with alternating hot/dry and rainy seasons. These climatic conditions enabled a diversification of fauna (invertebrate and vertebrates) and flora in a depositional environment with an alluvial plain, braided to meandering rivers and small lakes (Carvalho et al., 2004).

Paula e Silva et al. (2009) described the main stratigraphic units in light of the sequence stratigraphy and based on field and drill-hole information. They defined three main depositional phases separated by two erosive/non-depositional phases, as shown in figure 2. The initial phase of the deposition of the Bauru Basin, **Depositional Sequence 1**, is marked by the regional unconformity on the São Bento Group units, which is related to the tectonic

128   adjustment of the South America Platform due to thermal cooling of the lithosphere after

129   intense Paraná magmatism (Milani, 1997). The sedimentation was controlled by earlier

130   lineaments and manifested as aeolian-fluvial sandstones and lacustrine mudstones, which

131   filled the valley on the basaltic substratum. These units are interdigitated as part of the Caiuá

132   and Pirapozinho formations (Paula e Silva et al., 2005). They formed in an endorreic fluvial

133   system, which evolved into meandering rivers that flowed to a shallow lacustrine environment,

134   with main influx towards the northeast (Paula e Silva et al. 2009).

135   **Depositional Sequence 2** represents a new subsidence process associated with a

136   fluvial braided system, with dominant sand deposits and subordinate clay-rich sedimentation.

137   Meandering and aeolian dunes facies occurred locally. These sedimentary deposits compose

138   the Anastácio Fm (Fig. 2) and were deposited in erosional unconformity on the Caiuá and

139   Pirapozinho Formation units.

140   The third tectonic event occurred in the Bauru Basin with the deposition of the

141   sediments of **Depositional Sequence 3**. A local fluvial braided and channelized system was

142   installed over the Depositional Sequence 2 units, the sediment record of the Birigui Fm. (Fig.

143   2). The main sedimentation of **Depositional Sequence 3** was manifested as shallow

144   lacustrine and a meandering system as part of the Araçatuba and Lower Member of the

145   Adamantina Formation (Vale do Rio do Peixe Member, Fig. 2). Paula e Silva et al. (2009)

146   detailed the basal section of the Adamantina Formation, which formed by successive

147   sandstone bodies with increasing thickness and grain size. Alkaline extrusive bodies,

148   described as Taiúva Analcimite (Coutinho et al., 1982), occur in the lower Adamantina

149   Formation. Paula e Silva et al. (2006) interpreted the lower section to be small lacustrine

150   deltas. The upper portion of the Adamantina Fm. (sensu Paula e Silva et al., 2009), here

151   defined as Presidente Prudente Member (or Presidente Prudente Fm after Fernandes and

152   Coimbra, 1996), is represented by meandering to braided fluvial deposits, overlying the basal

153 deltaic-lacustrine sediments. The upper section of the Bauru basin is represented by the

154 Marilia Fm., which is characterized by an increase in the aridity of the basin. The Marília Fm.

155 is composed of alluvial deposits, such as an alluvial plain (ephemeral braided systems) with

156 small lakes (Carvalho et al., 2004) in the form of marginal fans (Paula e Silva et al. 2009) (Fig.

157 2).

158

159

160 **3. Materials and methods**

161

162 Twenty-nine sandstone samples were collected from the Caiuá, Santo Anastácio

163 and Lower (Vale do Rio do Peixe Member) and Upper (Presidente Prudente Member)

164 Adamantina Formation in the southwestern portion of the Bauru Basin, São Paulo State,

165 Brazil (Fig. 1). Previous analyses have already been published by Dias et al. (2010) and Dias

166 et al. (2011), which correspond to 12 samples dated by FTM and 5 samples dated by the U-

167 Pb zircon method. In this work, we carried out an additional 17 analyses using the FT method

168 and 5 analyses using the U-Pb zircon method. Thus, we integrated the information gathered

169 from 29 samples dated by FTM, 10 of which were dated by the combined FT and U-Pb dating

170 methods; thus, the FT apparent ages of 376 grains and U-Pb detrital zircon ages of 158

171 grains in total were determined. Figure 1 shows a geological map of the study area with the

172 sample locations, and figure 2 shows the stratigraphy and depositional environment of the

173 sedimentary units from Bauru Basin, as proposed by Paula e Silva et al. (2009).

174

175 *3.1. Materials*

176 Zircons were separated by conventional procedures using heavy liquids and a

177 magnetic separator after concentrating by hand panning. Zircons were handpicked for FTM

178 and LA-MC-ICP-MS analyses. First, the zircons were mounted and polished in Teflon for FT

179 analyses. During the assembly process, the zircons were ground, polished and etched; a

180 binocular magnifying glass Carl-Zeiss, model Citoval 2, was used to observe the materials. A

181 polishing machine and sandpapers with grit sizes of 1200, 2400 and 4000 were used to grind

182 the zircons, which were then polished using a polishing cloth and diamond paste, with 1 and

183 ¼ µm granulometries. Finally, a digitally controlled oven was used to etch the zircons. The

184 zircon FT ages were obtained at the Departamento de Física, Química e Biologia of UNESP,

185 Brazil, under a Leica DMRX microscope. For FT analyses, the samples were irradiated in the

186 nuclear reactor of IPEN/CNEN in São Paulo State, Brazil. After the FT zircon dating was

187 performed, the U-Pb zircon Teflon mounting was adapted to epoxy mounting for U-Pb dating

188 at the Isotope Geology Laboratory of Rio Grande University, Brazil, using a laser microprobe

189 (New Wave UP213) coupled to a MC-ICP-MS (Neptune).

190

191 **_3.2. Methods_**

192

193 **_3.2.1. Fission-track analysis (FT)_**

194 The Fission-track Method (FTM) has developed into one of the most useful

195 techniques that is used throughout the geological community to reconstruct the low-

196 temperature thermal history of rocks over geological time. The FT method is based on the

197 accumulation of narrow damage trails (i.e., fission tracks) in uranium-rich mineral grains (e.g.,

198 apatite, zircon, titanite) and natural glasses, which form as a result of spontaneous nuclear

199 fission decay of ^{238}U in nature (Price and Walker 1963; Fleischer et al. 1975; Tagami &

200 O'Sullivan 2005). Uranium fission creates latent tracks, which disrupt the crystalline structure

201 of materials as a result of the great charge, mass, and energy released during the fission

202 process. These tracks have a diameter of about 1 Å, which can be observed by optical

203   microscopy after etching (Wagner & Van den Haute, 1992; Dias et al., 2009). The total kinetic

204   energy of a fission fragment pair is about 170 MeV (Fleischer, 2004), corresponding to a

205   range of ~20 μm in fluorapatite and ~16 μm in zircon. By etching, the 5-10 nm wide fission

206   tracks are enlarged to several micrometers, which can be directly observed by optical

207   microscopy (Gleadow et al., 1986). During track formation, a fission track becomes

208   discontinuous at each end of the track trajectory, impeding chemicals from further etching the

209   material (Villa et al., 1999). This process results in etched lengths of ~16 μm in apatite (Green

210   et al., 1986) and ~11 μm in zircon (Yamada et al., 1995).

211   The time elapsed since fission tracks began to accumulate is estimated by

212   determining the density of accumulated tracks in a particular material in relation to the

213   uranium content of that material. Chemical etching can be used to enlarge fission tracks that

214   have formed within a mineral to make them readily observable under an ordinary optical

215   microscope (Price and Walker, 1962). The age is obtained by counting both the fossil (^{238}U

216   spontaneous fission) and the induced (^{235}U induced fission) tracks using an optical

217   microscope. The induced tracks are obtained by irradiating a sample with thermal neutrons in

218   a nuclear reactor, which causes the fission of the ^{235}U isotope. Within the FTM, two methods

219   are used to carry out dating. In the External Detector Method (EDM), spontaneous fission

220   tracks are measured in a mineral, and the induced fission tracks are measured using a

221   detector external to the mineral (mica muscovite, for instance). In the Population Method,

222   induced and spontaneous fission tracks are measured in the mineral itself (Wagner and Van

223   der Haute, 1992). In this study, the ages of the zircon fission tracks were determined using a

224   mathematical equation presented in Iunes et al. (2002, 2005).

225   Using the FTM, in zircon, both age and thermal events can be determined in

226   regions of geological interest. Because the closure temperature of zircon is ~ 240 ºC, which

227   corresponds to temperatures at which the tracks are retained over geological time, it is

228 possible to determine ages close to the crystallization ages of some minerals (Tagami, 2005).

229 This method can be also used in oil research because at the depths at which apatite (with a

230 closure temperature of ~ 120 ^{o}C) suffers total annealing zircon can still provide information

231 about the thermal evolution of the basin where the perforation was made (Yamada et al,

232 1998, 2003). For these and other reasons, the FTM has developed into one of the most useful

233 techniques used throughout the geological community,

234 Zircon has become one of the most important minerals for studying sediment

235 provenance and the exhumation history of orogenic belts. The usefulness of zircon lies in its

236 commonness in many igneous, metamorphic, and sedimentary rocks, its resistance to

237 weathering and abrasion, and its ability to be dated using various isotopic methods. With its

238 relatively high concentrations of uranium and thorium, zircon is one of the most useful

239 minerals used to unravel the Earth's history recorded in rocks (Bernet and Garver, 2005;

240 Tagami, 2005).

241 The ability of zircon to retain information about the most recent thermal history of a

242 source area is invaluable in elucidating the geological processes and system responses

243 experienced by the area over a range of geodynamic settings. As a consequence, the FTM

244 paired with zircon has been extensively employed, along with other radiometric dating

245 methods such as U-Pb (for instance, Davis et al. 2003; Chemale et al., 2012; Barredo et al.,

246 2012) and (U-Th)/He techniques (Reiners 2005), to understand the thermochronology of

247 rocks in a variety of geological settings, i.e., thermal history analysis of basement rocks for

248 orogenic studies, thermochronology using detrital zircon grains in sedimentary rocks for

249 provenance analysis and thermal history analysis in or near faults (Carter, 1999; Garver et al.

250 1999; DeCelles et al., 2000; Hasebe and Tagami, 2001; Spikings et al., 2001; Yamada et al.,

251 2003; Hasebe and Watanabe, 2004; Garver, 2003; Dias et al., 2010 and 2011).

252

3.2.1.1. FT annealing phenomena

Knowledge of the stability and annealing of fission tracks is critically important in decoding the geological history recorded by a host mineral. The thermal annealing of fission tracks at increased temperature (or time) is a process during which the amorphous, disordered core is gradually restored to the ordered structure of a crystalline matrix. This behavior in latent tracks can be directly observed by TEM (Paul and Fitzgerald, 1992; Paul, 1993; Jaskierowicz et al., 2004; Li et al., 2011).

The present understanding of the annealing process is largely limited to mathematical fits to data for etched track lengths as a function of temperature, time and composition. The internal structure of latent fission tracks controls the annealing process and, correspondingly, the shortening of track lengths. However, the empirical equations do not reflect the relationship between the internal structure of tracks and their annealing behavior because the structural information of tracks is lost as a result of chemical etching. Even a highly cited physical model of the process has met considerable criticism in the absence of actual observations of the atomic-scale process (Carlson, 1990; Crowley, 1993; Green et al., 1993). Atomic-scale studies of fission track fading have long been recognized as necessary for the development of quantitative models of fission track formation and annealing (Rabone et al., 2008; Li et al., 2011).

According to Tagami and O'Sullivan (2005), the annealing process is characterized by the development of irregular morphology at the track-matrix boundary, segmentation of the track, i.e., appearance of gaps, an increase in the spacing between segments, the shape of which approaches a sphere, and instantaneous healing of spheres, with an observable minimum diameter of ~3 nm. The annealing likely occurs through the diffusion of interstitial atoms and lattice vacancies, which recombine as a result of their thermal activation due to heating.

278   In a recent study, Li et al. (2011) performed in situ thermal annealing experiments

279   of latent tracks that demonstrated that the annealing mechanisms proposed for amorphous

280   tracks in zircon is a consequence of the recombination of vacancies and interstitials with an

281   amorphous track in zircon (entirely different from those of the porous tracks in apatite where

282   shrinkage of the track results from the thermo-emission of vacancies from the porous

283   channel). The composition of an amorphous track is not significantly different from that of the

284   surrounding solid. The small chemical difference results in a low surface tension and low

285   mobility of atoms along the track surface. This structure does not favor track segmentation.

286   Therefore, defect recombination is the main mechanism through which the amorphous track

287   decreases in size at elevated temperatures.

288   If a host rock is subjected to elevated temperatures, fission tracks that have formed

289   up to that point in time are shortened progressively and eventually erased by the thermal

290   recovery (i.e., annealing) of the damage. The FTM is based on the knowledge of the kinetics

291   of this length shortening due to time and temperature. Experimental studies have identified

292   several factors that may cause annealing, including temperature, time, pressure, chemical

293   solutions, and ionizing radiation (Fleischer et al., 1965; Ahrens et al., 1970; Gleadow, 1978;

294   Tagami et al., 1990). Of these factors, temperature is the most important for the minerals

295   commonly used in geological applications (Gallagher et al., 1998).

296   The quantitative description of annealing kinetics is provided by annealing models

297   (Yamada et al., 1995, Galbraith & Laslett, 1997; Tagami et al.,1998; Guedes et al., 2005a;

298   Murakami et al., 2006; Moreira et al., 2010). Some of these models attempt to establish a

299   correlation between certain parameters and physical phenomena (Carlson, 1990; Guedes et

300   al., 2005a, 2005b).

301   In Gallagher et al. (1998), the authors reported that annealing is a consequence of

302   a thermally activated diffusion process and that the temperature range over which annealing

303   occurs varies for different minerals and depends on the heating rate (see Wagner and Van

304   den Haute, 1992). The closure temperature is associated with the annealing concept. In a

305   geochronological system, the closure temperature may be defined as the temperature at the

306   time corresponding to the apparent age. The temperature recorded by a "frozen" chemical

307   system, in which a solid phase in contact with a large reservoir has cooled slowly from high

308   temperatures, is formally identical to the geochronological closing temperature (for more

309   details, see Dodson, 1973; Gallagher et al., 1998; Bernet, 2009).

310   Another important concept is the lag-time. The lag-time of a sample is the time

311   required for the sample to cool, be exhumed to the surface, and then become deposited in a

312   nearby basin. As a rock is exhumed to the surface, the rock cools below the closure

313   temperatures of various thermochronometers. Eventually, the rock reaches the surface,

314   where it is subject to erosion. Regarding time, the process of erosion and sediment transport

315   is generally regarded as geologically instantaneous (Heller et al. 1992; Bernet et al. 2004a),

316   but this is not always the case. The lag-time integrates the time between closure and the time

317   of deposition and mainly represents the time needed to exhume the rock to the surface

318   (Bernet and Garver, 2005).

319   Perhaps the most distinctive aspect of performing FT analysis on zircon that has

320   not been partially or fully reset after deposition is that the cooling ages recorded in the

321   sedimentary detritus can be related to past thermal events in the source terrain. In many

322   cases, these cooling events are directly related to the uplift and exhumation of source rock

323   such that cooling ages provide a direct link between long-term sediment supply and sediment

324   accumulation (see figure **3**). In this case, lag time is defined as the difference between the

325   peak age and the depositional age (Garver and Brandon, 1994a; Garver et al., 1999), and it

326   represents the lag or difference between closure in the source and deposition in the adjacent

327   basin.

328   On geological time scales, the latter interval is negligible. In the geological settings

329   of active volcanism, the lag-time is nearly zero as a result of eruption and deposition in

330   flanking basins. In non-volcanic cases, rock in the source area is exhumed and passes

331   through a closure isotherm at a certain depth, at which time the lag-time clock is set. In this

332   case, the lag time represents the time required for the rock to be exhumed to the surface and

333   eroded and for the zircon to then be transported to an adjacent basin. Thus, the lag time is a

334   function of the exhumation rate in a source area (Bernet and Garver, 2005; Hofmann, 2006).

335   A more detailed description about the consequences of the lag-time is provided in the next

336   section.

337

338   ***3.2.1.2. Provenance for detrital zircon fission track data***

339   The density of observable fission tracks in zircon is dependent upon past thermal

340   history, and the robustness of zircon is reflected by an FT partial annealing zone that occurs

341   at higher temperatures than those for apatite, ranging between 180 and 320ºC (for 10^6-10^8

342   years), although the upper bound is poorly defined because of a lack of suitable geological

343   constraint (Tagami et al., 1998) data that record the thermotectonic evolution of a source

344   terrain. Such information is central to understanding the temporal relationships between a

345   developing source region and sedimentation in adjacent basins.

346   The application of detrital zircon data to monitoring sediment source region

347   evolution, however, is dependent upon geological setting, and several factors should be

348   considered. Detrital zircon FT ages are therefore related to the time of cooling through this

349   temperature interval. For volcanic/igneous grains that have not experienced post-formation

350   track annealing temperatures, the measured FT age will record the original age of formation.

351   In contrast, zircons derived from a metamorphic terrain will record post-metamorphic

exhumational cooling with apparent ages related to the cooling path through the critical isotherms that define the zircon PAZ (Carter and Bristow, 2000).

Figure 3 (modified of Carter and Bristow, 2000) shows the potential range of detrital zircon FT source ages and associated cooling paths. Zircons derived from volcanic eruptions and tectonic denudation will undergo geologically instantaneous cooling (paths A and B), whereas zircons derived from interior stable cratons will generally experience more protracted cooling history paths (paths C and D). Recycled sediments may contain zircons derived from a variety of cooling paths (paths A, B, C and D).

Large temporal gaps between cooling, erosion and burial introduce uncertainty regarding the zircon origin (increased potential for sediment recycling), unless corroborated by independent data. Thus, in this study, double-dating was applied for detrital zircon of the Bauru sedimentary basin. Regarding the cooling paths (figure 3b), 37% of our grains presented instantaneous cooling and r mountain exhumation (paths A and B), 22% presented a protracted cooling history (path C) and 41.3% had a large time gap between zircon cooling and subsequent erosion, transport, and redeposition (path D). The results and discussion section will provide more details.

3.2.1.3. Analytical procedures

The amount of detritus rocks collected in exploration wells was ca. 1 kg, while in samples collected at the surface, it was over 15 kg. This difference in the amount of available material indicates the importance of the methodology employed, where grains hybrids (Tello et al., 2012 *in press*) and materials that present etching anisotropy are used (Dias et al., 2009). Zircons were separated from rock samples by conventional techniques, such as crushing, magnetic separation (isodynamic separator), using heavy liquids and handpicking.

376   The separated zircon grains were then collected with a sharp tip and, with the aid of

377 a binocular magnifying glass, mounted on an aluminum sheet. The grains were mounted with

378 their C-axes parallel to each other. The mounted grains formed a 10x10 square, totaling 100

379 zircon grains in each assembly. The grains were then encrusted in Teflon$^{®}$ PFA.

380   The assemblies were ground in three stages: polishing manually using 1200

381 sandpaper (~ 10 μm); polishing manually using 2400 sandpaper (~ 5 μm) for 2 minutes; and

382 polishing using sandpaper 4000 (~ 3 μm) for 5 minutes on a polishing machine at 60 rpm.

383 Then, the samples were polished with diamond paste with granulometries of 1 and ¼ μm for 5

384 and 10 minutes, respectively, by using a polishing machine at 60 rpm. All of the zircon

385 samples in this study were etched with a NaOH:KOH (1:1) solution at (225 ± 2) °C for 18 h.

386   The samples were then juxtaposed with muscovite micas (External Detector

387 Method - EDM) and stacked with uranium-doped glasses (CN5) calibrated against uranium

388 thin films (Iunes et al., 2002). Thermal neutron irradiation was performed in the nuclear

389 reactor of IPEN/CNEN – São Paulo. The mean neutron fluence obtained via the neutron

390 dosimeters was (5.98 ± 0.29) x 10^{14} cm^{-2}.

391   After counting the fossil (ρ_s) and induced tracks (ρ_i), the samples were dated by

392 using the absolute neutron dosimetry approach presented in Iunes et al. (2002), through

393 which the following values were used: C_{238} = 0.99275 (Lederer and Shirley, 1978), λ_F = 8.35 X

394 10^{-17} a^{-1} (Guedes et al., 2003a), λ = 1.55125 X 10^{-10} a^{-1} (Lederer and Shirley, 1978), g = 0.684

395 (Iwano & Danhara, 1998).

396

397   ### 3.2.2. U-Pb in situ dating

398   All zircon mountings used for FTM determination (ca. 1 cm x 1 cm) were mounted

399 in a 2.5-cm-diameter circular epoxy mount. Images of the zircons were obtained using an

400 optical microscope (Leica MZ 125) and a backscatter electron microscope (Jeol JSM 5800).

401   Zircon grains were dated using a laser ablation microprobe (New Wave UP213)

402   coupled to a MC-ICP-MS (Neptune) at the Isotope Geology Laboratory of UFRGS. Isotope

403   data were acquired under the static mode with a spot size of 25 µm for the same zircons

404   dated by FTM and, in most cases, in the same region of the zircon grains. Laser-induced

405   elemental fractional and instrumental mass discrimination were corrected using a reference

406   zircon (GJ-1) (Jackson et al., 2004), following the measurement of two GJ-1 analyses for

407   every ten samples of zircon spots. For common Pb correction, we assumed that the ^{204}Pb

408   values, obtained from zircons, share the same Pb composition (Stacey and Kramers, 1975),

409   assuming concordant ages of ^{206}Pb$^{/238}$U and ^{207}Pb/^{206}Pb (as estimated age).

410   The isotope ratios and inter-element fractionation of the data obtained by the MC-

411   ICP-MS instrument were evaluated by interspersing the GJ-1 standard zircon in every set of

412   zircon samples (spots). The number of analyzed spots varied because it depended on the

413   zircon homogeneity and the amount of Pb and U. Thus, the GJ-1 standard zircon was used to

414   estimate the necessary external corrections and corrections for internal instrumental

415   fractionation. The GJ-1 zircon and sample were assembled in the same mounting. The

416   operating conditions of the laser (New Wave UP213) and MC-ICP-MS (Neptune) were as

417   follows: laser output power: 6 J/cm^2; shot repetition rate: 10 Hz; laser spot: 25 and 40 µm; cup

418   configuration: Faradays ^{206}Pb, ^{208}Pb, ^{232}Th, ^{238}U; MIC's ^{202}Hg, ^{204}Hg+^{204}Pb, ^{20}7Pb; gas input:

419   coolant flow (Ar) 15 l/min, auxiliary flow (Ar) 0.8 l/min, carrier flow 0.75 l/min (Ar) + 0.45 l/min

420   (He); acquisition: 50 cycles of 1.048 s.

421   The ^{204}Pb values obtained from the zircons were assumed to share a common Pb

422   composition, assuming concordant ages of ^{206}Pb$^{/238}$U and ^{207}Pb/^{206}Pb (as estimated age). In

423   this case, we estimated the radiogenic composition of ^{206}Pb and Pb^{207} using the equation for

424   the fraction of non-radiogenic ^{206}Pb (Williams,1998): f_{206}= [^{206}Pb/^{204}Pb]$_c$/[^{206} Pb $^{/204}$Pb]$_s$ and

425 $f_{207}= [^{207}Pb/^{204}Pb]_c/[^{207}Pb /^{204}Pb]_s$. Additional details regarding U-Pb in situ dating can be

426 found in Chemale et al. (2011).

427

428

429 **4. Results of combined zircon dating**

430 The pioneering work in which FTM and U-Pb analysis were combined to study

431 detrital zircons was performed by Carter & Moss (1999) and Carter & Bristow (2000). While

432 each detrital zircon dating technique may provide unique source information, in any study,

433 there invariably remain outstanding questions that arise regarding the limitations of each

434 method. By adopting a dual zircon dating approach, combining both FTM and U-Pb analysis

435 to study the same samples and/or grains, it is possible to overcome such limitations and

436 extract the optimum amount of provenance information that is related to both the age

437 structure and thermal evolution of the immediate source terrains.

438 An improvement in the methodology described in Carter & Moss (1999) was carried

439 out and reported in Dias et al. (2010 and 2011). The ages found by both methods (detailed in

440 the table 2) were obtained in the same grains and, more specifically, in the same areas of the

441 grains (Figures 4 and 5). The grains were first dated by FTM and then by the U-Pb method.

442

443 *4.1. FTM results*

444 The results of the FTM analysis are shown in table S1, and figures 6 and 7 show

445 the fission track age distribution for 29 samples of Bauru Basin, which are divided into the

446 Cauiá Fm. (Depositional Sequence 1), Santo Anastácio Fm. (Depositional Sequence 2) and

447 Lower and Upper Adamantina Fm. (Depositional Sequence 3). Electron backscattering

448 images of the dated zircon grains are shown in figures 4 and 5, including the apparent FT and

449 U-Pb zircon age for the same grain. On the basis of all the FTM ages, including the three

450 depositional sequences, it was possible to distinguish the main age populations: 159 ± 8 Ma

451 (3%), 277 ± 6 Ma (26%), 390 ± 9 Ma (35%), 526 ± 29 Ma (24%), 654 ± 30 Ma (11%) and 780

452 ± 190 Ma (0.01%). This last population was estimated, whereas the five first were calculated

453 using an unmixed zircon histogram (Ludwig, 2003).

454 Individual histograms with normalized age probability (apparent zircon fission track

455 ages) are shown for each sample analyzed (Fig. 6).

456 Two samples of the Caiuá Fm. (Depositional Sequence 1) were dated, ZPS21 and

457 ZMDC20. They presented three main age populations: 323 ± 24 Ma, 467 ± 54 Ma and 540 ±

458 100 Ma. Only one zircon grain presented an age of 721 ± 155 Ma (sample ZMDC20).

459 Two samples of the Santo Anastácio Fm. (Depositional Sequence 2), ZPEB37 and

460 ZMP16, revealed three main populations: 130 ± 38 Ma, 306 ± 27 Ma and 538 ± 24 Ma. The

461 oldest age was 776 ± 159 Ma (sample ZPEB37), and the youngest was 121 ± 34 Ma

462 (ZMP15).

463 In the Vale do Rio do Peixe Member (Lower Adamantina Fm, Depositional

464 Sequence 3), 8 samples were dated (ZPP4, ZBV33, ZAMB6, ZMAB26, ZRF43, ZMA25 and

465 ZBC34). Three main age populations were determined: 288 ± 49 Ma, 420 ± 55 Ma ad 573 ±

466 34 Ma. The oldest age was 825 ± 200 Ma (sample ZRF43), and the youngest was 152 ± 41

467 Ma. (samples ZRF43 and ZMAB26).

468 In the Presidente Prudente Member (Upper Adamantino Fm., Depostional

469 Sequence 3), 7 samples were dated (ZPV22, ZFMB, ZTA2, ZAL13, ZTA3, ZSE12 and ZNP9).

470 The three main age groups identified in this member were 206 ± 16 Ma, 363 ± 17 Ma and 650

471 ± 38 Ma, with oldest and youngest ages being 865 ± 221 Ma (ZMA25- G01) and 93 ± 34 Ma

472 (ZRF43-G03), respectively.

473

474 **4.2. U-Pb zircon dating**

475   The U-Pb ages obtained from zircon grains are interpreted to be magmatic because

476   the grains' Th/U ratios vary from 0.20 to 1.72 (with exception of grain 4[B2], sample ZPE36).

477   The Th/U ratio > 0.2 is interpreted to be the limit for igneous versus metamorphic zircons,

478   which usually have very low values (10^{-2} to 10^{-3}) (e.g., Cates & Mojzsis, 2009).

479   The Caiuá Fm. (Depositional Sequence 1) presents three main age groups, 579 ± 3

480   Ma, 1144 ± 15 Ma and 2032 ± 13 Ma, and a subordinated group, 1589 ± 29 Ma. The Santo

481   Anastácio Fm. (Depositional Sequence 2) presents three main age groups, 638 ± 5 Ma, 1716

482   ± 27 Ma and 2775 ± 23 Ma, and a subordinate group, 1036 ± 13 Ma. As in the case of the

483   Vale do Rio do Peixe member (Lower Adamantina Fm - Depositional Sequence 3), three

484   main age groups were identified: 658 ± 3 Ma, 1635 ± 9 Ma ad 2003 ± 8 Ma, with

485   subordination in the Neoproterozoic (1008 ± 7 Ma). In the Presidente Prudente member

486   (Upper Adamantina Fm - Depositional Sequence 3), four age groups were recognized: 579 ±

487   5 Ma, 1020 ± 10 Ma, 1953 ± 15 Ma and 2819 ± 25 Ma. In this member, one detrital zircon

488   grain age of 90 ± 22 Ma was observed (see S2).

489

490   **5. Discussion**

491

492   ***5.1. Apparent FT zircon ages***

493   The obtained FT zircon ages (Table S1 and S2; and figs. 6, 7 and 9b) of the Bauru

494   Basin reveal a much more complex history when compared to modern orogenic belts. The

495   apparent zircon ages of the collected samples is herein evaluated after the three depositional

496   cycles of the Bauru Basin and are shown in Figures 6 and 7. Analyzed samples of

497   Depositional Sequence 1 belong to the fluvial meandering system of the Caiuá Fm. The

498   obtained zircon ages were clearly affected by the zircons, which passed the total annealing to

499   partial retention zone between 420 and 360 Ma and between 250 and 200 Ma; these results

could be related to the large tectonic events of the Famatinian and Gondwanides orogeny along the western margin of the South American Platform. The samples of the overlying Depositional Sequence 2, which belong to the Santo Anastácio Fm., contain apparent ages that are chronocorrelated with the Brasiliano, Famatianian and Gondwanides, but there are also some zircons that were denudated during the Tonian orogeny of the Brazilian Shield. Paula e Silva et al., (2009) report that the main river flow of the basal units was from SW to NE, while the overlying Santa Anastácio presented a paleocurrent running northward, southeast-eastward and probably westward. The zircons with apparent ages of about 750-850 Ma may have come from the west from the Bauru Basin,probable from the Goiás Magmatic Arc rocks.

During Depositional Sequence 3, a larger expansion of the Bauru Basin occurred. Samples from the Vale do Rio do Peixe Member showed apparent zircon age populations of 220-320 Ma, 350-450 Ma and 500-600 Ma. This time span was also the period of large crustal formation at the border and central part of South America, corresponding to the Gondwanides, Famatinian and Brasiliano orogenic time. The overlying lithologies from the Presidente Prudente Member (upper Adamantina Fm.) show behavior similar to those of the Vale do Rio do Peixe Member.

Individual apparent ages between 120 and 150 Ma were determined in the four stratigraphic units and interpreted to belong to the zircon formed during the Early Cretaceous Paraná magmatism (as path A in figure 3).

5.2. U-Pb zircon ages

In the histograms of individualized stratigraphic units, the Caiuá, Santo Anastácio Fm. and Vale Rio do Peixe and Presidente Prudente Mb. (Fig. 8), a strong component of the Brasiliano source (between 600 and 500) is recognized. The Early Brasiliano (Tonian ages),

Mesoproterozoic (Stenian ages) and Paleoproterozoic (Statherian and Rhyacian ages) occur as subordinate zircon age populations. Archean peaks are exhibited by a few zircons from the Santa Anastácio Fm. and Presidente Prudente Mb. Some Ordovician zircons were dated in the Caiuá Fm. and Adamantina Fm., which can correspond to the magmatism of the latest stage of the Brasiliano Cycle or were transported from the Famatinian Terrain situated to the west, in the Pre-Cordillera and main Andean region (e.g.: Ramos, 1988, Pankhurst et al., 1998). The Mesozoic zircon in the Presidente Prudente Mb. 90 ± 22 Ma (ZPP14-G4) is the youngest detrital zircon from the 158 dated grains in the studied samples; here, it is interpreted as the maximum depositional age for the Upper Section of the Bauru Basin.

5.3. Tracking the main tectonic events of South American Platform based on the Upper Mesozoic Intracratonic Basin

Through the analyses of the detrital zircon of the intracratonic Bauru Basin, formed between 90 and 73 Ma, it was possible to recognize the main tectonic events that took place in the South American Platform. The U-Pb zircon detrital ages provided information on the main source areas for the sedimentary rocks of the Bauru Basin, which can be grouped into the main Brasiliano Cycle (650-500 Ma), early Brasiliano (850 to 700 Ma), Sunsas-Grenvile Cycle (1000-1200), Statherian Cycle (1700-1800 Ma) , Rhyacian (2000-2200 Ma) and Jequié Cycle (Figs. 8 and 9). The sedimentary structures and isopach of the Caiuá and Pirapozinho Fm. point to main sedimentary transport from SW to NE, while the overlying sequences, the Santo Anastácio, Adamantina and Marilia Fm., present a more complex sedimentary infill, with sedimentary supply from the SW, W and E (Paula e Silva et al., 2009). In this case, the potential areas for the supply of sediments for the Depositional Sequence 1 would be mainly those areas situated to the SW of the Bauru Basin (the Pampean-Brasiliano terrains) and to the W (Goiás Magmatic Arch). The sediment source of the overlying units, Depositional

550   Sequence 2 and 3, were transported from the SW (the Pampean-Brasiliano terrains) and to

551   the W (Goiás Magmatic Arch), as well as probably from the E (Ribeira Belt).

552   In the diagram of U-Pb age versus FT age (Figure 9a) on detrital zircons of the

553   Bauru Basin, it is possible to distinguish four major epochs of denudation:

554   1) The first shows an apparent age concentrated between 850 and 700 Ma,

555   which corresponds to the time of the main oceanic arc collision of the Goiás

556   Magmatic Arc (Pimentel & Fuck, 1992, Pimentel et al., 2000b). The zircons

557   formed during the Rhyacian (Transmazonian Cycle), Statherian, Stenian

558   (Sunsas-Grenvile) and Tonian (time of the Goiás Island Arc collision).

559   2) The second group of apparent zircon age comprises those zircon samples

560   with TF ages ranging from 490 Ma to 650 Ma. There are five major

561   concentrations of U-Pb absolute age: the Rhyacian (Transamazonian),

562   Stahetrian, Stenian (Sunsas-Grenvile Cycle), Tonian (early Brasiliano) and

563   Brasiliano. The last concentration is the direct record of the exhumation

564   process of the Brasiliano Orogeny.

565   3) The third group of sample consists of FT ages ranging from 480 to 360 Ma,

566   with the U-Pb age of the Rhyacian, Stenian, Tonian and dominant Brasiliano

567   ones (650-500 Ma). Although these zircons came from Brasiliano and

568   Paleoproterozoic rocks, many of these zircons passed the total annealing to

569   partial retention zone during the period of the Famatinian Orogenic process

570   along the western margin of the South American Platform, which is

571   estimated to have occurred between 510 and 360 Ma (Pankhurst et al.,

572   1998; Loewy et al., 2004; Ramos, 1998; Bahlburg et. al., 2009 and

573   references therein).

4) The last group is represented by those zircons with FT apparent ages between 350 and 220 Ma, which correspond to the span of the Gondwanides Cycle active along the western margin of the South American Platform and Pangaea formation. The U-Pb ages of the same zircons indicate a sedimentary component of the following crustal accretion: Rhyacian (Transmazonian Cycle) Steneian (Sunsas-Grenvile Cycle), Tonian (Early Brasiliano Cycle) and dominant Brasiliano cycle (650 to 500 Ma)

The Mesozoic extensional events of the South American Platform can be recorded by those FT zircon ages between 120 and 150 Ma and U-Pb zircon at 90 ± 22 Ma (Figs. 6 and 7).

The main crustal accretion of the Brazilian Shield, the crystalline basement of the Bauru Basin and surrounding areas were very well tracked by the U-Pb zircon ages obtained from samples of Depositional Sequences 1, 2 and 3. The following sedimentary sources were recognized: Transamazonain or Rhyacian rocks (2.2-1.9 Ga) (e.g., Almeida et al., 2000; Santos et al., 2003), the Staherian extensional event (1.8 to 1.68 Ga) (Chemale et al., 2012), the Sunsá-Greenvile (1.2-10 Ga) (e.g., Fuck et al., 2008; Santos et al., 2008), Tonian or Early Brasiliano (0.9-0.7 Ga) (Pimentel & Fuck, 1992; Pimentel et al., 2000b) and Brasiliano Cycle (650-500 Ma) (e.g., Almeida et al., 2000; Cordani et al., 2003 and references therein). Some local Archean zircons dated to the time of the Jequié Cycle were also found.

The FTM zircon ages provided very important information on these recycled zircon grains or denudation processes, which span from the total annealing zone to the partial annealing, because we can track the main orogenetic deformation at the border of the South America Platform during the Famatian and Gondwanides Cycles and the Brasiliano Cycle (Fig. 9b). The overlap of the FT apparent ages and U-Pb zircon ages corresponds mostly to the rapid uplift with erosion and the removal of thrusted slices (or exhumation process) of the

599　Brasilaino Belts (Fig. 9b), as described for the modern orogenic belts (e.g., Bernett et al.,

600　2009). Figure 10 shows the extension of the magmatic arc generated during these orogenic

601　cycles.

602　　　　The Famatinian Orogenic Cycle evolved from 510 to 360 Ma (Pankhurst et al.,

603　1998; Loewy et al., 2004; Ramos, 1998; Bahlburg et al., 2009 and references therein). The

604　Gondwanides along the margin western of the South American Platform formed between 345

605　and 245 Ma, with a subduction process having started at 345 Ma (Bahlburg et al., 2009) and

606　a subduction-related process followed by extensive crustal magmatism (collapse-related

607　magmatism) of the Choyoi type (Kay et al., 1989). The Choiyoi and related magmatic rocks

608　extend 2500 km from northern Chile to North Patagonia in Argentina, formed between 300

609　and 245 Ma (Rocha Campos et al., 2011; Fannig et al., *in press*). This orogenic cycle is very

610　well constrained to the Chilenia Terrain, Central Andes (Figure 10), which corresponds to the

611　South American margin against the Cuyania in the Upper Devonian (Ramos, 2000) or

612　Carboniferous (Bahlburg et al., 2009).

613

614

615　**6. Conclusions**

616

617　　　　The use of double thermochronometer methods, namely, high-temperature U-Pb

618　and low-temperature FT methods, in the same detrital zircon grains from sedimentary rocks of

619　the intracratonic Bauru Basin formed between 73 Ma and 90 Ma ago and located in the

620　interior of the South America Platform, is undeniably a powerful tool that can be used to

621　unravel the main provenance sources for the basin and the main crustal accretion processes

622　(orogenic and extensional ones) that occurred in the South America Platform between the

623　Archean and the Upper Mesozoic.

624   Samples were collected from the three depositional sequences of the basin that

625   were deposited in the dominant fluvial and lacustrine environment under arid to semi-arid

626   conditions, and it was possible, through the in situ U-Pb analyses of detrital zircons, to

627   distinguish the major accretional events that took place during the Precambrian in the South

628   American Platform, namely, Archean (Jequié Cycle, 3.0 to 2.7 Ga), Rhyacian (Transmazonian

629   Cycle, 2.2-1.90 Ga), Statherian (1.80-1.68 Ga), Sunsás (1.2-0.90 Ga), Tonian (Early

630   Brasiliano, 0.9-075 Ga) and Upper Neoproterozoic (Brasiliano , 0.65-0.50 Ga).

631   The FT apparent zircon ages of the same zircons complemented the provenance of

632   the sedimentary units of the Bauru Basin as well as the additional crustal accretion in the

633   South America Platform from the Neoproterozoic to Mesozoic. The FT zircon ages of the

634   Tonian and Cryogenian-Ediacaran, most of which show U-Pb zircon ages close to those

635   determined by the FTM, suggest that these zircons passed the total annealing zone to the

636   partial retention zone during the exhumation process of the Early and Main Brasiliano

637   Orogenic Cycle. However, two major concentrations of ages between 500 and 360 Ma and

638   between 345 and 230 Ma are also recognized, which may track the two main Paleozoic

639   Orogenic Cycles along the western border of the South American Platform and the

640   Famatinian and Gondwanides Cycles in the Upper Cretaceous Bauru Basin. Thus, the

641   integration of sedimentary flow, as determined by the paleocurrent and isopach information,

642   during the deposition of the Bauru Basin with the potential source areas and the combination

643   of U-Pb and FT zircon dating enabled us to distinguish the main source areas as well as the

644   main tectonic events in the South America Platform.

645   The most significant contribution of this study was the ability to address the different

646   paths of sample cooling through the zircon FT partial annealing zone, paths A, B, C and

647   D.(Fig. 3), and estimate the proportion of zircons that cooled during rapid uplift (exhumation)

648   or magma cooling versus those grains that presented steady, long-term cooling associated

649 with slow exhumation or that spent a long time in the partial retention zone and passed to

650 zone of stability as a result of rapid exhumation. The difficulty associated with this study is

651 attributed to the fact that an intracratonic basin has a polyhistoric memory and has a variety of

652 zircons with a single or even multiple cooling histories (PAZ).

653

654

655 **Acknowledgements**

656

661

662

663 **References**

664

665 Ahrens, T. J.; Fleischer, R. L.; Price, P. B.; Woods, R. T.; 1970. Erasure of fission tracks in

666   glasses and silicates by shock waves. Earth Planet. Sci. Lett., 8, 420-426.

667 Allen, P. A. and Armitage, J.J. 2012 Cratonic Basins. In: Busby, C. and Azor, A. (eds)

668   2012.Tectonics of sedimentary basins: Recent advances. Wilery-Blackwell, 602-620.

669 Almeida, F.F.M., 1964. Fundamentos geológicos do relevo paulista. In: Instituto Geográfico e

670   Geológico. Geologia do Estado de São Paulo, IGG. 41, 167-263.

671 Almeida, F. F. M. & Carneiro, C. R.; 1998. Origem e evolução da Serra do Mar. Revista

672   Brasileira de Geociências, 28(2), 135-150.

673   Almeida, F. F. M., Brito Neves, B.B, Carnerio, C. Dal R. 2000. The origin and evolution of the
674   South American Platform. Earth-Sc. Reviews, 50(1-2), 77-111.

675   Bahlburg, B., Vervoort , J. D. Du Frane , S. A. Bock, B., Augustsson, C., Reimann, C. 2009.
676   Timing of crust formation and recycling in accretionary orogens: Insights learned from
677   the western margin of South America. Earth-Science Reviews, 97, 215–241

678   Barredo, S.; Chemale, F.; Marsicano, C.; Ávila, J. N.; Ottone, E. G.; Ramos, V.A.; 2012. .
679   Tectono-sequence stratigraphy and U Pb zircon ages of the Rincón Blanco
680   Depocenter, northern Cuyo Rift, Argentina. Gondwana Research, 21, 624-636.

681   Bernet, M.; Zattin, M.; Garver, J.I.; Brandon, M. T.; Vance, J.A., 2001. Steady-state
682   exhumation of the European Alps. Geology 29, 35-38.

683   Bernet, M.; Brandon, M. T.; Garver, J. I.; Molitor, B. R.; 2004a. Downstream changes of
684   Alpine zircon fission-track ages in the Rhôneand Rhine rivers. J Sed Research, 74, 82-
685   94.

686   Bernet, M. and Garver, J. I., 2005. Fission-track Analysis of Detrital Zircon. Reviews in
687   Mineralogy and Geochemistry, 58 (1), 205-237.

688   Bernet, M., Beekn, P.van der, Pikw, R. I., Huyghez, P., Mugnierz, J-L., Labrinz, E. and Szulc,
689   A. 2006. Miocene to Recent exhumation of the central Himalaya determined
690   fromcombined detrital zircon fission-track and U/Pb analysis of Siwalik sediments,
691   western Nepal. Basin Research , 18, 393–412.

692   Bernet, Mathias, 2009. A field-based estimate of the zircon fission-track closure temperature.
693   Chemical Geology, 259 (3-4), 181–189.

694   Carlson, W. D.; 1990. Mechanisms and kinetics of apatite fission-track annealing. *Amer.*
695   *Mineral.* 75, 1120-1139.

696 Carrapal,B., DeCelles, P.G., Reiners, P.W., Gehrels, G. E. and Sudo, M. Apatite triple dating
697   and white mica $^{40}Ar/^{39}Ar$ thermochronology of syntectonic detritus in the Central Andes:
698   A multiphase tectonothermal history Geology, 37 (5), 407-410.

699 Carter, A. and Bristow, C. S., 2000. Detrital zircon geochronology: enhancing the quality of
700   sedimentary source information through improved methodology and combined U-Pb
701   and fission-track techniques. Basin Research, 12, 47-57.

702 Carter, A. and Moss, S. J., 1999. Combined detrital-zircon fission-track and U-Pb dating: A
703   new approach to understanding hinterland evolution. Geology, 27 (3), 235–238.

704 Carter, A., 1999. Present status and future avenues of source region discrimination and
705   characterization using fission track analysis. Sedimentary Geology, 124, 31-45.

706 Carvalho, I. S.; Ribeiro, L. C. B.; Avilla, L. S.; 2004. Uberabasuchus terrificus sp. nov., a new
707   crocodylomorpha from the Bauru Basin (Upper Cretaceous), Brazil. Gondwana
708   Research, 7 (4), 975-1002.

709 Chemale Jr., F., Dussin, I. A., Alkmim, F. F., Martis, M. S., Queiroga, G., Armstrong, R.,
710   Santos, M. N. 2012. Unravelling a Proterozoic basin history through detrital zircon
711   geochronology: The case of the Espinhaço Supergroup, Minas Gerais, Brazil.
712   Gondwana Research (in press)

713 Cordani, U.G.; Brito-Neves, B. B.; D´Agrella, M. S.; 2003. From Rodinia to Gondwana: A
714   Review of the Available Evidence from South America. Gond. Res., 6 (2), 275–283

715 Coutinho, J. M. V; Coimbra, A. C.; Brandt Neto, M.; Rocha, G. A.; 1982. Lavas alcalinas
716   analcimíticas associadas ao Grupo Bauru (Kb) no Estado de São Paulo, Brasil. In:
717   Congreso Latinamericano de Geologia, 5, Buenos Aires. Actas, Buenos Aires, Serviço
718   Geologico Nacional, 2; 185-196.

719 Crowley, K. D.; Cameron, M.; Shaefer, R. L.; 1991. Experimental studies of annealing of etched
720   fission tracks in fluor apatite. Geoch. Cosmoch., 55, 1449-1465.

721 Davis, D. W.; Williams, I. S.; Krogh, T. E.; 2003. Historical development of zircon geochronology. Reviews in Mineralogy & Geochemistry, 53, 145-181.

723 DeCelles, P. G.; Gehrels, G. E.; Quade, J.; LaReau, B.; Spurlin, M.; 2000. Tectonic Implications of U-Pb zircon ages of the Himalayan Orogenic Belt in Nepal. Science, 288, 497.

726 Dias, A. N. C., Tello S., C. A., Constantino, C. J. L., Soares, C. J. , Osório, A. M., Novaes, F. P., 2009. Micro-Raman spectroscopy and SEM/EDX applied to improve the zircon Fission Track Method used for dating geological formations. Journal of Raman Spectroscopy 40, 101-106.

730 Dias, A. N. C., Tello, C. A. S., Chemale Jr., F., Godoy, M. C. T. F., Guadagnin, F., Iunes, P. J., Soares, C. J., Osório, A. M. A., Bruckmann, M. P., 2011. Fission track and U-Pb in situ dating applied to detrital zircon from the Vale do Rio do Peixe Formation, Bauru Group, Brazil. Journal of South American Earth Sciences, 31, 298-305.

734 Dias, A. N. C., Tello, C. A., Chemale Jr., F., Iunes, P. J., Soares, C. J., Curvo, E. A., Guedes, S., Barra, B. C., Constâncio Jr., M. and Hadler, J.C., 2010. Zircon fission track and U-Th-Pb in situ dating of Rio Paraná Formation, Parana Basin, Brazil. Revista Mexicana de Fisica, 56 (1), 16-21.

738 Dodson M.H. 1973. Closure temperature in cooling geochronological and petrological systems. *Contrib. Mineral. Petrol.,* **40**:259-274.

740 Fanning, C. M., Hervè, F, Pankhurst, R. J., Rapela, C. W., Kleiman, L. E., Yaxley, G. M., Castillo, P. Lu-Hf isotope evidence for the provenance of Permian detritus in accretionary complexes of western Patagonia and the northern Antarctic Peninsula region. Journal of South American Earth Sc., *in press*.

744 Fernandes, L.A., Coimbra, A.M., 1996. A Bacia Bauru (Cretáceo Superior, Brasil). Anais da Academia Brasileira de Ciências, 68 (2), 195–205.

746 Fleischer, R.L., Price, P.B. and Walker, R.M., 1965. The ion explosion spike mechanism for
747   formation of charger particles tracks in solids. Journal Appl. Phys., 36, 3645-3652.

748 Fleischer, R. L.; Price, P. B.; Walker, R. M. Nuclear tracks in solids: Principles and
749   Applications. University of California Press, Berkeley, 1975.

750 Fleischer, R.L., 2004. Fission tracks in solids-production mechanisms and natural origins. J.
751   Mater. Sci. 39, 3901–3911.

752 Fuck, R.A., Brito Neves, B.B., Schobbenhaus, C. 2008 Rodinia descendants in South
753   America. Precambrian Research, 160(1-2): 108-126

754 Galbraith, R. F.; Laslett, G. M.; 1997. Statistical modelling of thermal annealing of fission
755   tracks in zircon. Chemical Geology, 140, 123-135.Gallagher, K.; Brown, R.; Johnson,
756   C.; 1998. Fission Track Analysis and its applications to geological problems. Annual
757   Review Earth Planet. Science, 26, 519-572.

758 Garver, J. I.; Brandon, M. T.; Roden-Tice, M.K.; Kamp, P, J. J.;1999. Exhumation history of
759   orogenic highlands determined by detrital fission track thermochronology.
760   **In:**Exhumation processes: Normal faulting, ductile flow, and erosion. Ring U, Brandon
761   MT, Willett SD, Lister GS (eds) Geol Soc London Spec Pub 154:283–304.

762 Garver, J. I., 2003. Etching zircon age standards for fission-track analysis. Radiation
763   Measurements 37, 47-53.

764 Garver, J. and Brandon, M.; 1994. Fission-track ages of detrital zircons from Cretaceous
765   strata, southern British Columbia: Implications for the Baja BC hypothesis. Tectonics,
766   13 (2), 401-420.

767 Gleadow, A. J. W., 1978. Comparison of Fission-track dating methods: effects of anisotropic
768   etching and accumulated alpha-damage. In: R.E. Zartman (Ed.), Short Papers of the
769   Fourth International Conference on Geochronology, Cosmochronology and Isotope

770   Geology, Snowmass Colorado,August 1978, US. Geological Survey, Open File Report

771   78-701.

772 Green, P. F.; Duddy, I. R.; Gleadow, A. J. W.; Tingate, P. R. and Laslet, G. M.; 1986.Thermal

773   annealing of fission tracks in apatite, 1. A qualitative description. Chem. Geol. (Isot.

774   Geosci. Sect.), 59, 237-253.

775 Green, P. F.; Laslett, G. M.; Duddy, I.R.; 1993. Mechanisms and kinetics of apatite fission

776   track annealing - discussion. Am. Mineralog., 78, 441-445.

777 Guedes O., S., Hadler N J.C.., Iunes P.J., Zuñiga A. G., Tello S. C.A. and Paulo S.R.; 2003a.

778   The use of the U(n,f) reaction dosimetry in the determination of the λ_f value through

779   fission-track techniques. Nuclear Instruments and Methods in Physics Reseach A, 496,

780   215-221.

781 Guedes, S., Iunes P. J.; Neto J. C. H.; Bigazzi G.; Tello C. A. S.; Alencar I.; Palissari R.;

782   Curvo E. A.; Moreira P.; 2005b. Kinetic model for the relationship between mean

783   diameter shortening and age reduction in glass samples. Radiat. Meas., 39, 647-652.

784 Hasebe, N., Tagami T., 2001. Exhumation of an accretionary prism; results from fission track

785   thermochronology of the Shimanto Belt, Southwest Japan. Tectonophysics, 331, 247-

786   267.

787 Hasebe, N., Watanabe, H., 2004. Heat influx and exhumation of the Shimanto accretionary

788   complex: Miocene fission track ages from the Kii Peninsula, southwest Japan. Island

789   Arc 13, 533-543.

790 Heller, P. L.; Tabor, R. W.; O'Neil, J. R.; Pevear, D. R.; Shafiquillah, M.; Winslow, N. S.;

791   1992. Isotopic provenance of Paleogene sandstones from the accretionary core of the

792   Olympic Mountains, Washington: GSA Bull, 104, 140-153.

793 Iunes, P.J., G. Bigazzi, J.C. Hadler N., M.A. Laurenzi, M.L. Balestrieri, P. Norelli, A. M. Osório

794   A., Guedes, S, C.A. Tello. and Paulo, S. R. 2005. Fission-track dating of Jankov

795   Moldavite using U and Th thin films neutron dosimetry. Radiation Measurements, 39

796   (6), 665-668.

797 Iunes, P.J., J.C. Hadler N., G. Bigazzi, C.A. Tello., S. Guedes and S.R. Paulo, 2002.

798   Durango apatite fission-track dating using length-based age corrections and neutron

799   fluence measurements by thorium thin films and natural U-doped glasses calibrated

800   through natural uranium thin films. Chemical Geology 187, 201-211.

801 Iwano, H.; Danhara, T., 1998. A re-investigation of the geometry factors for fission-track

802   dating of apatite, sphene and zircon. In P. Van den Haute and F. De Corte (eds.).

803   Advances in Fission-Track Geochronology, 47-66.

804 Jaskierowicz, G., Dunlop, A., Jonckheere, R., 2004. Track formation influorapatite

805   irradiated with energetic cluster ions. Nucl. Instrum. Meth. Phys. Res. B

806   222, 213–227.

807 Jackson, S. E.; Pearsona, N. J.; Griffina, W. L.; Belousova, E. A.; 2004. The application of

808   laser ablation-inductively coupled plasma-mass spectrometry to in situ U-Pb zircon

809   geochronology. Chemical Geology, 211, 47-69.

810 Kay, S.M., Ramos, V.A., Mpodozis, C., Sruoga, P., 1989. Late Paleozoic to Jurassic silicic

811   magmatism at the Gondwana margin: analogy to the Middle Proterozoic in North

812   America?. Geology, 17, 324-328.

813 Lederer, C. M. and Shirley, V. S., 1978. Table of Isotopes, Seventh edition. John Wiley and

814   Sons, Inc., New York, USA. 1523pp.

815 Li, W.; Wang, L.; Lang, M.; Trautmann, C.; Ewing, R. C.; 2011. Thermal annealing

816   mechanisms of latent fission tracks: Apatite vs. zircon. Earth and Planetary Science

817   Letters, 302, 227–235.

818   Lindsay, J.F., 2002. Supersequences, superbasins, supercontinents – evidence from the
819   Neoproterozoic-Early Palaeozoic basins of central Australia. Basin Research 14, 207-
820   223.

821   Liu, T. K.; Hseih, S.; Chen, Y. G.; Chen, W. S.; 2001. Thermo-kinematic evolution of the
822   Taiwan oblique-collision mountain belt as revealed by zircon fission track dating. Earth
823   and Planetary Science Letters, 186, 45–56.

824   Loewy, S. L.; Connelly, J. N.; Dalziel, I. W. D.; 2004. An orphaned basement block: the
825   Arequipa-Antofalla Basement of the central Andean margin of South America. Geol.
826   Soc. Am. Bull., 116, 171-87.

827   Milani, E.J. 1997. Evolução tectono-estratigráfica da Bacia do Paraná e seu relacionamento
828   com a geodinâmica fanerozóica do Gondwana sul-ocidental. Instituto de Geociências,
829   Universidade Federal do Rio Grande do Sul, Tese de Doutoramento, 255 p.

830
831   Moreira, P. A. F. P.; Guedes, S.; Iunes, P. J., Hadler, J. C.; 2010. Fission track chemical
        etching kinetic model. Radiation Measurements, 45,157-162.

832   Murakami, M.; Yamada, R. and Tagami, T.; 2006. Short-term annealing characteristics of
833   spontaneous fission tracks in zircon. Chemical Geology, 227, 214–222.

834   Pankhurst, R.J., Rapela, C.W., Saavedra, J., Baldo, E, Dahlquist, J., Pascua, I., Fanning,
835   C.M., 1998. The Famatinian magmatic arc in the central Sierras Pampeanas: an Early
836   to Mid-Ordovician continental arc on the Gondwana margin. In: Pankhurst, R.J.,
837   Rapela, C.W. (Eds.), The Proto-Andean Margin of Gondwana: Geological Society,
838   London, Special Publication, 142, 343–367.

839   Paul, T. A., and P.G. Fitzgerald, 1992. Transmission electron microscopy investigation of
840   fission tracks in fluorapatite: American Mineralogist, 77, 336-344.

841   Paul, T.A., 1993. Transmission electron microscopy investigation of unetched fission tracks in
842   fluorapatite-physical process of annealing. Nucl. Tracks Radiat. Meas. 21, 507–511.

843 Paula e Silva, F., Chang, H.K., Caetano-Chang, M.R., Stradioto, M.R., 2006. Sucessão
844   sedimentar do Grupo Bauru na região de Pirapozinho (SP). Geociências, Rio Claro 25
845   (1), 17–26.

846 Paula e Silva, F. P., Kiang, C. H. and Caeteno-Hang, M. R. 2009. Sedimentation of the
847   Cretaceous Bauru Group in São Paulo, Paraná Basin, Brazil. Journal of South
848   American Earth Sciences 28: 25–39

849 Pereira, M.J., Barbosa, M.C., Agra, J., Gomes, J.B., Aranha, L.G., F., Saito, M., Ramos, M.A.,
850   Carvalho, M.D., Stamato, M., Bagni, O., 1986. Estratigrafia da Bacia de Santos:
851   análise das sequências, sistemas deposicionais e revisão litoestratigráfica. In:
852   Congresso Brasileiro de Geologia 34, v. 1, Goiânia, GO, Anais, pp. 65–79.

853 Pimentel, M. M. and Fuck, R. A.; 1992. Neoproterozoic crustal accretion in Central Brazil.
854   Geology 20: 372- 379.

855 Pimentel, M. M.; Fuck, R. A.; Jost, H.; Ferreira Filho, C. F.; Araújo, S. M.; 2000b. The
856   basement of theBrasília Fold Belt and the Goiás Magmatic Arc. In: Cordani UG et al.
857   (Eds); Tectonic Evolution of South America. Rio de Janeiro: 31st IGC,190-229.

858 Price, P. B.; Walker, R. M.; 1962. A new detector for heavy particle studies. Phys. Lett., 3,
859   113-115.

860 Price, P. B.; Walker, R. M.; 1963. Fossil tracks of charged particles in mica and the age of
861   minerals. J. Geophys. Res., 68, 4847−4862.

862 Ramos, V. A., Aleman, A., 2000. Tectonic evolution of the Andes. In: Cordani, U.G., Milani,
863   E.J., Thomaz Filho, A.M, Campos, D. A. (Eds.), Tectonic evolution of South America,
864   31st International Geological Congress, Rio de Janeiro, 636–685

865 Ramos, V.A., Dallmeyer, D. and Vujovich, G.,1998. Time constraints on the Early Paleozoic
866   docking of the Precordillera, Central Argentina. In: Pankhurst, R. and Rapela, C.W.

(Eds.), The Proto-Andean margin of Gondwana, Geol. Soc. Lon. Spec. Pub.. 142,143-158

Ramos VA. 1988. Tectonics of the Late Proterozoic - Early Paleozoic: a collisional history of Southern South America. *Episodes* 11:168--74

Rabone, J. A. L.; Carter, A.; Hurford, A. J.; Leeuw, N. H.; 2008. Modelling the formation of fission tracks in apatite minerals using molecular dynamics simulations. Phys. Chem. Miner. 35, 583-596.

Rahl, J.M., Reiner, P. W., Campbell, I. H., Nicolescu, S. & Allen, C, 2003. Combined single-grain (U-Th)/He and U/Pb dating of detrital zircons from the Navajo Sandstone, Utah. Geology, 31 (9), 761-764.

Reiners, P.W., 2005. Zircon (U-Th)/He thermochronometry. Reviews in Mineralogy & Geochemistry 58, 151-179.

Rocha-Campos, A.C., Basei, M.A., Nutman, A.P., Kleiman, Laura E., Varela, R., Llambias, E., Canile, F.M., da Rosa, O.C.R., 2011. 30 million years of Permian volcanism recorded in the Choiyoi igneous province (W Argentina) and their source for younger ash fall deposits in the Paraná Basin: SHRIMP UePb zircon geochronology evidence. Gondwana Research, 19, 509-523.

Santos, J.O. S., Hartmann, L;. A., Bossi, J., Campal, N., Schipilov, A., Pinero, D., McNaughton, N. J. . 2003. International Geol. Rev. , 45(1), 27-48.

Santos, J.O. S., Rizzoto, G.J., Potter, P.E., McNaughton, N. J., Matos, R.S., Hartmann, L.A., Chemale Jr, F., Quadros, M.E.S.; 2008. Age and autochthonous evolution of the Sunsás Orogen in West Amazon Craton based on mapping and U–Pb geochronology. Prec. Res., 165(3-4), 120-152.

890   Shaw, R., Etheridge, M., Lambeck, K., 1991. Development of the Late Proterozoic to Mid-
891   Paleozoic intracratonic Amadeus Basin in Central Australia: a key to understanding
892   tectonic forces in plate interiors. Tectonics, 10, 688-721.

893   Sloss, L.L., 1963. Sequences in the Cratonic Interior of North America. Geological Society of
894   America Bulletin 74, 93-114.

895   Sloss, L.L., and Speed, R. C. 1974. . Relationship of cratonic and continental margins tectonic
896   episodes, in tectonics and sedimentation. Special Pub. Soc. Economic Paleontologists
897   and Mineralogists, 22: 38-55.

898   Spikings, R.A., Winkler, W., Seward, D., Handler, R., 2001. Along-strike variations in the
899   thermal and tectonic response of the continental Ecuadorian Andes to the collision with
900   heterogeneous oceanic crust. Earth Planetary Science Letters, 186, 57-73.

901   Stacey, J. S., Kramers, J. D., 1975. Approximation of terrestrial lead isotope evolution by a
902   two-stage model. Earth and Planetary Science Letters 26, 207–221.

903   Stuart, F. M.; 2002. The exhumation history of orogenic belts from $^{40}Ar/^{39}Ar$ ages of detrital
904   micas. Mineralogical Magazine. 66 (1), 121-135.

905   Suguio, K., Fulfaro, V.J., Amaral, G., Guidorzi, L.A., 1977. Comportamentos estratigráfico e
906   estrutural da Formação Bauru nas regiões administrativas 7 (Bauru), 8 (São José do
907   Rio Preto) e 9 (Araçatuba) no Estado de São Paulo. In: Simpósio Regional de
908   Geologia, 1, São Paulo, SP, Atas, 231–247

909   Tagami, T., 2005. Zircon fission-track thermochronology and applications to fault studies.
910   Reviews In Mineralogy & Geochemistry 58, 95-122.

911   Tagami, T. and O'Sullivan, P. B.; 2005. Fundamentals of Fission-Track Thermochronology.
912   Reviews in Mineralogy and Geochemistry**, 58 (1), 19-47.**

913   Tagami, T.; Galbraith, R.F.; Yamada, R. and Laslett, G. M.; 1998. Revised annealing kinetics
914   of fission tracks in zircon and geological implications. In: P. Van den haute and F. De

915 Corte, Editors, Advances in Fission-Track Geochronology, Kluwer Academic

916 Publishers, Dordrecht, The Netherlands, 99-112.

917 Tagami, T., Ito, H., Nishimura, S., 1990. Thermal annealing characteristics of spontaneus

918 fission tracks in zircon. Chemical Geology, 80, 159-169.

919 Tello, C. A. S.; Curvo, E. A. C.; Dias, A. N. C.; Soares, C. J.; Constantino, C. J. L.; Alencar,

920 I.; Guedes, S.; Palissari, R.; Hadler, J. C.; 2012. Effects of etching on zircon grains and

921 its implications to Fission Track Method. Applied Spectroscopy, *in press.*

922 Thomson, S. N. & Hervé, F. 2002. New time constraints for the age of metamorphism at the

923 ancestral Pacific Gondwana margin of southern Chile (42-52°S). Revista Geológica de

924 Chile, 29(2), 151-165.

925 Villa, F., Grivet, M., Rebetez, M., Dubois, C., Chambaudet, A., Chevarier, A., Martin, P.,

926 Brossard, F., Blondiaux, G., Sauvage, T., Toulemonde, M., 1999. Damage morphology

927 of Kr ion tracks in apatite: dependence on dE/dx. Radiat. Meas. 31, 65–70.

928 Wagner,G. A. and P. Van Den Haute, Fission-track dating. Kluwer Acad., Norwell, Mass., 1992;

929 6, 285p.

930 Yamada, K., Tagami, T., Shimobayashi, N., 2003. Experimental study on hydrothermal

931 annealing of fission tracks in zircon. Chemical Geology (Isot. Geosci. Sect) 201, 351-

932 357.

933 Zalán, P.V.; Wolff, S.; Astolfi, M.A.M.; Vieira, I.S.; Conceição, J.C.J.; Appi, V.T.; Neto, E.V.S.;

934 Cerqucira, J.R.; Marques, A. 1990. The Paraná Basin, Brazil. In: M. W. Leighton; D. R.

935 Kolata; D. F. Oltz; J. J. Eidel (eds). Interior cratonic hasins. Tulsa: American

936 Association of Petroleum Geologists Memoir, 51, 681-708.

937

938

939

940 **FIGURE CAPTIONS**

941

942 **Figure 1. (A)** Simplified map of the Bauru Basin showing the location of the study area and a
943 map of South America. **(B).** Geological map of the SW sector of the Bauru Basin with the
944 main stratigraphic units and location of samples used for FT and U-Pb zircon analyses.

945

946 **Figure 2.** Stratigraphy chart of the Bauru Basin (modified after Paula e Silva et al., 2009),
947 where the stratigraphic section of the study area is the sector SW.

948

949 **Figure 3. (A)** Different types of detrital zircon FT ages. For post-metamorphic and/or
950 exhumation cooling, the measured age is related to the rate at a which the samples cool
951 through the zircon FT partial annealing zone, e.g., paths A-D. Sediments may contain variable
952 proportions of any of these different source age types as well as polycyclical grains (modified
953 of Carter and Bristow, 2000). **(B)** The percentage of U-Pb ages of zircon FT belonging to
954 each path. **(C)** The lag-time, which is the time required to cool, be exhumed to the surface,
955 and become eroded and then deposited in a nearby basin. Regarding time, the process of
956 transportation is regarded as geologically instantaneous (extracted of Bernet and Garver,
957 2005).

958

959 **Figure 4**. Backscattered electron images of the zircons analyzed by the FT and U-Pb
960 methods (samples from CFm, SAFm and VRPMb). The laser spot analysis for U-Pb isotope
961 acquisitions was performed at the same site where the FT analyses were performed. Age
962 plus error in orange = U-Pb and white = FTM.

963

964 **Figure 5.** Backscattered electron images of the zircons analyzed by the FT and U-Pb
965 methods (samples from CFm, PPFm and VRPMb). The laser spot analysis for U-Pb isotope

966   acquisitions was performed at the same site where the FT analyses were performed. Age

967   plus error in orange = U-Pb and white = FTM.

968

969   **Figure 6.** Histograms with normalized age probability for individualized samples of the Caiuá

970   Fm. (CF), Santo Anastácio Fm. (SAF), Vale do Rio do Peixe Mb. (VRPMb) and Presidente

971   Prudente Mb. (PPMb).

972

973   **Figure 7**. Composite histograms with normalized FT age probability for the main stratigraphic

974   units (legend see fig. 5). EBr = Early Brasilaino or Tonian, Br = Brasiliano Cycle (650-500

975   Ma), Fa = Famatinian Cycle (500-350 Ma), Go= Gondwanides Cycle (345 Ma-230 Ma) and

976   R= Mesozoic Rifting.

977

978   **Figure 8**. Composite histograms with normalized U-Pb age probability for the main

979   stratigraphic units.

980

981   **Figure 9. (A)** Fission-track (FT) versus U/Pb ages on single detrital zircons. One hundred

982   nine zircon grains were analyzed by the combined method (see table S2). A histogram with

983   the normalized ages of the U-Pb zircons is shown in blue. The symbols and error bars

984   correspond to the central apparent FT age and error (2 sigma level). The orange = Early

985   Brasiliano, Red = Brasiliano (650-500 Ma), Green = Famatinian (510-455 Ma) and blue =

986   Gondwanides (345-245 Ma). **(B)** Overlap of the FT apparent ages and U-Pb zircon ages

987   correspond mostly to the rapid uplift with the erosion and removal of thrusted slices (or

988   exhumation process) of the Brasiliano Belts. For further explanation, see the text.

989

990   **Figure 10.** Orogenic provinces of South American Platform (modified after Bahlburg et al.,

991   2009) AM, Arequipa Massif; CA, Central Amazonian Province; SF, Sao Francisco craton;

992   TBL: Transrasiliano Lineament. The black insert is the Bauru Basin.

993 **TABLE CAPTIONS (Supplementary Material)**

994 **S1.** Zircon FTM data for samples of Bauru Basin.

995

996 **S2.** Zircon U-Pb and FTM data for samples of Bauru Basin

997

Combined FT/U-Pb dating of detrital zircons reveals the polyhistory of the Bauru Basin►Main contribution of sedimentary rocks were from Transamazonian and Brasiliano Cycle►Minor sources from Sunsás and Statherian cycles and local Jequié cycle and Mesozoic extensional event►FT data provide evidence of rapid uplift during the Early Brasiliano and Brasiliano►Other main ages of 500-360 and 345-230 Ma records the Famatinian and Gondwanides cycle

Graphical Abstract_ Dias et al.

Figure 1 Dias et al

Figure2_Diasetal
Click here to download high resolution image
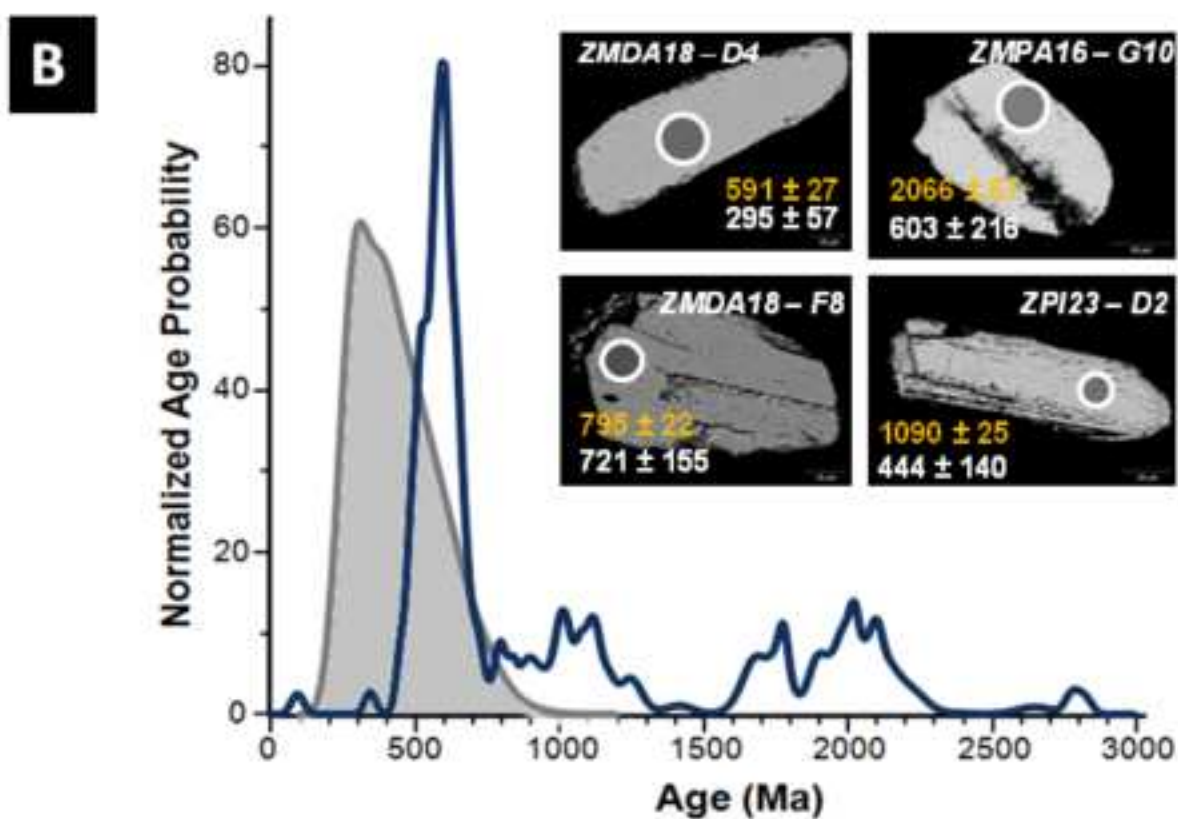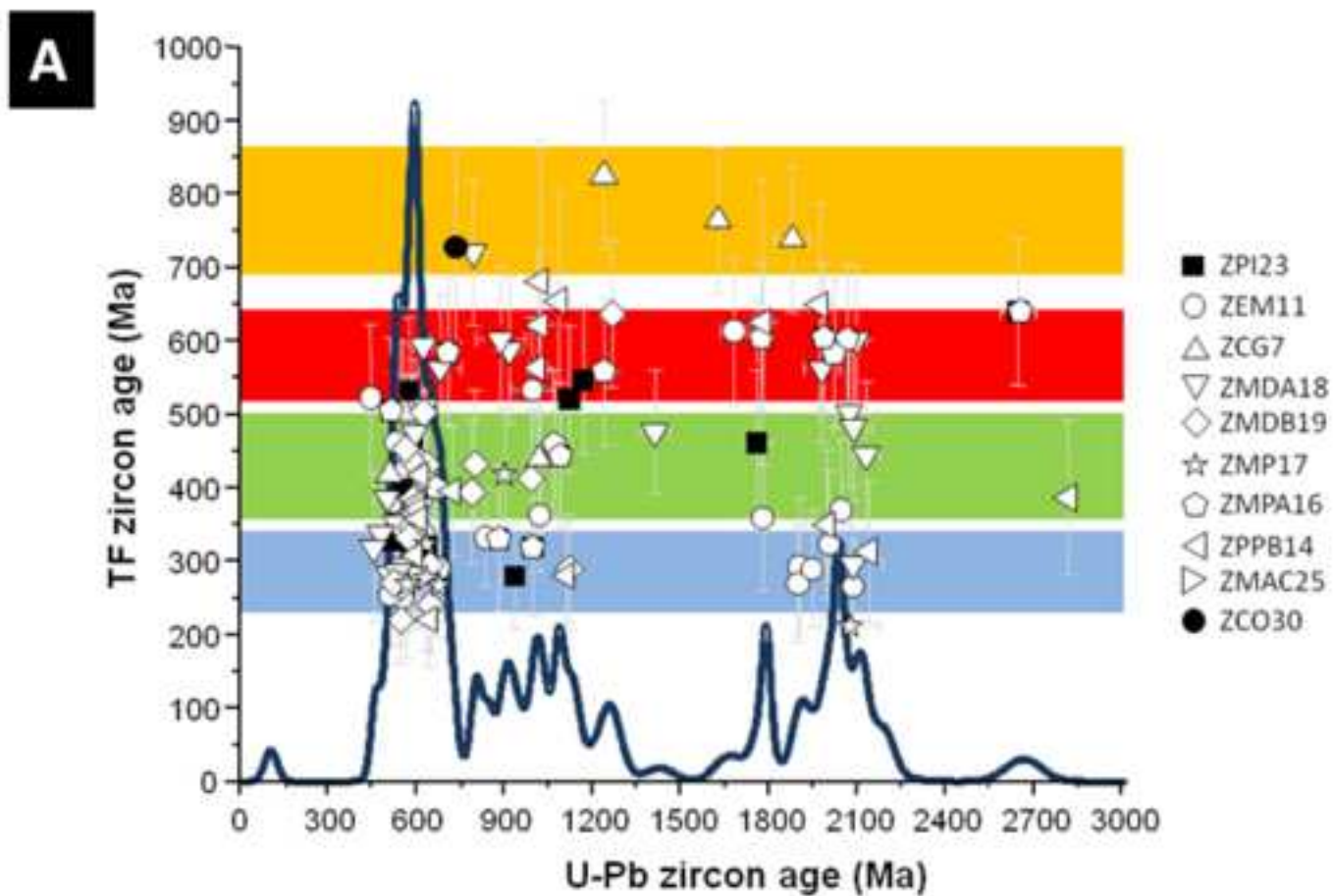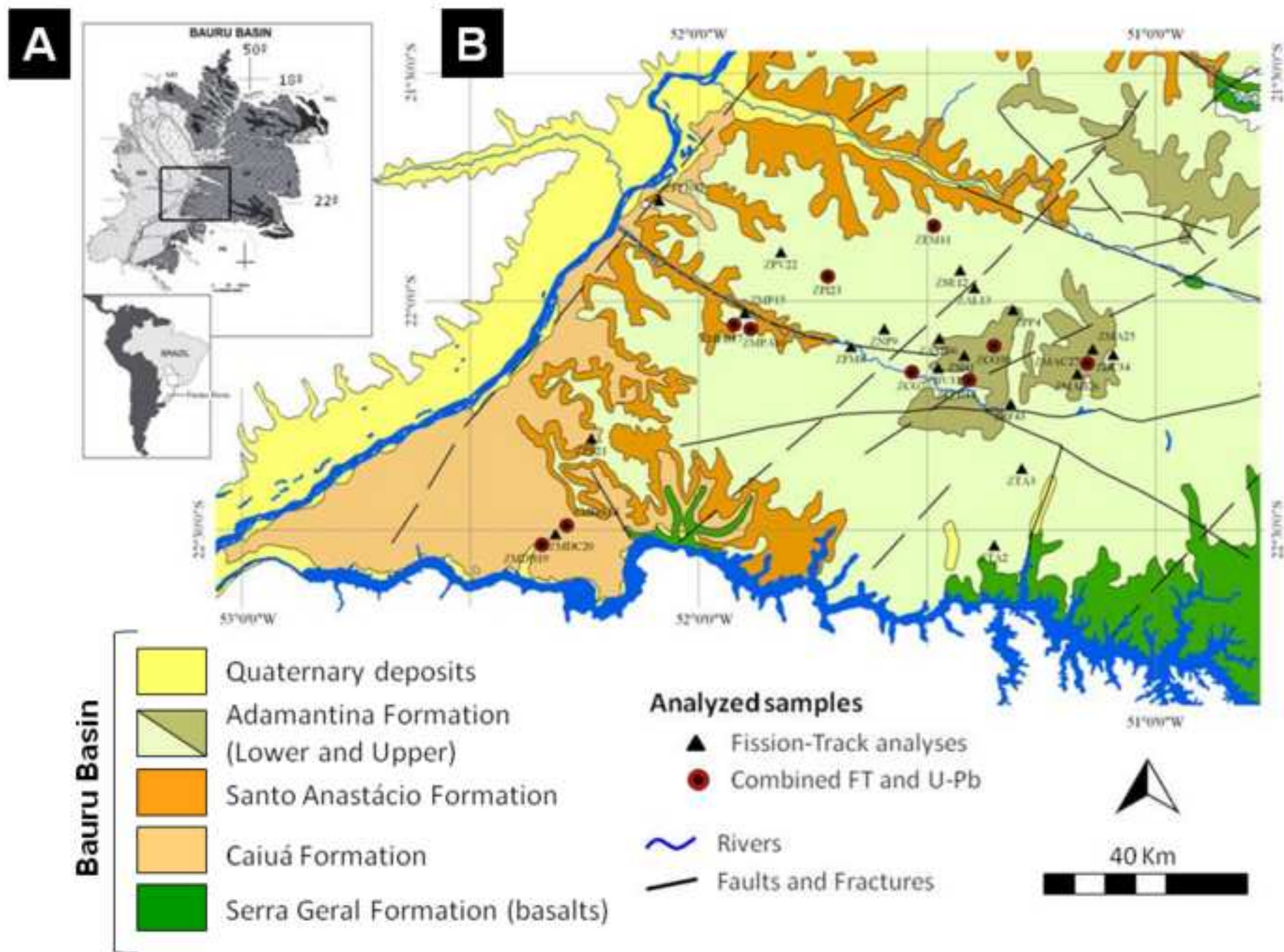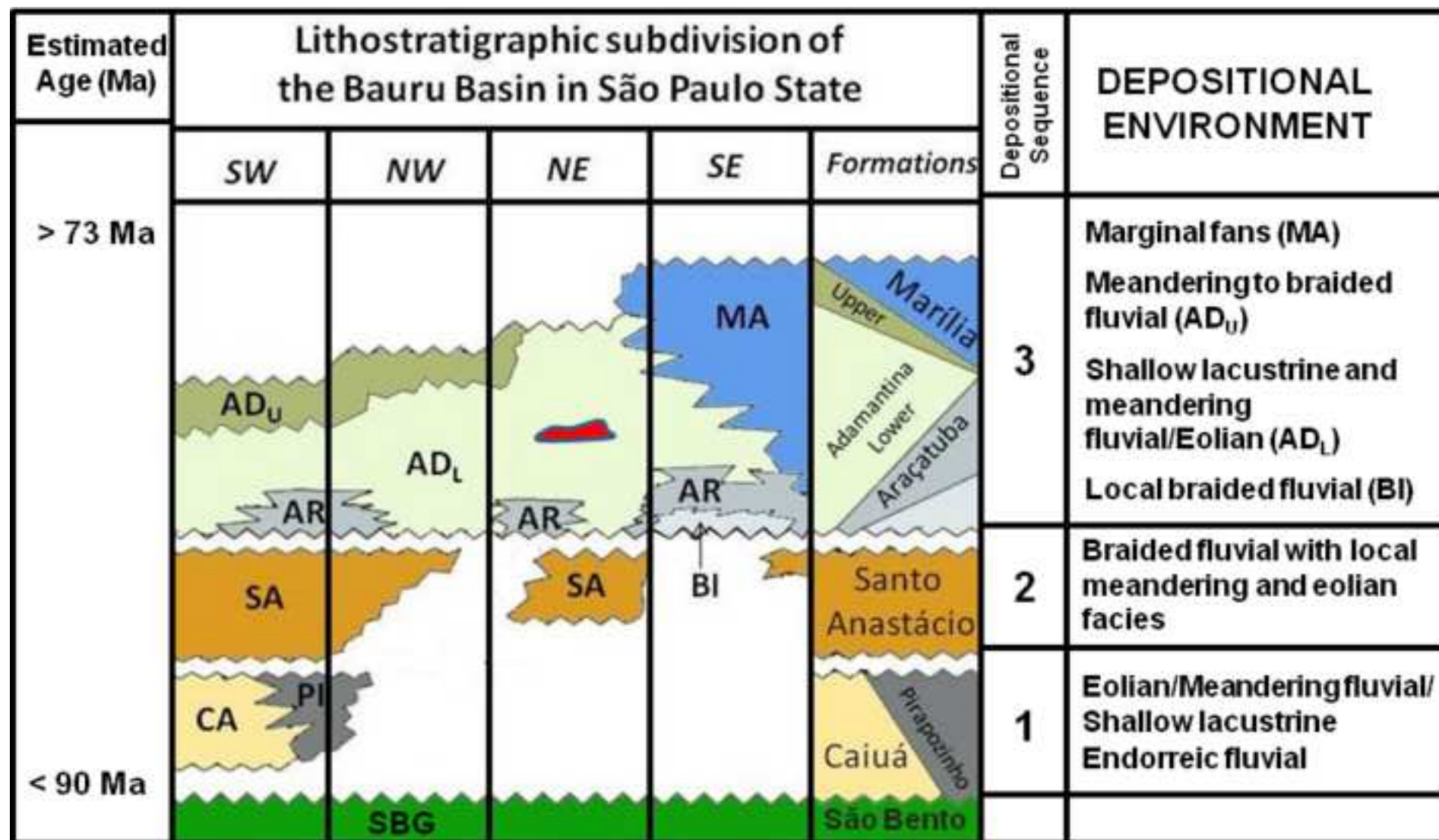
Taiúva Analcimite (in red)   AD$_U$ = Upper Adamantina Fm.   MA = Marília Fm.

AR = Araçatuba Fm.   BI = Birigui Fm.   AD$_L$ = Lower Adamantina Fm.

CA = Caiuá Fm.   PI = Fm. Pirapozinho   AS = Santo Anastácio Fm.

SBG = São Bento Group (Paraná lava flows and Botucatu eolian sediments)

Figure 2 Dias et al.

Figure3_Diasetal
Click here to download high resolution image
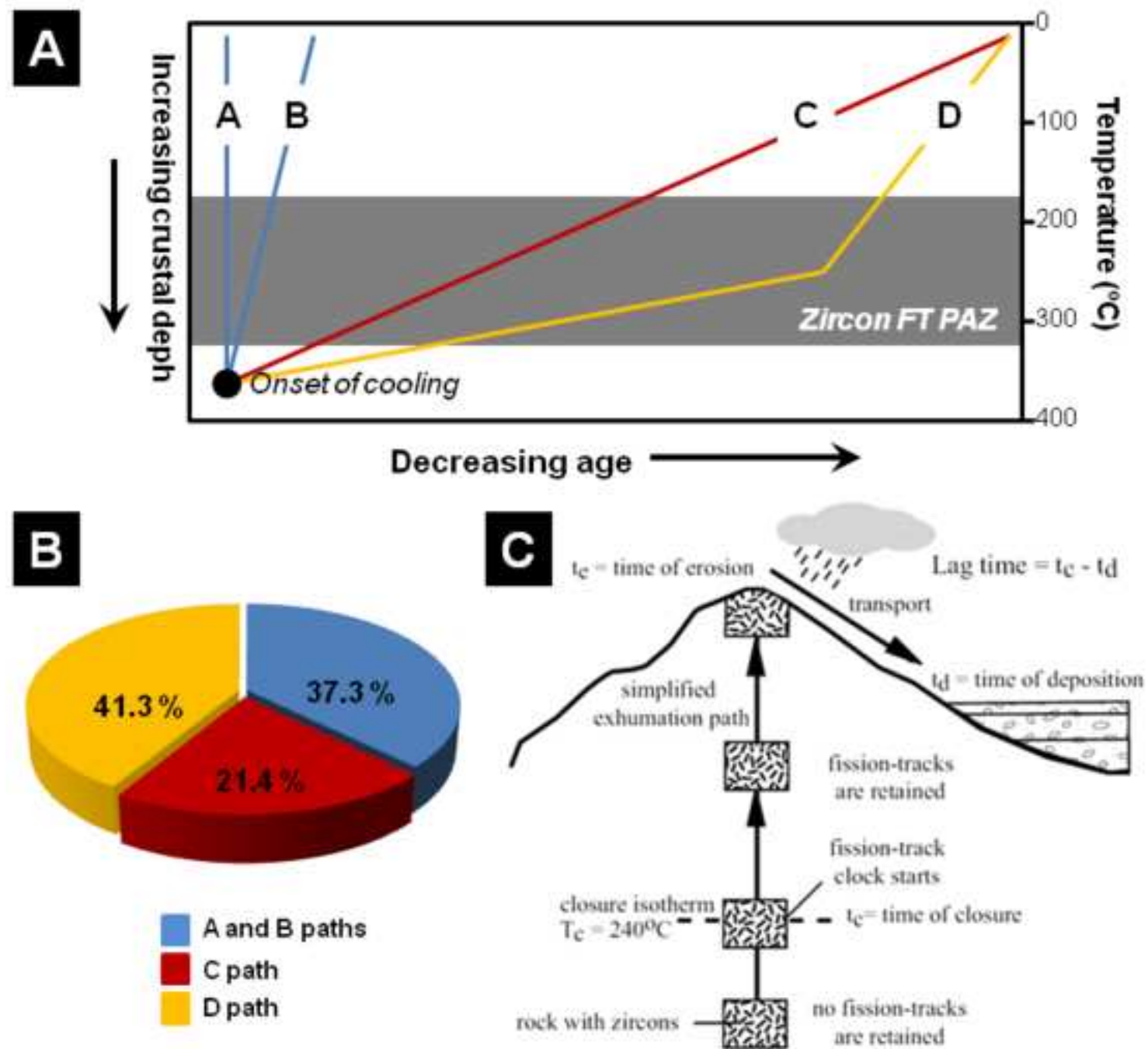
Figure 3 Dias et al

Figure4_Diasetal
Click here to download high resolution image
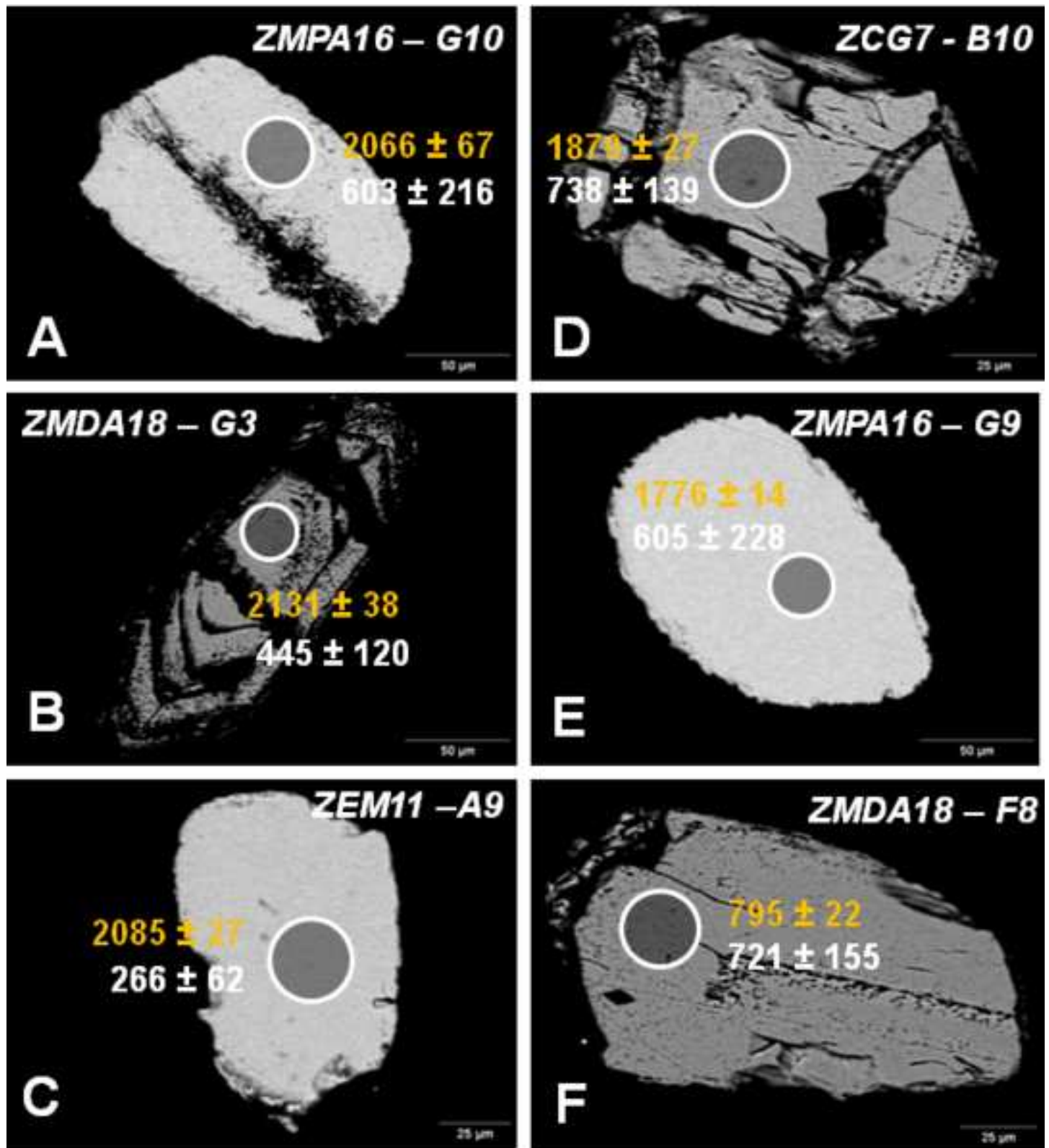
Figure 4 Dias et al

Figure5_Diasetal
Click here to download high resolution image

ZPPB14 – G10
1021 ± 25
622 ± 250
A
25 µm

ZMDA18 – F6
625 ± 32
594 ± 116
D
25 µm

ZPI23 – D2
1090 ± 25
444 ± 140
B
25 µm

ZMDB19 – A1
606 ± 69
440 ± 109
E
25 µm

ZPI23 – E8
936 ± 25
280 ± 73
C
25 µm

ZMDA18 – D4
591 ± 27
295 ± 57
F
25 µm
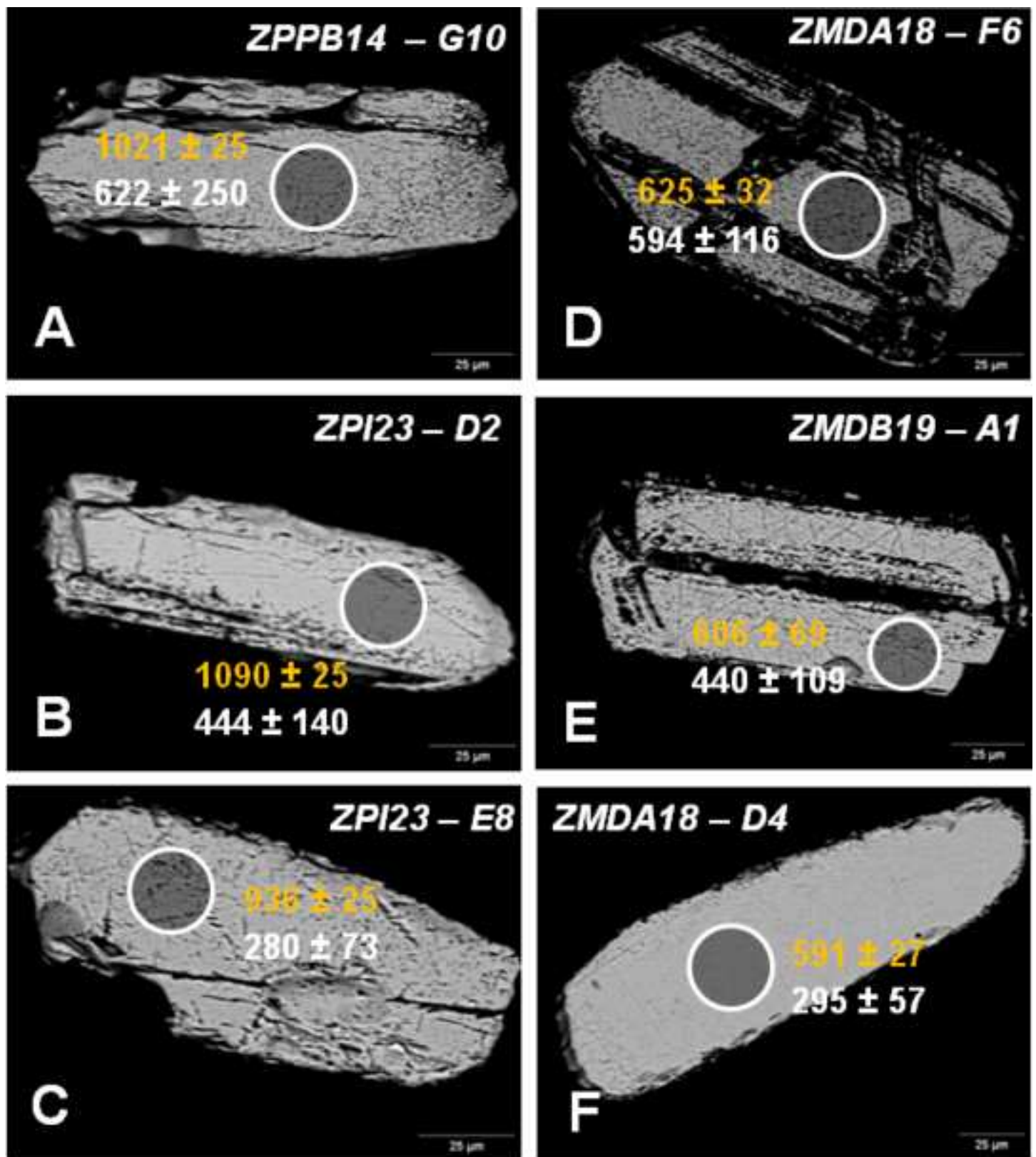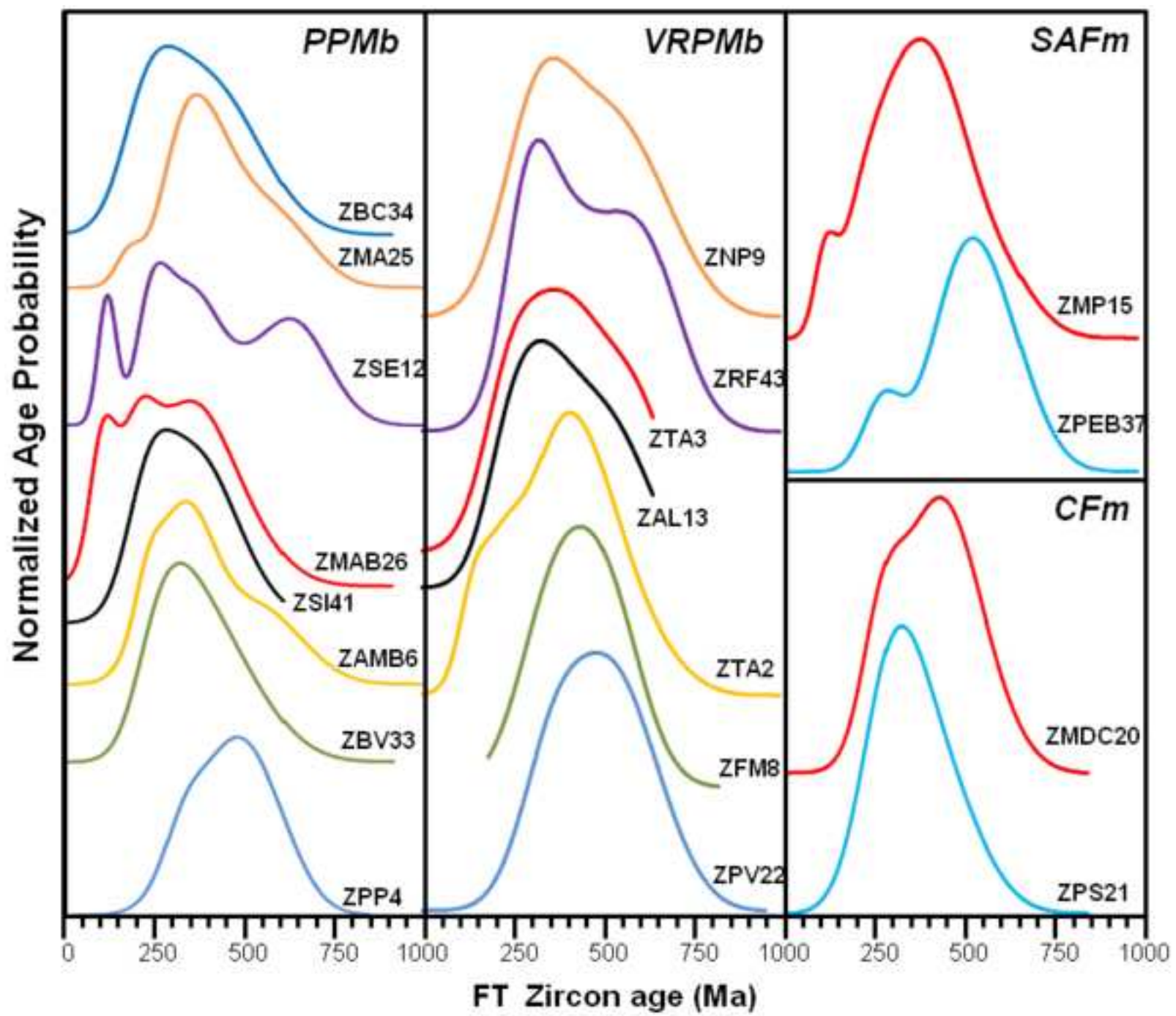
Figure 5 Dias et al

Figure 6 Dias et al.
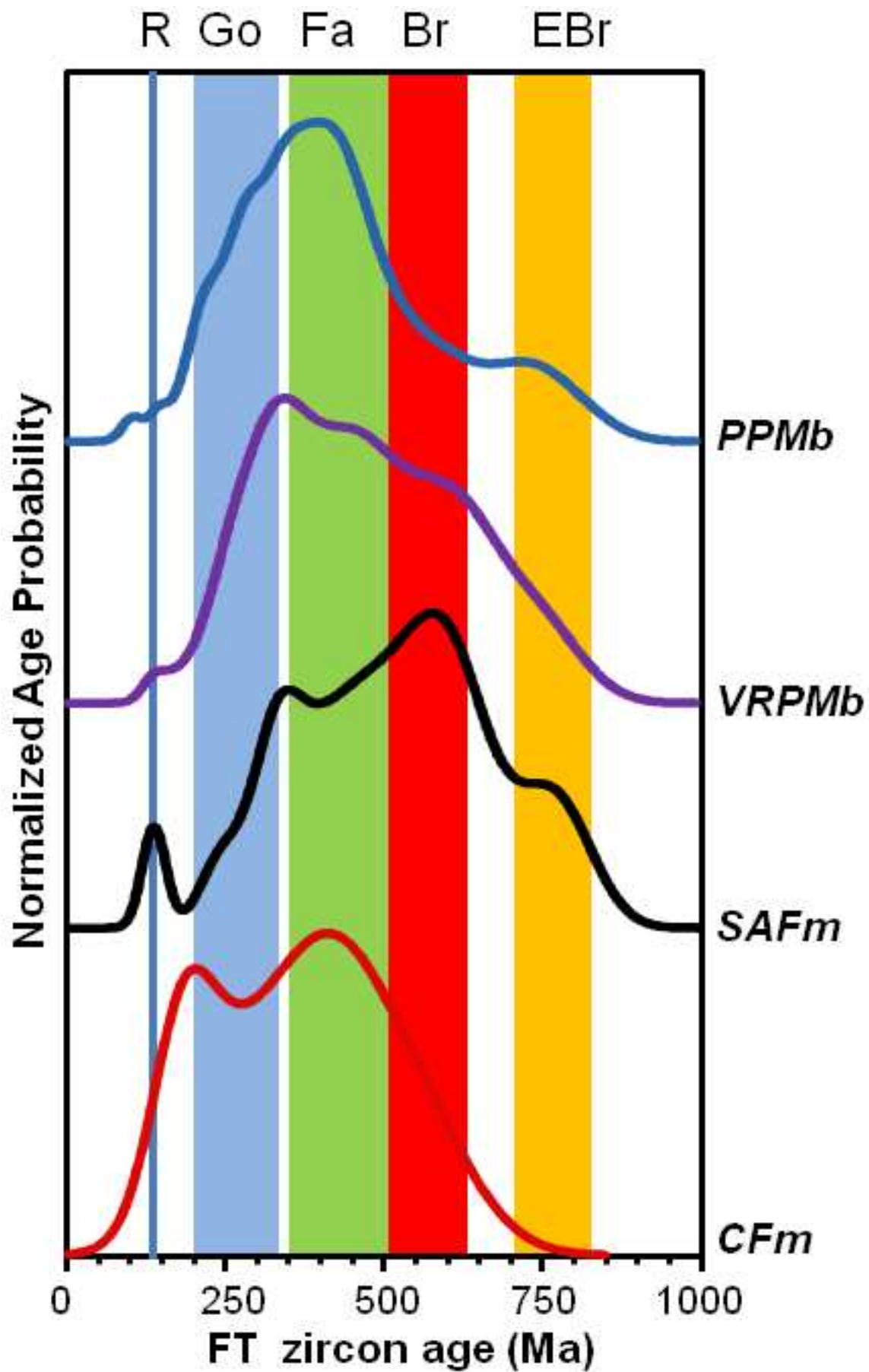
Figure 7 Dias et al.
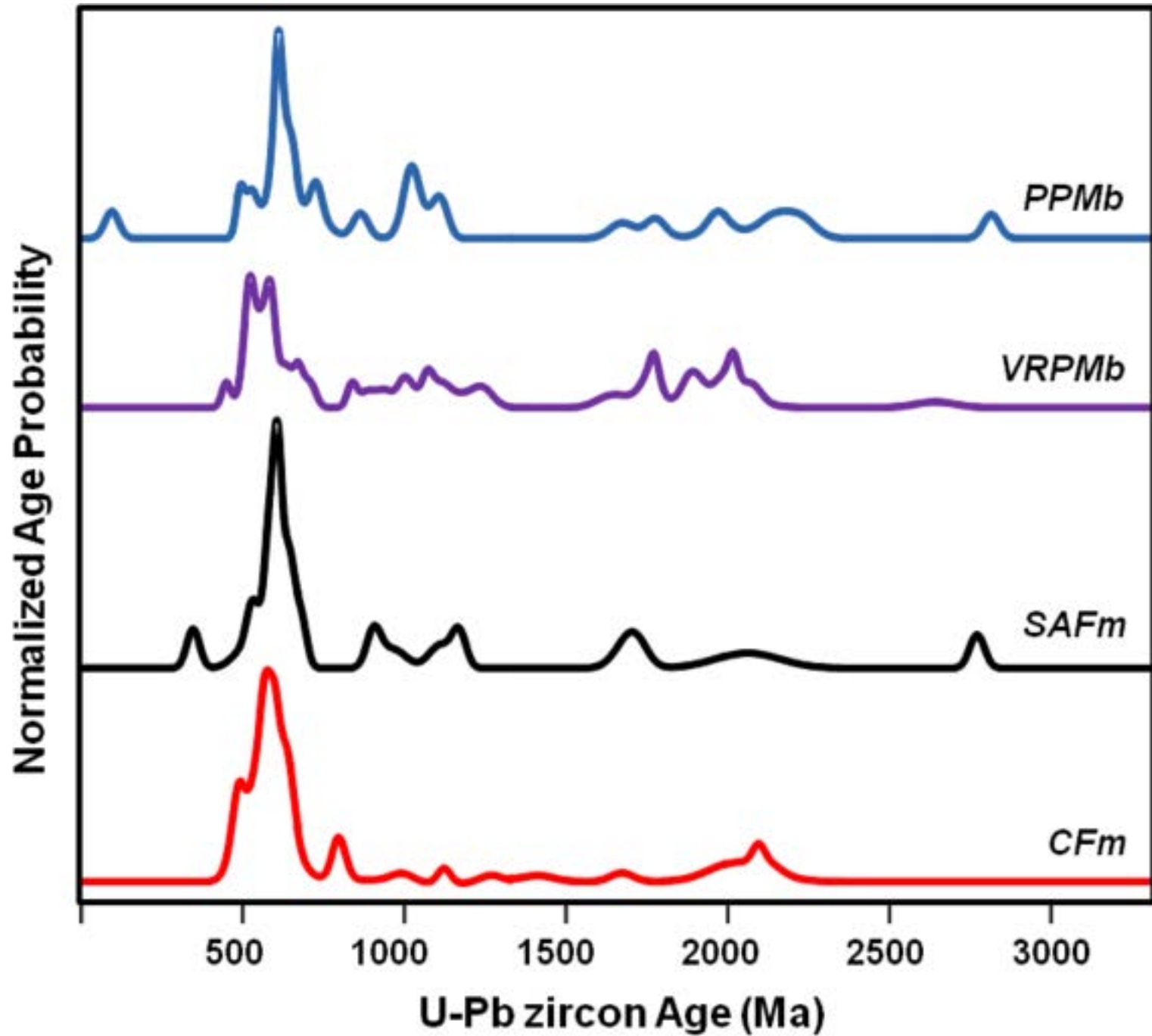
Figure 8 Dias et al
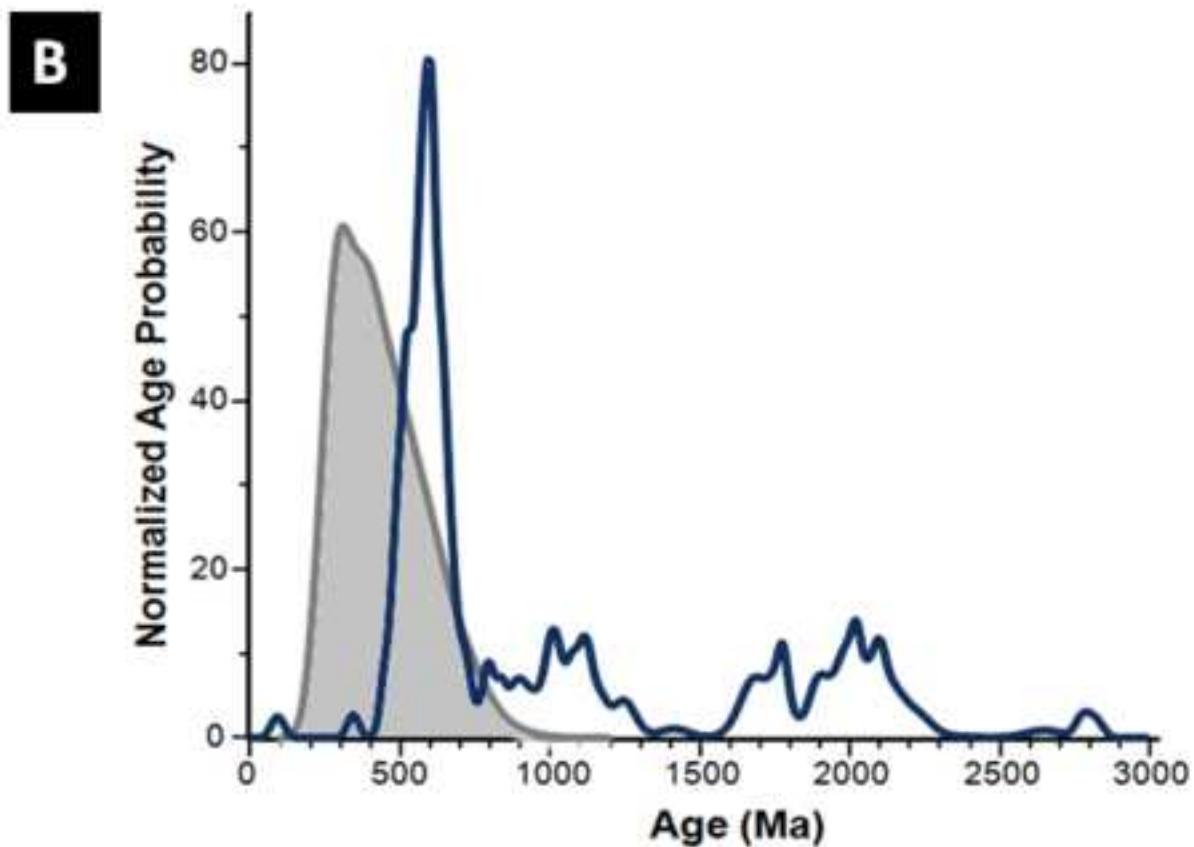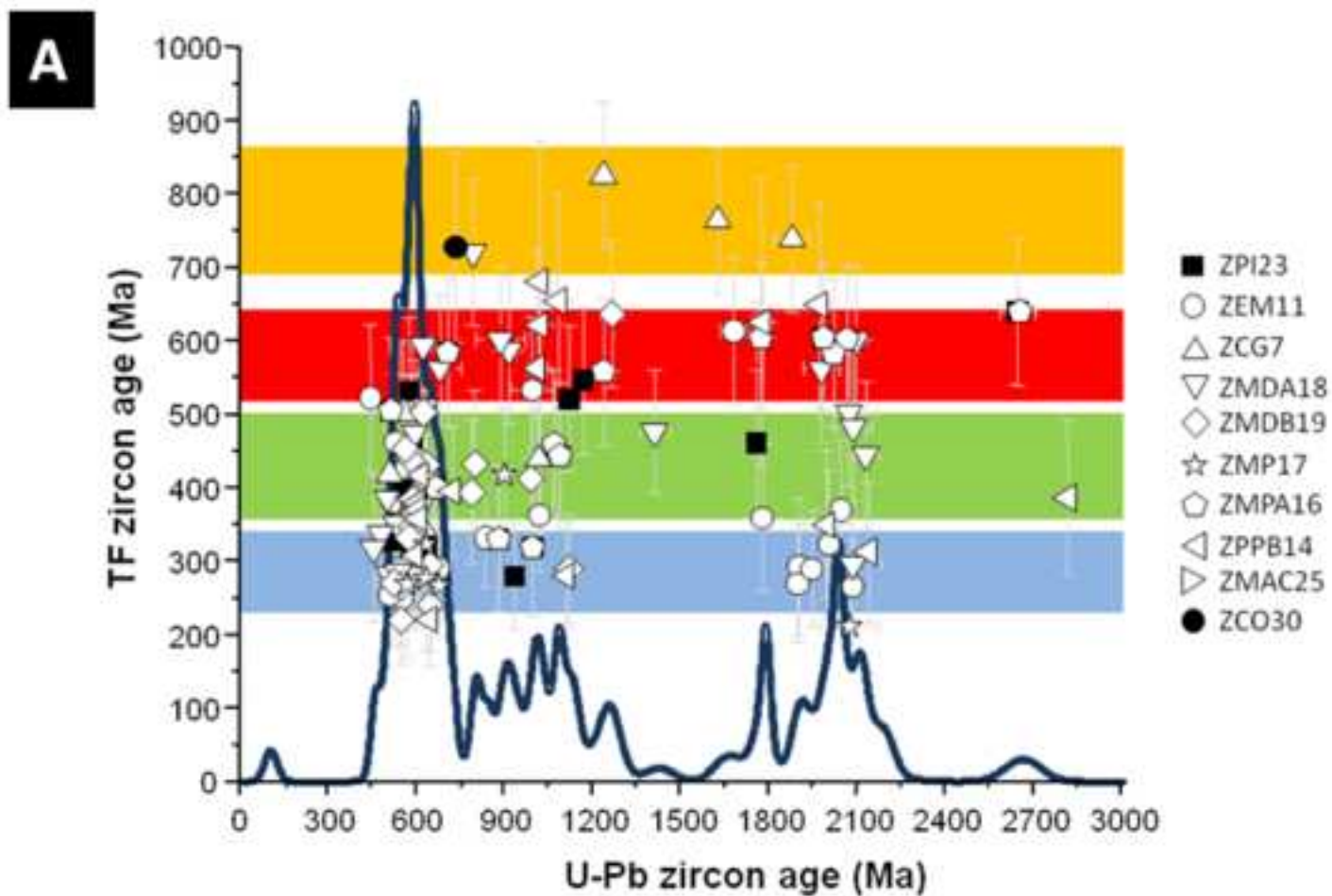
Figure 9 Dias et al.

Figure10_Diasetal
Click here to download high resolution image
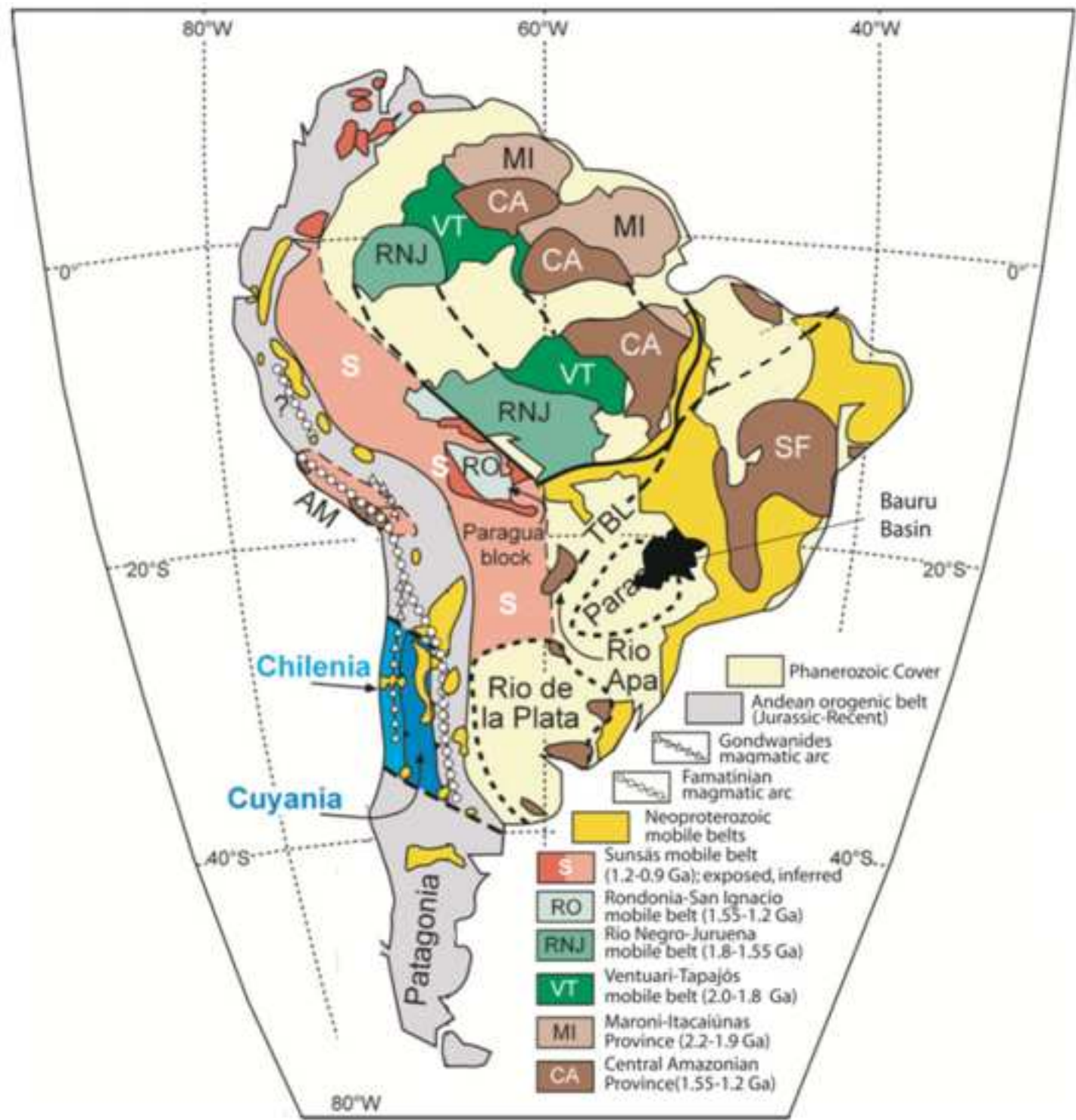
Figure 10 Dias et al

S1 (TF)_Diasetal

S1 (TF)_Diasetal

S2 (TFandUPb)_Diasetal

ANEXOS

Artigo publicado

1. Tello, C. A. S.; Curvo, E. A. C.; Dias, A. N. C. et al., 2012. Effects of etching on zircon grains and its implications to Fission Track Method. Applied Spectroscopy, 66 (5), 545-551.

Apresentação em congresso (Resumos e Resumos expandidos)

2. Dias, Airton Natanael Coelho, Chemale Jr., F., Tello, C. A. S. et al., Recognition of the early orogenic cycles of the South American Platform and adjacent areas by detrital zircon Fission Track and U-Pb dating of the Mesozoic Bauru Basin. 12th International Conference on Thermochronology - Thermo2010, 2010, Glasgow, Scotland - *(artigo submetido)*.

3. Dias, Airton Natanael Coelho, Chemale Jr., F., Tello, C. A. S. et al., Detrital zircon fission track and U-Pb dating applied in samples of Presidente Prudente formation, Bauru Basin, Brazil. VII SSAGI - South American Symposium on Isotopic Geology, 2010, Brasilia-DF, Brasil.

4. Dias, Airton Natanael Coelho, Tello, C. A., Chemale Jr., F. et al., Método de Traços de Fissão e U-Th-Pb in situ em zircão: geocronologia da Província Borborema. XXIII Simpósio de Geologia do Nordeste, 2009, Fortaleza-CE, Brasil - *(artigo em preparação)*.

5. Dias, Airton Natanael Coelho, Tello, C. A., Chemale Jr., F. et al., Zircon fission track and U-Pb dating of Bauru group, Parana Basin, Brazil. V International Symposium on Radiation Physics, 2009, Cidade do México, México - (*artigo publicado*).

6. Curvo, E. A. C.; Tello, C.A.; Dias, Airton Natanael Coelho. et al., Zircon fission track and U-Pb dating methods applied to São Paulo and Taubaté Basins located in the Southeast Brazil. 25th International Conference on Nuclear Tracks in Solids, 2011, Puebla, México - (*artigo submetido*).

7. Dias, Airton Natanael Coelho; Chemale Jr., F.; Tello, C. T. S., et al., Análise integrada pelos Métodos de Traços de Fissão e U-Pb aplicada a zircões detríticos da Bacia Bauru, Brasil. 46º Congresso Brasileiro de Geologia, 2012, Santos, Brasil.

Effects of Etching on Zircon Grains and Its Implications for the Fission Track Method

CARLOS ALBERTO TELLO SÁENZ,* EDUARDO AUGUSTO CAMPOS CURVO, AIRTON NATANAEL COELHO DIAS, CLEBER JOSÉ SOARES, CARLOS JOSÉ LEOPOLDO CONSTANTINO, IGOR ALENCAR, SANDRO GUEDES, ROSANE PALISSARI, and JULIO CESAR HADLER NETO

Departamento de Física Química e Biologia, UNESP Universidade Estadual Paulista, 19060-900 Presidente Prudente, SP, Brazil (C.A.T.S., E.A.C.C., A.N.C.D., C.J.L.C.); Instituto de Geociências e Ciências Exatas, UNESP Universidade Estadual Paulista, 13506-900, Rio Claro, SP, Brazil (C.J.S.); and Instituto de Física "Gleb Wataghin", Universidade Estadual de Campinas, UNICAMP, 13083-970 Campinas, SP, Brazil (I.A., S.G., R.P., J.C.H.N.)

Studies of zircon grains using optical microscopy, micro-Raman spectroscopy, and scanning electron microscopy (SEM) have been carried out to characterize the surface of natural zircon as a function of etching time. According to the surface characteristics observed using an optical microscope after etching, the zircon grains were classified as: (i) homogeneous; (ii) anomalous, and (iii) hybrid. Micro-Raman results showed that, as etching time increases, the crystal lattice is slightly altered for *homogeneous* grains, it is completely damaged for *anomalous* grains, and it is altered in some areas for *hybrid* grains. The SEM (energy dispersive X-ray spectroscopy, EDS) results indicated that, independent of the grain types, where the crystallinity remains after etching, the chemical composition of zircon is approximately 33% SiO_2:65% ZrO_2 (standard natural zircon), and for areas where the grain does not have a crystalline structure, there are variations of ZrO_2 and, mainly, SiO_2. In addition, it is possible to observe a uniform surface density of fission tracks in grain areas where the determined crystal lattice and chemical composition are those of zircon. Regarding hybrid grains, we discuss whether the areas slightly altered by the chemical etching can be analyzed by the fission track method (FTM) or not. Results of zircon fission track and U-Pb dating show that hybrid and homogeneous grains can be used for dating, and not only homogeneous grains. More than 50 sedimentary samples from the Bauru Basin (southeast Brazil) were analyzed and show that only a small amount of grains are homogeneous (10%), questioning the validity of the rest of the grains for thermo-chronological evolution studies using zircon FTM dating.

Index Headings: Zircon; Micro-Raman spectroscopy; Fission track method; Scanning electron microscopy; SEM; Energy dispersive X-ray spectroscopy; EDS; Zircon crystal lattice; Zircon chemical etching.

INTRODUCTION

The fission track method, FTM, is commonly used to evaluate thermo-chronological evolution in regions of geological interest. This application is based on the accumulation of fission tracks, originating from spontaneous fission decay of ^{238}U on the geological time scale, and the possibility that these tracks can be revealed when a mineral is submitted to appropriate etching. Some minerals to which FTM is commonly applied include, for instance, apatite and zircon, whose principal difference is the range of temperatures in which fission tracks have their lengths partially shortened (partial annealing zone, PAZ). Thus, from the measurement of fission track lengths it is possible to infer the interval of time

over which the mineral experienced PAZ temperatures and then reconstruct its geological thermal history. In the case of apatite, the PAZ spans between 60 and 110 °C (considering the time period of 1 Ma, where Ma is "million years"). The same interval is required for maturation of hydrocarbons in Ma (see Gallagher et al.[1] and references therein). For zircon, the PAZ spans between 190 and 380 °C (for heating durations of 1 Ma).[2] In this way, zircon enables the study of more intense thermal events and/or to find the crystallization age. An important example of its application is the geological fault dated by Murakami et al.[3] Thus, zircon fission track analysis complements the information given by the apatite fission track analysis.

Depending on the sample, laboratory treatments of zircon may be very laborious, reflecting the scarce annealing data previously presented.[4–6] However, it is possible to use this data for annealing modeling (e.g., Guedes et al.[7]). One of the major issues in the application of FTM to zircon is the track etching.[8] Etching and annealing (track fading by temperature[9]) of fission tracks in zircon are affected by: (i) crystallization through magmatic or metamorphic zonation; (ii) metamictization (partial or total damage of the crystal lattice caused by nuclide recoil during alpha decay) when the mineral has high concentration of uranium (U) and thorium (Th) (above 5000 ppm of $UO_2 + ThO_2$),[10,11] and (iii) the incorporation of other minerals. Such events can take place in zircons of igneous or detrital rocks. In general, at least one of these phenomena can be identified in natural zircons.

Over the last decade, micro-Raman spectroscopy has been applied to zircon to analyze radiation effects in the annealing process. Micro-Raman spectroscopy data present systematic changes in frequency, relative intensity, and/or band width according to the dose. These data are related to metamictization,[11–15] i.e., the loss of the periodic crystal structure. This phenomenon is the result of the accumulation of radiation damage over time in the geological timescale.[16] In natural zircons, metamictization is the result of the radioactive decay of U and Th incorporated during crystal growth (as well as the decay of their daughter products) and, therefore, the crystallization degree in a zircon sample may be described by the relative amounts of the amorphous and swelled crystalline fractions. According to Wasilewski et al.[17] and other researchers,[18–20] the α-recoil nuclei directly amorphize the structure, whereas point defects created by particles, together with the tangent stress from adjacent amorphous regions, induce swelling of the crystal structure. Palenik et al.[11] presented a micro-analytic study (optical microscopy, Raman spectroscopy, and

high-resolution transmission electron microscopy (HR-TEM)) of a zircon from Sri Lanka (alluvial zircon, with an estimated age of 570 ± 20 Ma), in which they observed zoning resulting from radiation damage (see also Chakoumakos et al.[21]). Evidence for the increased reactivity of metamict zircon is also given by the discordant ages determined from metamict areas of natural zircon samples.[22–24] However, little attention has been paid to the role of metamictization on the chemical stability of zircon at the Earth's surface.[25] Also, little is known about the effect of chemical etching over the zircon crystal lattice.

In the present work, the study of natural zircon surfaces was carried out using micro-Raman spectroscopy as a function of etching time. For this goal, we used a sample, denoted JP, collected in the Barreiras Formation, near the city of Matacara, State of Paraíba, northeast Brazil. The Barreiras Formation is a continental sedimentary deposit along the Brazilian coastline spanning from the State of Rio de Janeiro to the State of Amapá.[26] These detrital zircons present a mean uranium content of 130 ppm (calculated via neutron irradiation against standard uranium doped glasses) and mean Th/U ratio of 0.7 (calculated from inductively coupled plasma mass spectrometry (ICP-MS) measurements). The scanning electronic microscopy, SEM (energy dispersive spectroscopy (EDS)), was also used to characterize the zircon surface and to estimate the concentration of its main chemical oxide elements (ZrO_2 and SiO_2). Three types of zircon grains were identified after etching according to their response. They were classified here as *homogeneous*, *anomalous*, and *hybrid* grains. The aim of this work is to check the possibility of using *hybrid* grains in FTM. As a result, eight grains (*homogeneous* and *hybrid*) were dated by FTM and U-Pb dating to show that these zircon grains can be indeed used in thermo-geochronology. This work is complementary to the one carried out for *heterogeneous* grains, which show non-uniform fission-track distribution.[27]

EXPERIMENTAL PROCEDURES

The characterization of zircon grains was carried out before and after etching in terms of their surface morphology (optical microscopy) and crystalline structure (micro-Raman spectroscopy). Determination of the main chemical oxide elements (SEM/EDS) was carried out only after the etching. Optical microscopy and micro-Raman spectroscopy analyses were done for samples with no etching or with 6, 12, and 18 hours of etching. The experimental procedure for standard etching is described by Tagami et al.[5] Etching took place in steps until surface tracks perpendicular to the crystallography C-axis reach approximately 2 μm width.[4] The ideal etching time for samples used in this work was 18 hours. The SEM (EDS) analyses were carried out only for 18 hours of etching. The optical microscopy images were recorded using a microscope Leica DMRX, with nominal magnification up to 1500×, digital camera (ExwaveHAD Sony, model SSC-DC54A), and Image-Pro Plus 4.0 program for image acquisition. After etching, it shows that (i) a typical *homogeneous* grain surface has its crystallinity slightly changed after the chemical etching and presents a uniform fission-track distribution; (ii) an *anomalous* grain surface loses the crystallinity presented before etching, being heavily etching damaged. This etching damage may be occurring due to several physicochemical phenomena, and not only due to metamictization. Another possibility is the incorporation of other minerals;[28] and (iii) a *hybrid* grain surface presents preserved areas (with crystallinity and fission

tracks, as in the homogeneous grain case) and damaged areas (as in the anomalous grain case). The zircon classification used in this work tries to describe an etched surface characteristic, which may be well known in the fission track community but has not yet been reported. We could call the *hybrid* grain (for instance) a "patchily over-etched" grain, but this classification implies that one area reveals tracks and another does not. However, this is typical of grains that present etching anisotropy, which is not the case here. The *hybrid* grain maintains (after etching) areas with tracks while other areas are completely damaged by the etching.

Micro-Raman spectroscopy was carried out using a spectrograph micro-Raman Renishaw model in-Via equipped with a charge-coupled device (CCD) detector, Leica Microscope, lasers at 514.5, 633, and 785 nm, an automatic sample holder base (which allows X, Y, and Z translations with steps of 0.1 μm), and gratings with 1800 and 1200 grooves/mm. The Raman spectra were collected with spatial resolution around 1 μm^2, spectral resolution of approximately 2.5 cm^{-1}, and directly from the grains without any further treatment beyond the one necessary for the fission track analysis (i.e., polishing and etching). The measurements were done with the 514.5 nm laser line focused perpendicular to the C-axis using the 50× objective lens and gratings with 1200 grooves/mm. The SEM (EDS) measurements[29] were performed with a scanning electron microscope LEO430. The electron beam operated with energy of 20 keV, working distance of 19 mm, beam current of 3×10^{-9} A, and vacuum of 1×10^{-5} torr. Samples were coated with carbon before measurement to avoid charge effects. The process to obtain grains of zircon utilized conventional techniques, i.e., by crushing, grinding, magnetic, and heavy liquid separations. After these, zircon grains were mounted in a sheet of Teflon PFA and polished. Before etching, all grains were observed by optical microscopy and presented a flat surface from characteristic zircon grains. The etching was done with an eutectic mixture of KOH : NaOH at $(225 \pm 2)° C.$[8,30]
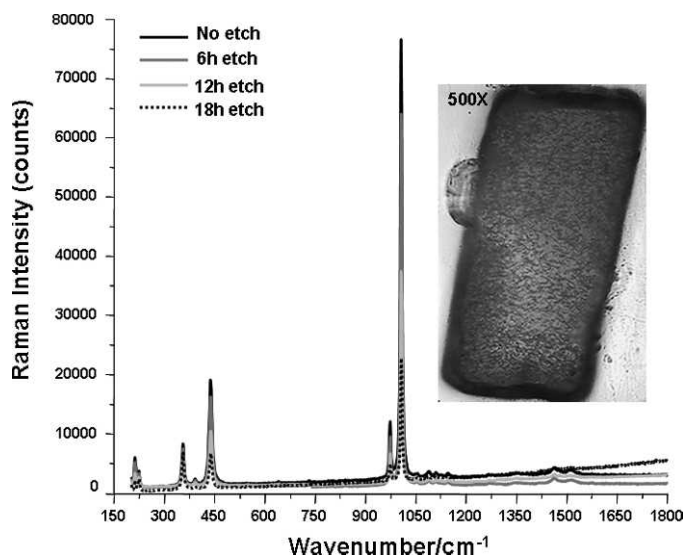

FIG. 1. *Homogeneous grain:* grain after 18 hours of etching with 500× nominal magnification (inset) and surface analyses using micro-Raman spectroscopy as a function of etching time.

TABLE I. Raman assignments for the zircon mineral.[a]

Raman (514.5 nm) (cm^{-1})	Assignments
356	(E$_g$) or SiO$_4$ υ$_4$
393	(E$_g$) or (B$_{1g}$)
439	SiO$_4$ υ$_2$ (A$_{1g}$)
974	SiO$_4$ υ$_1$ (A$_{1g}$)
1008	SiO$_4$ υ$_3$ (B$_{1g}$)

[a] υ$_1$, symmetric stretching; υ$_2$, symmetric bending; υ$_3$, antisymmetric stretching; υ$_4$, antisymmetric bending; A$_{1g}$, B$_{1g}$, internal vibrational modes; E$_g$, external modes

RESULTS

Micro-Raman Spectroscopy. Figures 1, 2, and 3 present the Raman spectra for *homogeneous*, *anomalous*, and *hybrid* grains, respectively, whose optical images are given in figure insets. The assignments of the main Raman bands are given in Table I, which summarizes literature data.[31,32] The vibrational modes are related to Si–O bonding. Raman data (wavenumber, intensity, relative intensity, and full width at half-maximum (FWHM)) are shown in Table II.

Homogeneous Grain. The inset in Fig. 1 shows an optical image obtained with 500× nominal magnification and reveals a uniform density of fission tracks for a grain surface after 18 hours of etching. Four Raman spectra were collected over sequential etching times (without etching and with 6, 12, and 18 hours of etching, see Fig. 1). It can be seen that the absolute and relative intensity of the peaks decreases as etching time
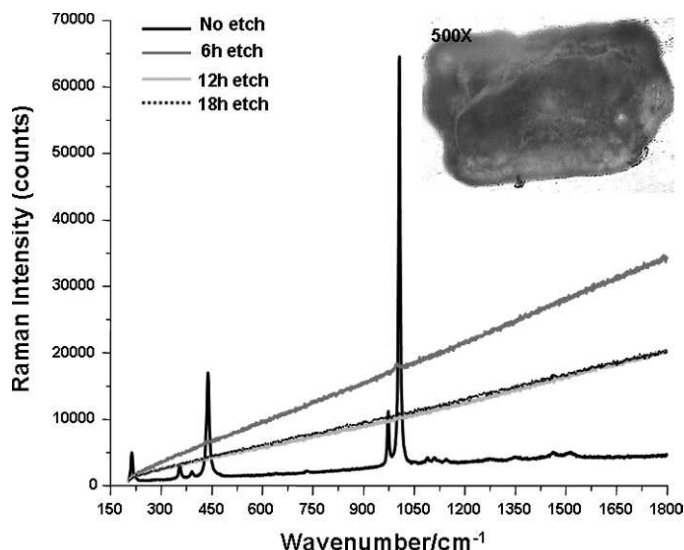

FIG. 2. *Anomalous grain:* grain after 18 hours of etching with 500× nominal magnification (inset) and surface analyses using micro-Raman spectroscopy as a function of etching time.

increases (Table II), but even after 18 hours of etching a significant percentage of the crystalline structure is maintained. The latter indicates that this type of grain is suitable for zircon FTM dating. The same analyses were done for other *homogeneous* grain areas and the results are similar. Similar results were also found for *heterogeneous* grains.[27] However,

TABLE II. Raman data (wavenumber, intensity, relative intensity, FWHM) for the natural zircon grains (JP sample), with and without chemical etching.[a]

		Etched					
Not-etched		6 hours		12 hours		18 hours	
ῡ (cm^{-1})	Intensity [RI] (FWHM)	ῡ (cm^{-1})	Intensity [RI] (FWHM)	ῡ (cm^{-1})	Intensity [RI] (FWHM)	ῡ (cm^{-1})	Intensity [RI] (FWHM)
HOMOGENEOUS GRAINS							
223.8	6123 [8.26%] (7.34)	224.1	5209 [7.03%] (7.63)	224	3865 [5.21%] (7.62)	223.5	2486 [3.35%] (7.88)
355.1	7937 [10.71%] (7.19)	355.5	7691[10.38%] (7.21)	355.6	7201 [9.72%] (6.98)	355.5	6974 [9.41%] (7.14)
390.6	1703 [2.30%] (7.02)	390.5	1555 [2.10%] (7.11)	390.5	1346 [1.80%] (7.14)	390.5	1037 [1.4%] (7.29)
437.8	19463 [26.27%] (9.38)	438.1	17817 [24.05%] (9.41)	438.1	11549 [15.59%] (9.07)	437.9	6038 [8.15%] (8.92)
974.2	11449 [15.45%] (6.14)	974	10102 [13.63%] (6.56)	974.5	7641 [10.31%] (6.71)	974.3	4723 [6.37%] (6.67)
1006	74085 [100%] (5.94)	1006.5	62380 [84.20%] (6.04)	1006.6	37489 [50.60%] (5.69)	1006.5	22607 [30.51%] (5.63)
ANOMALOUS GRAINS							
224	5011 [7.81%] (7.44)	–	–	–	–	–	–
355.5	3297 [5.38%] (8.33)	–	–	–	–	–	–
390	1816 [2.97%] (8.42)	–	–	–	–	–	–
437	16920 [27.60%] (9.96)	–	–	–	–	–	–
975	9142 [14.90%] (6.65)	–	–	–	–	–	–
1007.3	61214 [100%] (6.75)	1005.7	1156 [1.89%] (11.40)	–	–	–	–
HYBRID GRAINS – Area A							
224	4911 [8.27%] (7.02)	224.2	4792 [8.07%] (7.24)	224.5	4255 [7.17%] (7.35)	224.5	3551 [5.98%] (7.42)
355.1	3844 [6.48%] (6.89)	355.1	3671 [6.18%] (6.92)	355.5	3288 [5.54%] (7.01)	355.5	2790 [4.70%] (7.13)
390.6	1476 [2.49%] (7.66)	391	1387 [2.33%] (7.85)	391	1002 [1.68%] (8.31)	391.2	833 [1.40%] (8.44)
437.8	14569 [24.55%] (9.41)	437.8	14023 [23.63%] (9.69)	437.8	10723 [18.07%] (9.98)	438.1	7610 [12.83%] (10.11)
974.2	7832 [13.19%] (6.02)	974.5	7534 [12.69%] (6.13)	974.5	4365 [7.35%] (6.26)	974.8	2968 [5.00%] (6.34)
1006.5	59354 [100%] (6.70)	1007.1	55263 [93.10%] (6.94)	1007.5	38452 [64.78%] (7.11)	1007.8	24199 [40.77%] (7.27)
HYBRID GRAINS – Area B							
224.5	5452 [8.92%] (7.59)	–	–	–	–	–	–
355	3877 [7.98%] (8.54)	–	–	–	–	–	–
390	1204 [1.97%] (9.61)					–	–
438.5	15798 [25.86%] (9.90)	438.6	2935 [4.80%] (12.48)	438.6	1129 [1.85%] (13.23)	–	–
975.3	6843 [11.20%] (7.25)	–	–	–	–	–	–
1007.7	61085 [100%] (6.73)	1006.9	7127 [11.7%] (10.35)	1007.8	1567 [2.56%] (8.9)	–	–

[a] ῡ is the Raman wavenumber, RI is the relative intensity regarding the 1008 cm^{-1} peak, FWHM is the Full Width at Half Maximum (cm^{-1}).

TABLE III. Main oxide chemical elements estimative obtained through SEM (EDS).

Grain classification	Areas	ZrO$_2$ (%)	SiO$_2$ (%)	HfO$_2$ (%)
Homogeneous (Fig. 4)	P1	67.75	30.25	2
	P2	67.49	30.52	1.99
	P3	67.37	30.53	1.92
Anomalous (Fig. 5)	P1	73.82	0.72	2.22
	P2	60.65	0.62	1.99
	P3	56.15	0.63	1.67
Hybrid (Fig. 6)	P1	68.13	30.8	1.07
	P3	67.94	30.55	1.5
	P4	67.69	30.62	1.69
	P5	68.52	29.96	1.52

because only about 10% of the grains we have so far analyzed in over 50 sedimentary samples from the Bauru Basin are of the *homogeneous* type, it is important to pursue other grain types that allow the use of FTM dating. A thorough counting performed of 500 grains from the Bauru Basin lead to the following proportions of grains: anomalous, 60%; hybrid, 20%; and heterogeneous, 10%. The cretaceous rocks from the Paraná Basin, where the Bauru Group is located, are composed predominantly of sandstones with different grain sizes (coarse, medium, fine, and very fine grained), colors (pale brown to reddish), and characteristics (conglomeratic, clay, mudstone). They present a mean uranium content of 150 ppm and mean Th/U ratio of 0.7. The grains described in this work (homogeneous, anomalous, and hybrid) are present both in the samples from the Bauru Group and from the Barreiras Formation (JP sample). The mean uranium content obtained for both suites of detrital zircon are: Bauru Group $\sim$ 150 ppm and Barreiras Formation $\sim$ 130 ppm (Table III).

Anomalous Grain. The inset in Fig. 2 shows an optical image obtained with 500$\times$ nominal magnification for an *anomalous* grain after 18 hours of etching. It is observed that the grain surface is totally damaged. Raman spectra were measured for the grain without etching and after 6, 12, and 18

hours of etching (Fig. 2). The crystallinity of the *anomalous* grains is more affected by etching than the crystallinity of *homogeneous* grains (Table II). The Raman spectra are already flattened in the first hours of etching, indicating that the grain crystalline structure is completely damaged. As mentioned in the Experimental Procedures section, this etching damage may be occurring due to several physicochemical phenomena, and not only due to metamictization. It is also possible to have incorporation of other minerals. Other grains of this kind were analyzed, showing similar results. Therefore, these grains cannot be used for FTM dating.

Hybrid Grain. The inset in Fig. 3 shows an optical image obtained with nominal magnification of 500$\times$ for a *hybrid* grain after 18 hours of etching. For this grain, fission tracks are uniformly distributed within certain areas (e.g., area A) while for other areas (e.g., area B) fission tracks are not observed. In both areas, Raman spectra were obtained for the grain without etching and after 6, 12, and 18 hours of etching (Fig. 3 and Table II). The *hybrid* grain can be interpreted as a mixture of the *homogeneous* and *anomalous* grains. Area A presents a similar trend (Raman data) to that found for the *homogeneous* grains, i.e., a significant portion of the surface and mineral crystalline structure is preserved. On the other hand, in area B, the results are similar to those found for *anomalous* grains, i.e., loss of crystalline structure during the first hours of etching. Other grains of this type were analyzed showing similar results. This trend indicates that, if at least one area with uniform density is found (*hybrid* grain area A), then the *hybrid* grains could be used for FTM through the external detector method.

Scanning Electronic Microscopy. The SEM (EDS) analyses were carried out for *homogeneous*, *anomalous*, and *hybrid* grains in order to qualitatively investigate their chemical composition. The analyses of SEM (EDS) were done on the same grains used to obtain the micro-Raman spectroscopy after 18 hours of etching.

Homogeneous Grain. An SEM (back-scattered electron, BSE) image and an estimate of the main chemical oxide elements (ZrO$_2$, SiO$_2$, and HfO$_2$) obtained through SEM (EDS) for a *homogeneous* grain are shown in Fig. 4A and Table III,
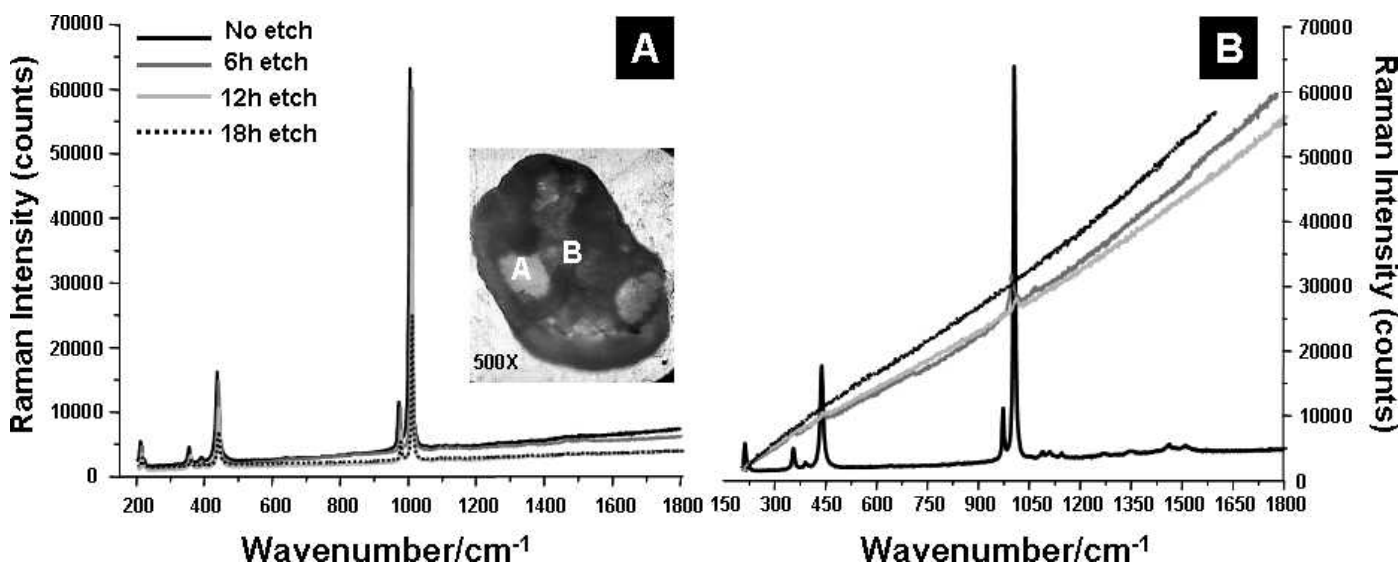

FIG. 3. *Hybrid grain:* grain after 18 hours of etching with 500$\times$ nominal magnification (inset) and surface analyses using micro-Raman spectroscopy as a function of etching time in areas A and B.
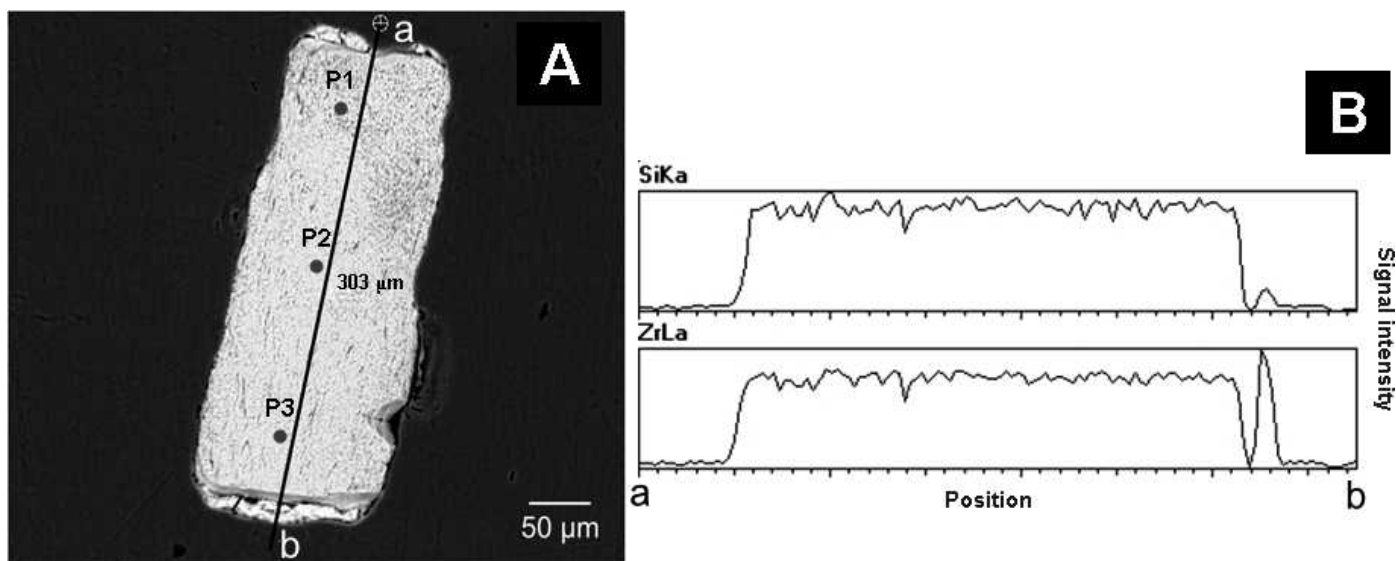
FIG. 4. *Homogeneous grain:* (**A**) SEM (BSE) grain image after 18 hours of etching and (**B**) SEM (EDS) line profile analysis.

respectively. The chemical analysis was done in three different areas, approximately in the same areas used to record the micro-Raman spectra. A SEM (EDS) line profile analysis was also done and the result is shown in Fig. 4B. Table III shows that the measurements of ZrO_2, SiO_2, and HfO_2 in three different areas agree with natural zircon (e.g., sample 4403 from Sri Lanka: 67.8% ZrO_2; 32.0% SiO_2; and 0.95% HfO_2).[24] The line profile (Fig. 4B) shows that zirconium and silicon measurements are uniform in the whole grain. In this kind of grain, even after 18 hours of etching, the crystallinity could be verified by micro-Raman spectroscopy (Fig. 1). It is worth noting that non-standard zircon[27] also presented similar main chemical oxide elements and micro-Raman spectra.

Anomalous Grain. Figure 5A shows a SEM (BSE) image of an *anomalous* grain damaged due to the chemical etching. Table III shows the quantity of ZrO_2, SiO_2, and HfO_2 obtained in three areas of the grain. This grain is different from the one

used in the micro-Raman spectroscopy measurement (Fig. 2) because background noise during the SEM measurements prevented the EDS analysis. Instead, another anomalous grain was chosen and characterized. Because the anomalous grains present similar characteristics, the final result was not changed. The values obtained from this analysis were not in accordance with the chemical composition of standard zircon. It can be seen in Fig. 5B that the SEM (EDS) line profile shows a greater change of the zirconium and silicon amount in this grain than in the *homogeneous* grain. Also, from Table III, a drastic decrease in SiO_2 can be seen, reaching almost null concentration. The amount of ZrO_2 varies, usually also decreasing. However, the latter variation is much smaller than the former. With these observations, it could be possible to conclude that the zircon crystallinity depends on the amount of silicon. This crystallinity loss could also be observed in the micro-Raman spectra evolution (Fig. 2).
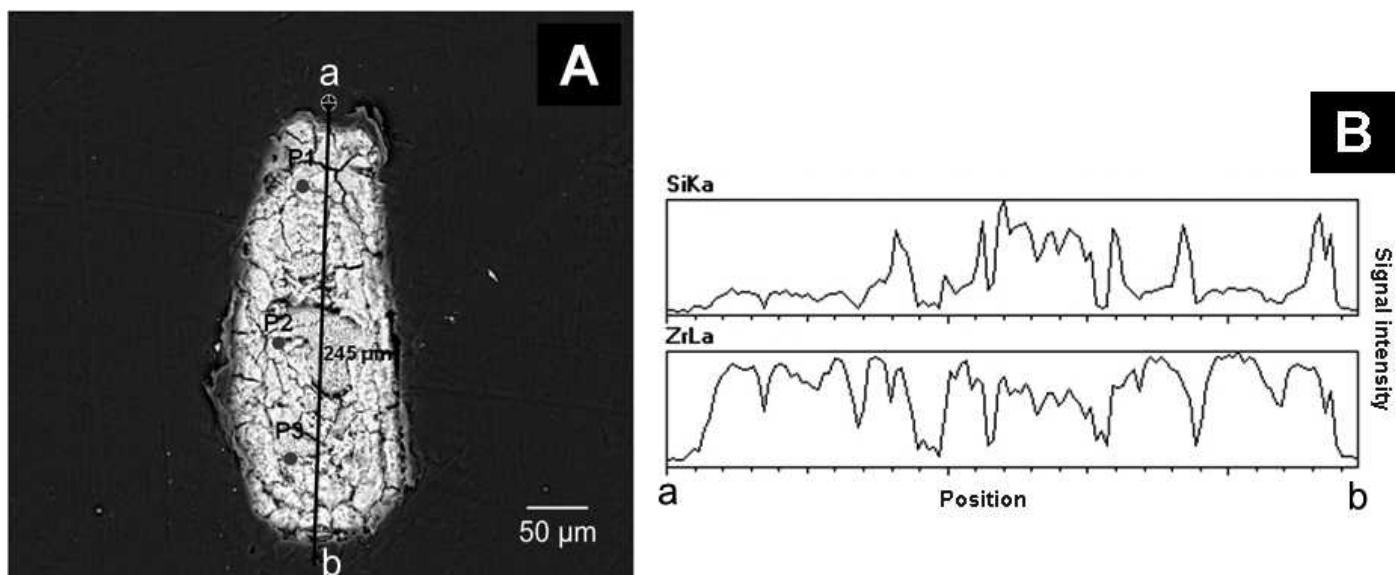

FIG. 5. *Anomalous grain:* (**A**) SEM (BSE) grain image after 18 hours of etching and (**B**) SEM (EDS) line profile analysis.
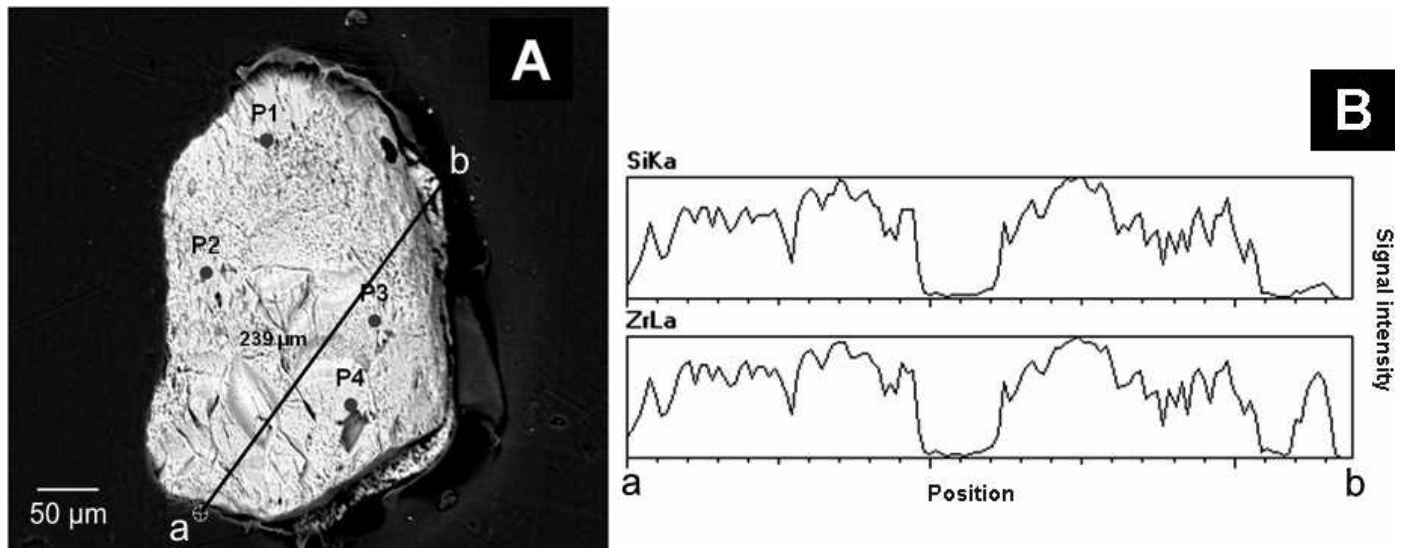
Fig. 6. *Hybrid grain:* (**A**) SEM (BSE) grain image after 18 hours of etching and (**B**) SEM (EDS) line profile analysis.

Hybrid Grain. A SEM (BSE) image of a *hybrid* grain is presented in Fig. 6A. In this grain the analysis of the main chemical oxide elements was carried out in four areas using SEM (EDS). The results are shown in Table III. It can be seen that the values of ZrO_2 and SiO_2 are similar to those of standard zircon. These areas can be related to the presence of uniform fission track density. Micro-Raman spectra indicated the existence of crystallinity for these areas even after 18 hours of etching (Fig. 3A). So, these areas could be used for FTM dating through the external detector method. On the other hand, the SEM (EDS) line profile analysis (Fig. 6B) shows areas that have different characteristics compared to *homogeneous* grains (Fig. 4B). It is important to observe an almost null value for SiO_2 and ZrO_2 in certain areas. These areas can be related to a totally damaged surface (like the *anomalous* grain). The presence of totally damaged areas does not prohibit the utilization of the hybrid grains for FTM, since it is possible to work within the homogeneous areas.

Fission Track Method and U-Pb in Situ Dating. As an example, eight zircon grains from Barreiras Formation (JP sample), near the city of Matacara, State of Paraíba, Brazil, are shown in Table IV. These grains were dated by both FT and U-Pb dating methods. The U/Pb ages were obtained by aiming the laser at the areas where fission tracks were developed, which improved the agreement of the obtained U/Pb ages (Table IV). The ages obtained by FTM in homogeneous and hybrid grains are consistent. As also shown in Table IV, the ages found using the U-Pb method are systematically higher than those found via FTM. The latter is also consistent since the closure temperature for the U-Pb system is approximately 700 °C and for zircon FTM is approximately 240 °C.[30] The FTM dating data strengthen the conclusion that the *hybrid* grains can be used in FTM analyses. Further dating data and more details about geological interpretations are beyond the scope of this article and might be subjects of future research.

TABLE IV. Zircon U-Pb and FTM data for JP sample.[a]

| | | | LA-MC-ICP-MS DATA | | | | | | | | | | AGES (Ma) | | | |
| | | | | | Ratios # | | | | | FTM DATA | | | | U-Pb in situ | | FTM |
Grain #	$^{232}Th/$ ^{238}U	U (ppm)	$^{207}Pb/$ ^{235}U	$\pm \sigma$ (%)	$^{206}Pb/$ ^{238}U	$\pm \sigma$ (%)	$^{207}Pb/$ ^{206}Pb	$\pm \sigma$ (%)	$\rho_S \times$ 10^7 cm^{-2}	N_S	$\rho_i \times$ 10^6 cm^{-2}	N_I	($\pm$ 2σ)	% Conc	($\pm$ 2σ)
2 [B1]	0.49	115.8	11.70205	0.68	0.47702	0.44	0.17792	0.52	2.85	73	0.923	30	2634	17	95	371	80
3 [B3]*	0.88	76.0	0.82775	3.53	0.09963	1.71	0.06026	3.09	3.39	130	1.323	43	612	20	100	373	80
8 [C3]*	0.78	45.0	3.87207	2.24	0.28044	0.98	0.10014	2.01	2.63	118	1.931	63	1597	26	98	346	72
10 [D7]	0.66	87.7	6.52885	1.39	0.37460	0.86	0.12641	1.09	3.56	114	1.204	39	2050	24	100	356	79
11 [D9]*	1.01	33.3	3.60351	2.85	0.26737	1.26	0.09775	2.56	3.03	97	1.441	47	1533	32	97	319	67
17 [F3]*	0.80	110.3	6.41747	1.37	0.36455	0.93	0.12767	1.00	2.92	112	2.002	29	2066	36	97	353	73
23 [G6]	1.32	39.4	3.79171	2.53	0.27693	1.38	0.09931	2.12	2.86	28	1.052	38	1582	35	98	342	72
28 [H6]*	0.42	112.9	9.09817	1.09	0.41532	0.51	0.15888	0.97	3.27	48	0.593	38	2444	33	92	365	76

[a] The U-Th-Pb ages (concordant ages) are calculated after Ludwig program for those zircons with discordance <10%; Sample and standard are corrected after Pb and Hg blanks; $^{206}Pb/^{207}Pb$ and $^{206}Pb/^{238}U$ are corrected after common Pb presence; Common Pb assuming $^{206}Pb/^{238}U$ and $^{207}Pb/^{235}U$ concordant age; $^{235}U = 1/137.88*U_{total}$; Standard GJ-1; Th/U $= {}^{232}Th/^{238}U*0.992743$; the isotope ratios errors in the table are calculated with 1σ and the age with 2σ error; otherwise the concordant age is after $^{207}Pb/^{206}Pb$ age. ρ_S (ρ_i), spontaneous (induced) track density; N_S (N_i), number of tracks counted to determine ρ_S (ρ_i); ρ_i, induced track density was measured in muscovite mica acting as an external detector (EDM). The grains with * are examples of *hybrid* grains.

CONCLUSION

Three types of zircon grains were identified according to the way they react to chemical etching. After being analyzed through optical microscopy, micro-Raman spectroscopy, and SEM they were classified as *homogeneous*, *anomalous*, and *hybrid* grains. After etching, the *homogeneous* grains have their crystal lattice slightly altered and present a uniform fission-track distribution. The *anomalous* grains surfaces are strongly etching-damaged just after the first hours of etching and accordingly do not reveal fission tracks. On the other hand, the *hybrid* grains present a special characteristic: after the etching procedure some grain areas have no crystalline structure (as the *anomalous* grains), while other areas of the same grain reveal fission tracks (as the *homogeneous* grains).

The results obtained through micro-Raman spectroscopy (as a function of etching time) and SEM (EDS) analyses on the zircon surface indicated that areas with standard main oxide element concentrations and characteristic Raman spectra present a uniform fission track density, which can be used for FTM dating (through the external detector method). In other words, the areas that could reveal fission tracks are essentially zircon. In this way, not only *homogeneous* grains but also *hybrid* grains can be used for dating purposes. This result is very important for FTM because in many cases the natural zircon samples, after the etching procedure, have been damaged. Using the *hybrid* grains as well will increase the statistics of the analysis significantly. An interesting result obtained in this work is that in the case of the *anomalous* grains there is an accentuated reduction of the silicon oxide content, which may indicate the influence of the silicon in the structural stability of the mineral.

1. K. Gallagher, R. Brown, C. Johnson. "Fission Track Analysis and Its Applications to Geological Problems". Annu. Rev. Earth Planet. Sci. 1998. 26(1): 519–572.

2. T. Tagami. "Zircon Fission-Track Thermochronology and Applications to Fault Studies". Rev. Mineral. Geochem. 2005. 58(1): 95–122.

3. M. Murakami, J. Kosler, H. Takagi, T. Tagami. "Dating pseudotachylyte of the Asuke Shear Zone using zircon fission-track and U–Pb methods". Tectonophys. 2006. 424(1-2): 99–107.

4. R. Yamada, T. Tagami, S. Nishimura, H. Ito. "Annealing kinetics of fission tracks in zircon: an experimental study". Chem. Geol. (Isot. Geosci. Sect.). 1995. 122(1-4): 249–258.

5. T. Tagami, A. Carter, A.J. Hurford. "Natural long-term annealing of the zircon fission-track system in Vienna Basin deep borehole samples: constraints upon the partial annealing zone and closure temperature". Chem. Geol. (Isot. Geosc. Sect. 3). 1996. 130(1-2): 147–157.

6. M. Murakami, K. Yamada, T. Tagami. "Short-term annealing character-istics of spontaneous fission tracks in zircon: A qualitative description". Chem. Geol., (Isot. Geosc. Sect.). 2006. 227(3-4): 214–222.

7. S. Guedes. J. Hadlern, P.J. Iunes, K.M.G. Oliveira, P.A.F.P. Moreira, and C.A. Tellos. "Kinetic model for the annealing of fission tracks in zircon". Radiat. Meas. 2005. 40(2-6): 517–521.

8. J.I. Garver. "Etching zircon age standards for fission-track analysis". Radiat. Meas. 2003. 37(1): 47–53.

9. G. Wagner, P. van den Haute. Fission-track Dating. Kluwer Academic: Norwell, 1992. 6th vol., pp. 285.

10. E. Balan, D.R. Neuville, P. Trocellier, E. Fritsch, J.P. Muller, G. Calas. "Metamictization and chemical durability of detrital zircon". Am. Mineral. 2001. 86(9): 1025–1033.

11. C.S. Palenik, L. Nasdala, R.C. Ewing. "Radiation damage in zircon." Am. Mineral. 2003. 88(5-6): 770–781.

12. L. Nasdala, G. Irmer, D. Wolf. "The degree of metamictization in zircons: a Raman spectroscopic study". Eur. J. Mineral. 1991. 7: 471–478.

13. L. Nasdala, M. Wenzel, G. Vavra, G. Irmer, T. Wenzel, B. Kober. "Metamictisation of natural zircon: accumulation versus thermal annealing of radioactivity-induced damage". Contr. Min. Petr. 2001. 141(2): 125–144.

14. M. Zhang, E.K.H. Salje, I. Farnan, A. Graeme-Barber, P. Daniel, R.C. Ewing, A.M. Clark, H. Leroux. "Metamictization of zircon: Raman spectroscopic study". J. Phys.: Condens. Matter. 2000. 12(8): 1915–1925.

15. M. Lodzinski, R. Wrzalik, M. Sitarz. "Micro-Raman spectroscopy studies of some accessory minerals from pegmatites of the Sowie Mts and Strzegom-Sobótka massif, Lower Silesia, Poland". J. Mol. Struct. 2005. 744: 1017–1026.

16. H.D. Holland, D. Gottfried. "The effect of nuclear radiation on the structure of zircon". Acta Cryst. 1955. 8(6): 291–300.

17. P.J. Wasilewski, F.E. Senftle, J.E. Vaz, A.N. Thorpe, C.C. Alexander. "A study of the natural α-recoil damage in zircon by infrared spectra". Radiat. Eff. 1973. 17(3-4): 191–199.

18. E.K.H. Salje, J. Chrosch, R.C. Ewing. "Is "metamictization" of zircon a phase transition?" Am. Miner. 1999. 84(7-8): 1107–1116.

19. S. Ríos, E.K.H. Salje, M. Zhang, R.C. Ewing. "Amorphization in zircon: evidence for direct impact damage". R.C. J. Phys.: Cond. Matter. 2000. 12(11): 2401–2412.

20. K.T. Trachenko, M.T. Dove, E. Salje. "Modelling the percolation-type transition in radiation damage". J. Appl. Phys. 2000. 87(11): 7702–7707. 2000.

21. B.C. Chakoumakos, T. Murakami, G.R. Lumpkin, R.C. Ewing. "Alpha-Decay–Induced Fracturing in Zircon: The Transition from the Crystalline to the Metamict State". Science. 1987. 236(4808): 1556–1559.

22. A.C. McLaren, J.D. Fitz Gerald, I.S. Williams. "The microstructure of zircon and its influence on the age determination from Pb/U isotopic ratios measured by ion microprobe". Geochim. Cosmochim. Acta. 1994. 58(2): 993–1005.

23. L. Nasdala, R.T. Pidgeon, D. Wolf, G. Irmer. "Metamictization and U-PB isotopic discordance in single zircons: a combined Raman microprobe and SHRIMP ion probe study". Mineral. and Petrol. 1998. 62(1-2): 1–27.

24. T. Geissler, H. Schleicher. "Improved U–Th–total Pb dating of zircons by electron microprobe using a simple new background modeling procedure and Ca as a chemical criterion of fluid-induced U-Th-Pb discordance in zircon". Chem. Geol. 2000. 163(1-4): 269–285.

25. G.R. Lumpkin. "Alpha-decay damage and aqueous durability of actinide host phases in natural systems". J. Nucl. Mater. 2001. 289(1-2): 136–166.

26. V.D. Araújo, Y.A. Reyes-Peres, R.O. Lima, A.P. Pelosi, L. Menezes, V.C. Córdoba, F.P. Lima-Filho, Geol. USP Sér. Cient. 2006. 6(2): 43–49, in Portugeuse.

27. A.N.C. Dias, C.A. Tello Saenz, C.J.L. Constantino, C.J. Soares, F.P. Novaes, A.M.O.A. Balan. J. Raman Spectrosc. 2009. 40(1): 101–106.

28. M. Menneken, A.A. Nemchin, T. Geisler, R.T. Pidgeonl, S.A. Wilde. "Hadean diamonds in zircon from Jack Hills, Western Australia". Nature. 2007. 448(7156): 917–920.

29. C.W. Passchier, R.A.J. Trouw. Micro-tectonics. New York: Springer, 2005. 2nd ed., pp. 366.

30. M.T. Brandon, M.K. Roden-Tice, J.I. Garver. "Late Cenozoic exhumation of the Cascadia accretionary wedge in the Olympic Mountains, northwest Washington State". Bull. Geol. Soc. Am. 1998. 110(8): 985–1009.

31. T. Geisler, R.T. Pidgeon, W. van Bronswijk, R. Kurtz. "Transport of uranium, thorium, and lead in metamict zircon under low-temperature hydrothermal conditions". Chem. Geol. (Isot. Geosci. Sect.). 2002. 191(1-3): 141–154.

32. L. Nasdala, M. Zhang, U. Kempe, G. Panczer, M. Gaft, M. Andrut, M. Ploetze. "Spectroscopic methods applied to zircon". Rev. Mineral. Geochem. 2003. 53(1): 427–467.

Recognition of the early orogenic cycles of the South American Platform and adjacent areas by detrital zircon Fission Track and U-Pb dating of the Mesozoic Bauru Basin

A. N. C. Dias[1],*, F. Chemale Jr.[2], C. A. Tello S.[1], P.J. Iunes[3], J. C. Hadler[3], S. Guedes[3], E. Curvo[3], C. J. Soares[1], R.S. Resende[1], M. Constâncio Jr.[1], M. R. Gomes[1], L. A. Stuani[1]

[1]Dep. de Física, Química e Biologia – FCT/UNESP, Presidente Prudente-SP, Brazil
[2]Núcleo de Geologia – UFS, São Cristovão-SE, Brazil
[3] Instituto de Física Gleb Wataghin – DRCC/UNICAMP, Campinas-SP, Brazil.

*Correspondent Author: diasanc@bol.com.br

Ages of detrital zircon from sedimentary samples of the Conician-Maastrichtian Bauru Basin, an interior continental basin of the South American Platform, has been determined by zircon Fission Track and U-Pb *in situ* dating methods. The combination of the two thermochronometer techniques provides very important constraints on the source areas as well as the exhumation history of the South American Platform and adjacent orogenic areas. This study presents FT and U-Pb detrital zircon analysis from 9 samples collected along the stratigraphic profiles of the Bauru Basin. Based on detrital zircon U-Pb dating (DZUPbD) the main source area of the Mesozoic Basin are Brasiliano zircons, varying from 445 ± 14 to 708 ± 18 Ma with a main peak at 595 ± 2.2 Ma, a result of the late orogenic and collapse phases of the Brasiliano Mountains. Subordinate occurrences of Eoneoproterozoic are thus records of the early Brasiliano Magmatic arc. Mesoproterozoic zircons with peaks at 1025 ± 4.6 Ma, 1538 ± 32 Ma and 1794 ± 7.4 Ma are also recognized, interpreted to be related to the rock formation in a period of stable conditions on the South America plataform. The oldest zircons are Paleoproterozoic (1879 ± 27 Ma to 2186 ± 28 Ma) formed mostly during the Rhycian (Trans-Amazonian) Cycle and Archean 2648 ± 61 to 2815 ± 25 Ma. The youngest dated detrital zircon (90 ± 11Ma) is probably related to the synvolcanic process during the Bauru sedimentation. The Detrital Zircon FT (DZFT) analysis is a well established tool to study long term exhumation history of the orogenic mountains, although it can also provide information on the early orogenic process in the recycled material exposed on a stable platform. Moreover the DZFT data of the Bauru Basin can be grouped into four main populations: Early Brasiliano (720 to 825 Ma), the Brasiliano (480 – 650 Ma), Silurian-Devonian (440 – 360 Ma) and Late Paleozoic (354 – 250 Ma). The combined information of DZUPbD and DZFT suggested that the main source area for the Brasiliano zircons came from the western of the Bauru Basin, precisely from the Goiás Massif, Central Brazil. The Silrurian-Devonian FT-zircon age population was mostly incorporated into the Fold-Thrust-Belt of the Famitinian Orogenic Cycle and recycled during the Phanerozoic. The Neopaleozoic FT zircon ages can be associated with one of the most important orogenetic process in the Westgondawana, the Gondwanides Orogeny. These zircons were incorporated to the Fold-Thrust Belt and then recycled into the foreland deposits or/and Paleozoic intraplate Paraná Basin. Renewed erosional process occurred and the sediments of the Late Cretaceous Bauru Basin were deposited with fingerprints of mountain buildings of the South American Platform and surrounded by Paleozoic orogenic zones.

Detrital zircon Fission Track and U-Pb dating applied in samples of Presidente Prudente Formation, Bauru Basin, Brazil

A. N. C. Dias[1], F. Chemale Jr.[2], C. A. Tello S.[1], C. J. Soares[3], R. S. Resende[1], M. R. Gomes[1], M. Constâncio Jr.[1], L. A. Stuani[1], G. V. M. Pereira[1], M. C. T. F. de Godoy[1]

1 - Dep. de Física, Química e Biologia – FCT/UNESP, 19050-900, Presidente Prudente-SP, Brazil.
2 - Núcleo de Geologia – UFS, 49100-000, Aracajú-SE, Brazil.
3 – IGCE/UNESP, 13506-900, Rio Claro-SP, Brazil.

INTRODUCTION

As the Fission Track (FT) method, the U-Pb geochronology is becoming an increasingly important tool in Earth Science research because of the technical developments; they have provided opportunities for improved precision and accuracy, finer spatial resolution, and more efficient data acquisition (Gehrels and Juiz, 2007). The strength of the FT technique is that it can provide low-temperature (200 - 320 °C, e.g., Tagami et. al., 1998) data that record the thermotectonic evolution of a source terrane. Such information is central to understanding the temporal relationships between a developing source region and sedimentation in adjacent basins. While FT detrital zircon data are ideally used to provide low-temperature information, U-Pb single detrital grain ages (measured using techniques such as the SHRIMP or Laser Ablation ICP-MS), record the time of zircon formation in igneous or high grade metamorphic environments (Carter & Moss, 1999; Dias et al., 2010).

Were determined Zircons ages from sedimentary rocks (igneous and metamorphic) from Presidente Prudente Formation, Bauru Group, São Paulo state, Brazil, using FT method and U-Pb *in situ* dating with LA-MC-ICP-MS.

GEOLOGICAL SETTING

The Bauru Basin is a Coniacian–Maastrichtian (LateCretaceous) continental basin developed as a result of subsidence within the central-southern part of the South- American Platform (Fernandes, 2004), following the break up and separation of Gondwana. The depression was created in part as an isostatic response to the accumulation of almost 2000 m of the Early Cretaceous basaltic lavas of the Serra Geral Formation. The basin has an area of about 370,000 km^2 and was filled with sandy strata that have a preserved maximum thickness of almost 300 m. The basin substratum consists of volcanic rocks (mainly basalts) of the Serra Geral Formation, from which the sedimentary pile is separated by an erosive regional surface (non-conformity). Its upper erosive limit is demarcated by the Sul-Americana (King, 1956) or Japi (Almeida, 1964) Surface, and by its posterior dissection. According to Fernandes and Coimbra (2000a), the siliciclastic sequence is composed of two partially contemporaneous groups (Figure 1). The sedimentary succession is divided into two groups (details in figure 2): the Caiuá, formed by the Rio Paraná, Goio Erê and Santo Anastácio Formations, and the Bauru, consisting of the Uberaba, Vale do Rio do Peixe, Araçatuba, São José do Rio Preto, Presidente Prudente and Marilia Formations, including the Taiúva analcimites (Milani et al., 2007).

The Presidente Prudente Formation happens in the quotas highest of the regional interfluves; below of the Vale do Rio do Peixe level. The contact among these formations is showing the gradual settlement of the first (fluvial deposits) on second (aeolian deposits). This formation was deposited in meandering fluvial fine sandy system, of shallow channels with sinuosity relatively low. The unit is composed by the alternation of *i)* filling deposits of wide and shallow channels; and *ii)* floodplain deposits of marginal dikes *(crevasse)* (Fernandes & Coimbra, 2000a).
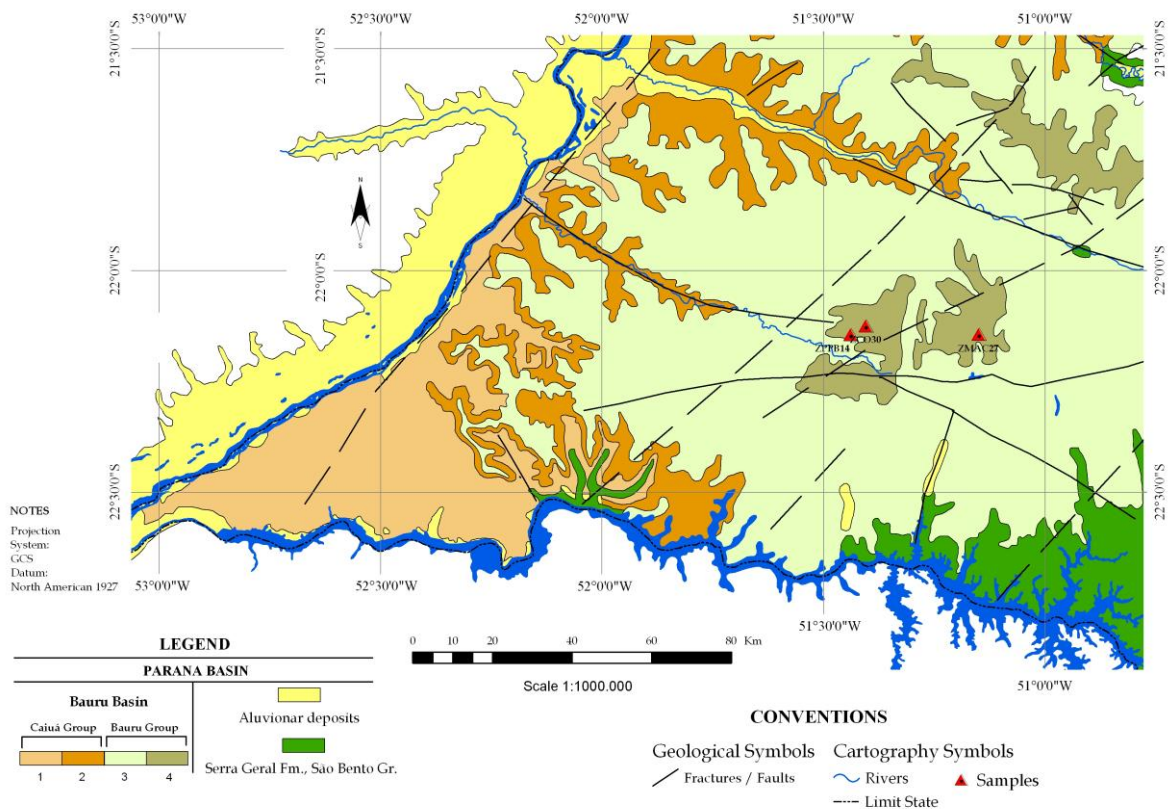

Figure 1 - Lithostratigraphic map of the Bauru Basin eastern. **Key: 1.** Rio Paraná Formation, **2.** Santo Anastácio Formation, **3.** Vale do Rio do Peixe Formation, **4.** Presidente Prudente Formation.

RESULTS

This study presents FT and U-Pb detrital zircon analysis from 3 samples collected along the Presidente Prudente Formation, Bauru Basin. The FT data of the Bauru Basin can be grouped into four main populations: the Brasiliano ages (480 to 680 Ma), as part of late stage of Brasiliano uplift, and Early-Famatian ages (220 to 340 Ma), as part of the main uplift in the South Platform during the Gondwanides, and Famatian ages (350 to 480 Ma), that record combined geological information from Late-Famatian and Early-Brasiliano cycles.

The obtained U-Pb ages of zircon grains are interpreted to be magmatic because the Th/U ratios vary from 0.26 to 1.57. The Th/U ratio > 0.20 is interpreted to be the limit for igneous versus metamorphic zircons, which they have usually very low values (10^{-2} to 10^{-3}) (e.g., Cates & Mojzsis, 2009). The analyzed zircons show a clear provenance of Brasiliano age zircons, ranging from 550 ± 28 to 735 ± 40 Ma. Minor occurrence of zircons formed from

862 ± 24 to 1756 ± 50 Ma (Early Neoproterozoic to Mesoproterozoic), as well as some zircons formed from 1973 ± 23 to 2819 ± 25 Ma (Paleoproterozoic) are also recognized.

CONCLUSIONS

It is possible conclude that the Mesozoic Basin are Brasiliano zircons (445 ± 14 to 708 ± 18 Ma) a result of the late orogenic and collapse phases of the Brasiliano Mountains. Subordinate occurrences of Eoneoproterozoic are thus records of the early Brasiliano Magmatic arc. Mesoproterozoic zircons with peaks at 1021 ± 22 Ma and 1756 ± 50 Ma are also recognized, interpreted to be related to the rock formation in a period of stable conditions on the South America plataform. The oldest zircons are Paleoproterozoic (1973 ± 31 Ma to 2189 ± 55 Ma) formed mostly during the Rhycian (Trans-Amazonian) Cycle and Archean (2819 ± 25 Ma). The detrital zircon FT analysis is a well established tool to study long term exhumation history of the orogenic mountains, although it can also provide information on the early orogenic process in the recycled material exposed on a stable platform.

The combined information of U-Pb and FT suggested that the main source area for the Brasiliano zircons came from the western of the Bauru Basin, precisely from the Goiás Massif, Central Brazil. The Silrurian-Devonian FT-zircon age population was mostly incorporated into the Fold-Thrust-Belt of the Famitinian Orogenic Cycle and recycled during the Phanerozoic. The Neopaleozoic FT zircon ages can be associated with one of the most important orogenetic process in the Westgondawana, the Gondwanides Orogeny. These zircons were incorporated to the Fold-Thrust Belt and then recycled into the foreland deposits or/and Paleozoic intraplate Paraná Basin. Renewed erosional process occurred and the sediments of the Late Cretaceous Bauru Basin were deposited with fingerprints of mountain buildings of the South American Platform and surrounded by Paleozoic orogenic zones.

REFERENCES

Almeida, F.F.M., 1964. Fundamentos geológicos do relevo paulista. Bol. Inst. Geogr. Geol. 41, 169–263.

Carter, A. and Moss, S. J., 1999. Combined detrital-zircon fission-track and U-Pb dating: A new approach to understanding hinterland evolution. Geology, 27 (3), 235–238.

Dias, A.N.C., C.A. Tello, F. Chemale Jr, P.J. Iunes, C.J. Soares, E.A. Curvo, S. Guedes, B.C. Barra, M. Constâncio Jr. and J.C. Hadler, 2010. Zircon fission track and U-Th-Pb in situ dating of Rio Paraná Formation, Paraná Basin, Brazil. Mexican Physics Review, 56:(1), 16–21.

Fernandes, L.A., 2004. Mapa litoestratigráfico da parte oriental da Bacia Bauru (PR, SP, MG), escala 1:1.000.000. Bol. Parana. Geocienc. 55, 53–66. 1 map (CD rom).

Fernandes, L.A., Coimbra, A.M., 2000a. Revisão estratigráfica da parte oriental da Bacia Bauru (Neocretáceo). Rev. Bras. Geo. 30 (4), 723–734.

Gehrels, G. E. and Juiz J., U-Th-Pb geochronology of zircon by Laser-Ablation Multicollector ICP Mass Spectrometry at the Arizona LaserChron Center. Journal of Analytical Atomic Spectrometry *(in press).*

King, L.C., 1956. A geomorfologia do Brasil oriental. Rev. Bras. Geog. 18 (2), 147–265.

Milani, E. J., Melo, J. H. G., Souza, P. A., Fernandes, L. A., França, A. B., 2007. Bacia do Paraná. Boletim de Geociências da Petrobrás, 15, 265–287.

Tagami, T., Ito, H., Nishimura, S., 1990. Thermal annealing characteristics of spontaneus fission tracks in zircon. Chemical Geology (Isot. Geosc. Sect.) 80, 159-169.

MÉTODO DE TRAÇOS DE FISSÃO E U-Th-Pb *IN SITU* EM ZIRCÃO: GEOCRONOLOGIA DA PROVINCIA BORBOREMA

Airton Natanael Coelho Dias[1]; Carlos AlbertoTello Saenz[1]; Farid Chemale Jr.[2]; Márcio Constâncio Jr.[1]; Cleber José Soares[3]; Beatriz Caroline Barra[1]; Mariana Rubira Gomes[1]; Luiz Augusto Stuani Pereira[1]
[1]Dep. de Física, Química e Biologia – FCT/UNESP, Presidente Prudente-SP – diasanc@bol.com.br;
[2]Dep. de Geografia – DGE/UFS, São Cristovão-SE; [3] Instituto de Geociências e Ciências Exatas – IGCE/UNESP, Rio Claro-SP.

Na última década, a obtenção de idades e histórias térmicas através do Método de Traços de Fissão (MTF) em zircão tem crescido rapidamente, bem como sua aplicação em diversas disciplinas das Ciências da Terra. O zircão contém altas concentrações de U e Th, bem como Elementos Terras Raras (ETR) e este pode ser encontrado como acessório em rochas ígneas, metamórficas e sedimentares. Não obstante, o zircão também é muito importante na datação absoluta (de alta precisão) de eventos magmáticos, metamórficos e sedimentares. Este tipo de datação é feita combinando a aquisição das quantidades dos isótopos de U, Th e Pb com uma análise *in situ* usando microscópio tipo *Laser Ablation*. O objetivo deste trabalho foi conectar estas duas técnicas de datação, pois esta combinação, aplicada a zircões detriticos de bacia sedimentares pode oferecer importantes informações sobre: *i)* eventos de baixa, intermediária e alta temperatura; *ii)* cristalização ígnea e metamórfica destes zircões; *iii)* eventos morfotectônicos (soerguimento, denudação, etc.) e; *iv)* estudos de proveniência sedimentar. Para isto, 57 zircões de rochas metamórficas e magmáticas da Província Borborema, próximo a Matacara, estado da Paraíba, Brasil, foram utilizados. Nas datações via U-Th-Pb, observa-se quatro principais grupos de idades: ~2600 Ma, 2129 Ma, 1593 Ma e 611 Ma, sendo relacionados aos ciclos do Jequié, ou equivalente, Neoarqueano (~2,6 Ga), Transamazônico (2,1 Ga) e Brasiliano (0,6 Ga). Já a concentração de idades de ~1,6 Ga estão relacionadas ao evento de magmatismo final do Ciclo Espinhaço, evento este de característica extensional. As análises dos zircões datados via MTF indicam dois principais grupos de idades: 370 Ma e 250 Ma, os quais podem estar relacionados aos eventos Gondwanides (250 Ma) e o Acadiana (África-América do Norte)/Famatina (América do Sul) (370 Ma). A maior concentração de idades MTF está entre 420-125 Ma, podendo incluir os registros dos eventos Acadiano (~354 Ma), Gondwanides (~280-250 Ma), como já citado, e rifteamento do início da separação Brasil-África (137 Ma). No entanto, observa-se que alguns zircões apresentam idades mais antigas (ciclos brasiliano, neo e mesoproterozóicos), indicando uma atuação significativa na construção do relevo no passado (como é de se esperar para região). Estas idades de MTF deixam evidente que os zircões tiveram apagados os eventos mais antigos que foram detectados pelo método U-Th-Pb. As idades obtidas via MTF indicam ainda que os zircões sofreram quase todos os eventos geológicos de baixa temperatura, o que implica na ocorrência de um maior número de eventos sofridos pelas amostras datadas com 1593 Ma, 2129 Ma e 2600 Ma.

ZIRCON FISSION TRACK AND U-Pb DATING OF BAURU GROUP, PARANA BASIN, BRAZIL

A. N. C. Dias[1] *, C. A. Tello S.[2], F. Chemale Jr.[1], P. J. Iunes[3], C. J. Soares[4], F. P. Novaes[3], B. C. Barra[2], M. Constâncio Jr. [2], J. C. Hadler[3]

(1) Laboratório de Geologia Isotópica – CPG*q*/UFRGS, 91501-970, Porto Alegre-RS, Brazil.
(2) Dep. de Física, Química e Biologia – FCT/UNESP, 19060-900, Presidente Prudente-SP, Brazil.
(3) Instituto de Física Gleb Wataghin – DRCC/UNICAMP, 13083-970, Campinas-SP, Brazil.
(4) Instituto de Geociências e Ciências Exatas – IGCE/UNESP, 13506-900, Rio Claro-SP, Brazil.

Ages of zircon samples of Bauru Group, north of Paraná Basin, Brazil, has been determined through Zircon Fission Track and U-Pb dating methods. In the Zircon Fission Track Method, ZFTM, studies realized with Optical Microscopy, micro-Raman Spectroscopy and Scanning Electron Microscopy, showed that the etching varies from grain to grain. This also happens in different areas of the same zircon grain surface doing with that just in a small area the tracks density is uniform. Through the analyses done in this study we can see that these grains also can be used to determine its age. This new methodology can be applied in samples from basin zircon samples where the amount of zircon grains for ZFTM is little (for instance, in samples from hydrocarbon exploration wells). The U-Pb ages were calculated using the conventional methodology and these results are compared with those obtained trough ZFTM.

---

* E-mail: diasanc@bol.com.br (Airton Natanael Coelho Dias)
  Telephone: 55 51 3308 7287

Zircon fission track and U-Pb dating methods applied to São Paulo and Taubaté Basins located in the southeast Brazil

E.A.C. Curvo[1*], C.A. Tello S.[1], A.N.C. Dias[1], C.J. Soares[2], W.M. Nakasuga[1], R.S. Resende[1], M.R. Gomes[1], I. Alencar[3], R. Palissari[3], S. Guedes[3], J.C. Hadler[3]

[1] Departamento de Física, Química e Biologia, Universidade Estadual Paulista, UNESP, 19060-900, Presidente Prudente, SP, Brazil

[2] Instituto de Geociências e Ciências Exatas, Universidade Estadual Paulista, UNESP, 13506-900, Rio Claro, SP, Brazil

[3] Instituto de Física "Gleb Wataghin", Universidade Estadual de Campinas, UNICAMP, 13083-970, Campinas, SP, Brazil

Zircon samples from the São Paulo and Taubaté Basins (southeast Brazil) were concomitantly dated by conventional zircon Fission Track Method (FTM) (i.e., with neutron irradiation), *in situ* U-Pb dating method and zircon Fission Track Method without neutron irradiation (by using a LA-MC-ICP-MS) [1]. While FTM detrital-zircon data are ideally used to provide low-temperature information, U-Pb single detrital grain ages record the time of zircon formation in igneous or high grade metamorphic environments [2]. The correlation with the possible source of the basins' sediments (Mar and Mantiqueira Mountain Ranges) is also discussed.

References

[1] Hadler, J. C.; Iunes, P. J.; Tello S., C. A.; F. Chemale Jr., K. Kawashita, E.A.C. Curvo, F.G.S. Santos, T.E. Gasparini, P.A.F.P. Moreira and S. Guedes (2009). Experimental study of a methodology for Fission-track Dating without neutron irradiation. Radiation Measurements, 44 (9-10), 955-957.

[2] Carter, A. and Moss, S. J. (1999). Combined detrital-zircon fission-track and U-Pb dating: A new approach to understanding hinterland evolution. Geology, 27 (3), 235–238.

---

[*] Corresponding author: curvo@ifi.unicamp.br

Análise integrada pelos Métodos de Traços de Fissão e U-Pb aplicada a zircões detríticos da Bacia Bauru, Brasil

Airton Natanael Coelho Dias[1]; Farid Chemale Jr.[1]; Carlos Alberto Tello Saenz[3]; Peter Christian Hackspacher[4]

[1] UFU; [2] UnB; [3] Unesp (Presidente Prudente); [4] Unesp (Rio Claro)

RESUMO: A combinação de duas técnicas termocronológicas, ou seja, uma de alta temperatura (U-Pb) e outra de intermediária/baixa temperatura (Método de Traços de Fissão, MTF), aplicadas nos mesmos grãos de zircão detríticos da Bacia Bauru, provou ser uma poderosa ferramenta para desvendar o proveniência de rochas decorrentes de eventos morfotectônicos. O método U-Pb forneceu informações consistentes sobre principais áreas fontes para esta bacia sedimentar formada entre 90 a 100 Ma. Tais fontes estão identificadas por zircões Brasilianos e fontes subordinadas como do início do Neoproterozóico e Mesoproterozóico (ou Greenviliano) e Paleoproterozóico (Transamazônico). A fonte para esta bacia é na maior parte dos sedimentos da Bacia do Paraná, que contêm zircões retrabalhados dessas idades, e de material do embasamento cristalino formado a partir de Paleoproterozóico até o Neopalezóico. Os dados obtidos pelo MTF produziram dois grupos principais de idades aparentes: a idade Brasiliano (480-600 Ma), como parte da fase tardia da elevação Brasiliano, Late-Devonian/Permian idades (250-380 Ma), como parte da elevação principal da Plataforma Sul durante os Gondwanides. A exumação entre 739-825 Ma que também é gravada nas idades aparentes obtidas via MTF, podem estar relacionados com os *inliers* situados a oeste das unidades da Bacia Bauru (por exemplo: Maciço de Goiás Central). Algumas amostras registram idades do Paleoproterozóico e Brasiliano (via U-Pb) e idades aparentes via MTF de 381-250 Ma. Amostras estas que foram retrabalhadas e suportaram a passagem pela zona de *annealing* total (ou parcial) durante o Ciclo Gondwanides.

PALAVRAS CHAVE: BACIA BAURU, U-Pb e MTF